

DEVELOPMENT AND OPTIMIZATION OF SELF-  
MICROEMULSIFYING ASTAXANTHIN DELIVERY  
SYSTEM USING THE DESIGN OF EXPERIMENT (DOE)  
APPROACH



A Thesis Submitted in Partial Fulfillment of the Requirements  
for the Degree of Master of Science in Pharmaceutical Sciences and  
Technology  
Common Course  
FACULTY OF PHARMACEUTICAL SCIENCES  
Chulalongkorn University  
Academic Year 2019  
Copyright of Chulalongkorn University

การพัฒนาและการหาค่าเหมาะที่สุดของระบบนำส่งแอสตาแซนธินชนิดเกิดไมโครอิมัลชันด้วย  
ตัวเองโดยใช้วิธีการออกแบบการทดลอง



วิทยานิพนธ์นี้เป็นส่วนหนึ่งของการศึกษาตามหลักสูตรปริญญาวิทยาศาสตรมหาบัณฑิต  
สาขาวิชาเภสัชศาสตร์และเทคโนโลยี ไม่สังกัดภาควิชา/เทียบเท่า  
คณะเภสัชศาสตร์ จุฬาลงกรณ์มหาวิทยาลัย  
ปีการศึกษา 2562  
ลิขสิทธิ์ของจุฬาลงกรณ์มหาวิทยาลัย

Thesis Title	DEVELOPMENT AND OPTIMIZATION OF SELF-MICROEMULSIFYING ASTAXANTHIN DELIVERY SYSTEM USING THE DESIGN OF EXPERIMENT (DOE) APPROACH
By	Miss Mo Mo Ko Zin
Field of Study	Pharmaceutical Sciences and Technology
Thesis Advisor	VEERAKIET BOONKANOKWONG, Ph.D.

---

Accepted by the FACULTY OF PHARMACEUTICAL SCIENCES, Chulalongkorn University in Partial Fulfillment of the Requirement for the Master of Science

-----  
 Dean of the FACULTY OF  
 PHARMACEUTICAL SCIENCES  
 (Assistant Professor RUNGPETCH SAKULBUMRUNGSIL,  
 Ph.D.)

THESIS COMMITTEE

----- Chairman  
 (Assistant Professor WALAISIRI MUANGSIRI, Ph.D.)  
 ----- Thesis Advisor  
 (VEERAKIET BOONKANOKWONG, Ph.D.)  
 ----- Examiner  
 (VARIN TITAPIWATANAKUN, Ph.D.)  
 ----- External Examiner  
 (Associate Professor SOMLAK KONGMUANG, Ph.D.)



จุฬาลงกรณ์มหาวิทยาลัย  
 CHULALONGKORN UNIVERSITY

โม โม โค ชิน : การพัฒนาและการหาค่าเหมาะที่สุดของระบบนำส่งแอสตาแซนทินชนิดเกิดไมโครอิมัลชันด้วยตัวเองโดยใช้วิธีการออกแบบการทดลอง. ( DEVELOPMENT AND OPTIMIZATION OF SELF-MICROEMULSIFYING ASTAXANTHIN DELIVERY SYSTEM USING THE DESIGN OF EXPERIMENT (DOE) APPROACH) อ.ที่ปรึกษาหลัก : อ. ภก. ดร.วีระเกียรติ บุญกนกวงศ์

วัตถุประสงค์ของงานวิจัยนี้คือเพื่อพัฒนาและหาค่าเหมาะที่สุดของระบบนำส่งชนิดเกิดไมโครอิมัลชันด้วยตัวเองและเพื่อปรับปรุงอัตราการละลายของแอสตาแซนทินซึ่งเป็นสารที่ละลายน้ำได้น้อยโดยใช้วิธีการออกแบบการทดลองชนิดของผสม การวิจัยเริ่มต้นจากการวัดค่าการละลายของแอสตาแซนทินในสารช่วยต่าง ๆ เพื่อหาชนิดของวัสดุภาคน้ำมัน สารลดแรงตึงผิว และสารลดแรงตึงผิวที่เหมาะสมในสูตรตำรับ และการทดสอบการเกิดไมโครอิมัลชันโดยการสร้างเป็นแผนภูมิไตรภาคเพื่อหาอัตราส่วนที่เหมาะสมที่สุดของส่วนประกอบต่าง ๆ ในสูตรตำรับ จากการทดลองพบว่าสูตรตำรับที่เหมาะสมของระบบนำส่งชนิดเกิดไมโครอิมัลชันด้วยตัวเองที่ประกอบด้วยไตรกลีเซอไรด์สายโซ่ยาวประกอบด้วยน้ำมันละหุ่งร้อยละ 19.59 ครีโมฟอร์® อาร์เอช 40 ร้อยละ 62.34 และทวิน® 80 ร้อยละ 18.03 ซึ่งทำให้ได้อิมัลชันที่มีขนาดอนุภาคเท่ากับ 20.71 นาโนเมตร คำนีการกระจายขนาดอนุภาคเท่ากับ 0.28 ค่าศักย์ซีต้าเท่ากับ -9.07 ปริมาณของสารสำคัญเท่ากับร้อยละ 97.87 และการส่งผ่านของแสงเท่ากับร้อยละ 98.38 ส่วนสูตรตำรับที่เหมาะสมของระบบนำส่งชนิดเกิดไมโครอิมัลชันด้วยตัวเองที่ประกอบด้วยไตรกลีเซอไรด์สายโซ่ปานกลางประกอบด้วยไตรกลีเซอไรด์สายโซ่ปานกลางร้อยละ 12.39 ครีโมฟอร์® อาร์เอช 40 ร้อยละ 44.98 และทวิน® 80 ร้อยละ 44.59 ซึ่งทำให้ได้อิมัลชันที่มีขนาดอนุภาคเท่ากับ 22.02 นาโนเมตร คำนีการกระจายขนาดอนุภาคเท่ากับ 0.17 ค่าศักย์ซีต้าเท่ากับ -10.69 ปริมาณของสารสำคัญเท่ากับร้อยละ 97.09 และการส่งผ่านของแสงเท่ากับร้อยละ 98.72 ผลการวิเคราะห์การหาค่าเหมาะที่สุดพบว่าฟังก์ชันความพึงพอใจของระบบนำส่งชนิดเกิดไมโครอิมัลชันด้วยตัวเองที่ประกอบด้วยไตรกลีเซอไรด์สายโซ่ยาวและสายโซ่ปานกลางเท่ากับ 0.8074 และ 0.7949 ตามลำดับ และค่าที่ได้จากการทำนายโดยใช้โมเดลเมื่อเทียบกับค่าที่ได้จากการทดลองพบว่ามีความใกล้เคียงกัน นอกจากนี้ยังได้ทำการทดสอบสูตรตำรับที่เหมาะสมของไมโครอิมัลชันชนิดเกิดด้วยตัวเองที่ประกอบด้วยไตรกลีเซอไรด์สายโซ่ยาวและสายโซ่ปานกลาง โดยการสังเกตด้วยตาเปล่า การวัดระยะเวลาในการเกิดอิมัลชันด้วยตัวเอง คำนีหักเหแสง การส่องด้วยกล้องจุลทรรศน์ชนิดส่องกราด การทดสอบความคงตัวโดยการเก็บในอุณหภูมิสูงและต่ำสลับกัน พบว่าสูตรตำรับที่พัฒนามีลักษณะทางเคมีกายภาพและความคงตัวดี การละลายของสูตรตำรับไม่ขึ้นกับค่าพีเอชของตัวกลางและสามารถปลดปล่อยแอสตาแซนทินออกมาได้มากกว่าร้อยละ 90 ภายในระยะเวลา 4 ชั่วโมงในทุกตัวกลางที่ทดสอบ จากการทดลองพบว่าการละลายที่เวลาต่าง ๆ ของแอสตาแซนทินจากระบบนำส่งชนิดเกิดไมโครอิมัลชันด้วยตัวเองมีค่ามากกว่าอย่างมีนัยสำคัญเมื่อเปรียบเทียบกับวัตถุดิบแอสตาแซนทินและผลิตภัณฑ์แอสตาแซนทินที่ขาย ในท้องตลาดที่นำมาทดสอบ ระบบนำส่งชนิดเกิดไมโครอิมัลชันด้วยตัวเองที่ได้พัฒนาขึ้นโดยใช้วิธีการออกแบบการทดลองจึงเป็นอีกหนทางหนึ่งที่เหมาะสมที่ใช้ปรับปรุงอัตราการละลายของสารที่ละลายน้ำน้อยอย่างแอสตาแซนทิน

สาขาวิชา เกษศาสตร์และเทคโนโลยี  
ปีการศึกษา 2562

ลายมือชื่อนิสิต .....  
ลายมือชื่อ อ.ที่ปรึกษาหลัก .....



## ACKNOWLEDGEMENTS

I would like to express my sincere gratitude to my advisor Dr. Veerakiet Boonkanokwong for providing me an opportunity to be a part of his research group and for his patience, enthusiasm, motivation, and immense knowledge. His advice and suggestions were very helpful to me throughout the two years of graduate study. He made all the possible resources available for me to succeed in the research project. His guidance helped me in all the time of research and writing for the thesis. I could not have imagined having a better advisor and mentor for my study.

I also would like to thank all members of thesis committees, Assistant Professor Dr. Walaisiri Muangsiri, Dr. Varin Titapiwatanakun, and Associate Professor Dr. Somlak Kongmuang for their valuable time, support, insightful comments, and suggestions.

In addition, I would like to gratefully thank the Grants for Development of New Faculty Staff, Ratchadaphiseksomphot Endowment Fund, Chulalongkorn University. The research fund granted from the Graduate Program of Pharmaceutical Sciences and Technology, Faculty of Pharmaceutical Sciences, Chulalongkorn University is also acknowledged. I gratefully thank the Scholarship Program for ASEAN Countries granted from the Office of Academic Affairs, Chulalongkorn University for the financial support, tuition fees, monthly allowance, and material expense.

Additionally, I would like to pay greatly thank to all my teachers, my fellow labmates, friends, colleagues, and staffs in Faculty of Pharmaceutical Sciences, Chulalongkorn University, for their encouragement and great support. We have had wonderful times over the past two years.

Also, I would like to express my deepest gratitude to all my teachers from University of Pharmacy, Mandalay for allowing me to study a master's degree in Thailand.

Finally, I would like to express my gratitude to my beloved father, mother, sister, and grandmother for their care, mental support, cheerfulness, and understanding throughout these two years.

Mo Mo Ko Zin

## TABLE OF CONTENTS

	<b>Page</b>
.....	iii
ABSTRACT (THAI) .....	iii
.....	iv
ABSTRACT (ENGLISH).....	iv
ACKNOWLEDGEMENTS.....	v
TABLE OF CONTENTS.....	vi
LIST OF TABLES.....	vii
LIST OF FIGURES .....	viii
LIST OF ABBREVIATIONS.....	0
CHAPTER I INTRODUCTION.....	1
CHAPTER II REVIEW LITERATURE .....	11
CHAPTER III MATERIALS AND METHODS .....	30
CHAPTER IV RESULTS AND DISCUSSION.....	45
CHAPTER V CONCLUSION.....	91
REFERENCES .....	96
APPENDIX.....	111
VITA.....	134

## LIST OF TABLES

	<b>Page</b>
Table 1. Independent variables and responses in the mixture design. ....	35
Table 2. Formulation table for AST-loaded SMEDS containing castor oil.....	36
Table 3. Formulation table for AST-loaded SMEDS containing MCT oil.....	37
Table 4. Evaluation standard for self-microemulsification efficiency.....	49
Table 5. Emulsification Efficiency of Various Surfactants. ....	50
Table 6. Emulsification Efficiency of Various Co-surfactants. ....	51
Table 7. Range of independent variables of LCT-SMEDS in the mixture design. ....	58
Table 8. Range of independent variables of MCT-SMEDS in the mixture design. ...	58
Table 11. Summary of results of statistical analysis and model equations for the measured responses of LCT-SMEDS. ....	60
Table 9. Mixture experimental design for optimizing LCT-SMEDS formulation and the associated response data.....	60
Table 10. Mixture experimental design for optimizing of MCT-SMEDS formulation and the associated response data.....	61
Table 12. Summary of results of statistical analysis and model equations for the measured responses of MCT-SMEDS.....	63
Table 13. Analysis of variance of measured responses for LCT-SMEDS. ....	64
Table 14. Analysis of variance of measured responses for MCT-SMEDS. ....	65
Table 15. Predicted and measured values of optimized LCT-SMEDS formulation. ..	82
Table 16. Predicted and measured values of optimized MCT-SMEDS formulation. .	82
Table 17. Results of visibility grade, precipitation, and phase separation.....	83
Table 18. Stability profile of optimized SMEDS formulations. ....	86



## LIST OF FIGURES

	<b>Page</b>
Figure 1. Chemical structure of astaxanthin (60).....	14
Figure 2. Three-component simplex region (88) .....	29
Figure 3. Solubility of astaxanthin in different oils .....	47
Figure 4. Solubility of astaxanthin in different surfactants.....	47
Figure 5. Pseudoternary phase diagram with the following components: castor oil, Cremophor <sup>®</sup> RH 40, and Tween <sup>®</sup> 80. Surfactant and cosurfactant ratio of (a) 1:1, (b) 2:1, (c) 3:1, (d) 4:1, and (e) 5:1 .....	54
Figure 6. Pseudoternary phase diagram with the following components: MCT oil, Cremophor <sup>®</sup> RH 40, and Tween <sup>®</sup> 80. Surfactant and cosurfactant ratio of (a) 1:1, (b) 2:1, (c) 3:1, (d) 4:1, and (e) 5:1 .....	55
Figure 7. Pseudoternary phase diagrams constructed (a) in absence and (b) in presence of astaxanthin respectively using castor oil as the lipid phase.....	56
Figure 8. Pseudoternary phase diagrams constructed (a) in absence and (b) in presence of astaxanthin respectively using MCT oil as the lipid phase. ....	56
Figure 9. Three-dimensional response surface plot for the effects of the independent variables on the responses, Y <sub>1</sub> , Y <sub>2</sub> , Y <sub>3</sub> , Y <sub>4</sub> , and Y <sub>5</sub> of LCT-SMEDS .....	73
Figure 10. Contour plots for the effects of the independent variables on the responses, Y <sub>1</sub> , Y <sub>2</sub> , Y <sub>3</sub> , Y <sub>4</sub> , and Y <sub>5</sub> of LCT-SMEDS .....	74
Figure 11. Three-dimensional response surface plot for the effects of the independent variables on the responses, Y <sub>1</sub> , Y <sub>2</sub> , Y <sub>3</sub> , Y <sub>4</sub> , and Y <sub>5</sub> of MCT-SMEDS .....	75
Figure 12. Contour plots for the effects of the independent variables on the responses, Y <sub>1</sub> , Y <sub>2</sub> , Y <sub>3</sub> , Y <sub>4</sub> , and Y <sub>5</sub> of MCT-SMEDS .....	76
Figure 13. Response optimizer plot for LCT-SMEDS .....	79
Figure 14. Response optimizer plot for MCT-SMEDS .....	80
Figure 15. Overlaid contour plot for LCT-SMEDS.....	81
Figure 16. Overlaid contour plot for MCT-SMEDS.....	81
Figure 17. TEM images (a) LCT-SMEDS and (b) MCT-SMEDS of AST .....	85

Figure 18. The AST release profiles of LCT-SMEDS, MCT-SMEDS, marketed preparation, and raw AST in different dissolution media (n = 3). (a) pH 1.2, (b) pH 4.5, (c) pH 7.4, and (d) various pH. ....89



## LIST OF ABBREVIATIONS

AD	Alzheimer's disease
APP	amyloid precursor protein
AST	astaxanthin
A $\beta$	amyloid beta
DOE	design of experiment
HLB	hydrophilic and lipophilic balance
LCT	long chain triglycerides
LCT-SMEDS	self-microemulsifying delivery system containing long chain triglycerides
LCT-SMEDS <sub>OTM</sub>	optimized formulation of self-microemulsifying delivery system containing long chain triglycerides
MCT	medium chain triglycerides
MCT-SMEDS	self-microemulsifying delivery system containing medium chain triglycerides
MCT-SMEDS <sub>OTM</sub>	optimized formulation of self-microemulsifying delivery system containing medium chain triglycerides
ME	microemulsions
NF-KB	nuclear factor kappa B
NSAIDs	nonsteroidal anti-inflammatory drugs
ROS	reactive oxygen species
SMEDS	self-microemulsifying delivery system

## CHAPTER I

### INTRODUCTION

Alzheimer's disease (AD) is considered as a common severe chronic neurodegenerative disease. The characterization of this disease is the cognitive dysfunction and the memory impairment. The etiology of this disease is multifactorial. One of these factors is pathologically related with the accumulation of neurofibrillary tangles and amyloid beta (1). Oxidative stress is led by mitochondrial dysfunction and the accumulation of amyloid beta. Through many cellular molecular pathways, damage of tissue is followed as the result of oxidative stress, which is caused by the reactive oxygen species (ROS) formation. By different modes of necrosis or apoptosis, proteins, lipids, and nucleic acids in the cell can be damaged by ROS, which is then followed by cell death (2). Thus, it is crucial that the redox status is maintained in our body.

Two possible theoretical approaches are discovered for the treatment of AD while no medicine was found to effectively protect the nerve cells (3). The symptomatic treatment is observed as one approach to treat and reduce the cognitive symptoms. Another approach for treatment is to prevent the onset of the disease by sequestering the primary precursors and to reduce the secondary pathologies of the disease. According to the specificity of each individual and the severity of the disease, the appropriate treatment strategies were selected. However, specific symptoms of AD are chiefly targeted by currently available therapeutic agents. These therapeutic agents include acetylcholinesterase inhibitors which suppress the acetylcholine degradation within the

synapse and enhance the cholinergic neurotransmission. Other therapeutic strategies and agents such as immunotherapy, secretase effectors, the A $\beta$  vaccine trials, neurotrophins, statins, and nonsteroidal anti-inflammatory drugs (NSAIDs) have also been observed. However, their use remains questionable and all the treatments undergo various side effects. Hence, further research studies are still required for the preventive and treatment of AD. The promising antioxidant therapy for the treatment of AD has been studied for years (4).

Especially, astaxanthin (AST) can oppose oxidative injuries by scavenging of radicals, regulating gene expression, inhibiting lipid peroxidation, and quenching of singlet oxygen, (5, 6). Since astaxanthin inhibits inflammation and oxidative stress for the treatment of chronic diseases as shown in many studies in recent years, astaxanthin is considered as a successful carotenoid on the market (7). Moreover, AST can easily cross the blood-brain barrier due to its unique chemical structure (8). Therefore, brain is regarded as a target organ of AST. AST is mainly found in the marine environment and microorganisms (6, 9, 10). Animals cannot synthesize AST, however, it can be acquired via the diet (11).

AST showed the effect of anti-inflammation by blocking nitric oxide production and the NF-KB-dependent signaling pathway and by inhibiting the inflammatory mediators expression (5, 12, 13). This finding validates the administration of astaxanthin as a co-treatment of AD. Unfortunately, AST is unstable during production and storage owing to its 3-hydroxy and 4-keto in the end of the molecule, and a chain of highly conjugated, double bond structure that is prone to chemical degradation (oxidation and isomerization) when exposed to light, oxygen, high

temperature, and pH extremes (14). This causes color fading of AST and a loss of its biological activity. Moreover, the bioavailability of astaxanthin is greatly reduced owing to its poor solubility in water, resulting in negative effect on its practical applications (15). For the purpose of increasing the stability and bioavailability of AST, various approaches such as formulation of liposomes (15) and nanoparticles (16) have been examined. In these formulations, high expense of ingredients and complicated method of formulation are needed.

Since most of the current therapies are only symptomatic but not curative, new drugs are highly demanded to be discovered for the effective medication of neurodegenerative diseases. Moreover, for the purpose of reaching the pathological site and minimizing unwanted side effects, highly effective targeted delivery systems of drug are required for the treatment of chronic neurodegenerative diseases which needs long-term drug administration. Thus, once the discovery of an optimal drug has been successful, it should be efficiently conveyed to the aimed cells.

In supplying drugs to patients with neurodegenerative diseases, one of the most patient-friendly and convenient methods is systemic non-invasive oral delivery. Nevertheless, the main drawbacks connected with the delivery via oral route involve drug degradation prior to reach the blood vessels and low drug hydrophilicity. Oral route has limited drug efficacy although it is the most applied method in supplying drugs. The main limits affecting drug-loaded pills to reach the systemic circulation involves poor bioavailability in body fluid, particularly owing to poor solubility in water, degradation within the gastrointestinal tract, pre-intestinal metabolism, and poor intestinal membrane permeability. By the use of absorption enhancers, the pharmaceutically active compounds are

modified to be able to overcome poor intestinal membrane permeability. The bioavailability of drugs administered through oral delivery are ensured to be enhanced on the usage of lipids and lipophilic excipients among others. The main mechanisms by which lipophilic excipients and lipids influence drug absorption are as follow (17):

1. by alterations of the composition of the colloidal environment targeted at drug solubilization improvement within the intestinal environment on the usage of vesicles and micelles
2. by enhancing drug uptake interacting with enterocyte-based transport and metabolic processes
3. by developing the transportation of drug to the systemic circulation through the intestinal lymphatics rather than the hepatic portal vein and as a result, reducing the first-pass metabolism of drug.

Currently, lipid-based formulations have gained much attention because of their ability to improve the solubility and bioavailability of poorly water soluble compounds (18). Solubilizing or encapsulating the active substances in lipid excipients can promote the enhancement of solubilization and absorption, resulting in improved bioavailability. The successful marketed lipid-based formulations consist of clofazimine (Lamprene<sup>®</sup>), saquinavir (Fortovase<sup>®</sup>), efavirenz (Sustiva<sup>®</sup>), and ritonavir (Norvir<sup>®</sup>) (19). Some examples of lipid-based formulations are oily liquids, micelles, liposomes, and self-microemulsifying delivery systems.

Some drugs such as steroids were formulated as oily liquids by dissolving the drugs in oils (e.g., triacylglycerols). But, the amount of oil needed to solubilize a unit dose of active substance is very large, that limits the preparation of active substance in oil (19).

The formation of micelles is induced by self-assembly of amphiphilic molecules. These molecules hold polar regions (heads) and a nonpolar regions (tails). Both hydrophilic and hydrophobic compounds can be delivered by micelles. The molecules of micelles are usually spherical in shape with 2 to 20 nm (20). The difficulty in drug loading and high cost of preparation hinder the industrial growth of polymeric micelles (21). The polymer may be solubilized directly with the active compound to produce drug-loaded polymeric micelles when it is sufficiently hydrophilic. Although this technique is applicable for hydrophilic polymers, it is generally related with low drug loading. Moreover, an organic solvent may be required to dissolve other amphiphilic polymers and the active compound with poorly water solubility which may cause safety and environmental concerns. Then, by dialysis or emulsification techniques, drug loading is performed in the polymeric micelles. However, the process of dialysis usually needs more than 36 hours for effective drug loading and water replenishment at regular intervals. Moreover, the process of emulsification usually contains the usage of chlorinated solvents that are not safe. Additionally, disadvantages of micelles include poor physical stability *in vivo* and poor drug loading efficiency (22).

Liposomes is a sphere-shaped vesicle with a membrane consisting of one or more phospholipid bilayers used to deliver active compound or genetic material into a cell. According to their lamellarity, these vesicles can be classified from single lamellar with a size ranging between 50 and 250 nm to multilamellar with size 1-5  $\mu\text{m}$ . They are capable of carrying either hydrophobic active compounds in their hydrophobic lipid bilayers or hydrophilic compounds in their inner aqueous phase. As the stability of



the vesicles is poor in the gastrointestinal tract, the oral delivery of liposomes is difficult and challenging. This is because the lipid bilayer structure may rapidly splinter in response to van der Waals, electrostatic, and hydrophobic forces, resulting in drug leakage, particle aggregation, and a reduced shelf life. Moreover, the loaded drug is frequently dispersed in a rapid burst release due to their poor control of drug release. Additionally, liposomes exhibit poor efficiency of drug encapsulation owing to low solubility of drugs in solution (22).

Self-microemulsifying delivery system (SMEDS) produces microemulsions with globule size ranging from 20 to 200 nm upon dilution (23, 24). Microemulsions (ME) are solution-like systems with an inner structure of nano droplets stabilized by a set of surfactants and co-surfactants (25). SMEDS formulation typically consists of a homogenous mixture of a surfactant, an oil, and an active ingredient, which is rapidly dispersed in the body. The size range of formed droplets are approximately the same as those mentioned in microemulsion.

Among various lipid-based formulations, self-microemulsifying systems have gained much interest by the researchers due to their self-emulsifying nature, their stability, ease of preparation, and scale-up (26). The oil presented in the SMEDS formulation could serve as the precursor for the chylomicrons and lipoproteins formation which may improve the drug absorption through the lymphatic pathway and hence increase the bioavailability of active compound by decreasing hepatic first-pass metabolism. Moreover, the presence of surfactant in SMEDS might alter the cell membrane permeability and thereby enhance permeability of drug. Additionally, due to their amphiphilic nature, the surfactants are absorbed at the oil-water interface, that can reduce the interfacial surface

tension and enhance the penetration of drug into the epithelial cells. The polar region of the surfactants interacts with the polar head region of the lipid bilayers, as a result modifying ionic forces and hydrogen bonding. The drug also presents in dissolved form, resulting in increasing absorption of drug. Owing to its reproducible drug release, SMEDS has also attracted attention because it is less dependent on the physiological conditions typically found in the gastrointestinal tract.

A self-microemulsifying delivery system (SMEDS) is a simple formulation produced by a simple technique method as well as required less time of formulation and available cheap excipients (27). Owing to small droplet sizes upon dispersion and their behavior of self-dispersion that has been shown to enhance drug absorption, SMEDS is a beneficial approach in delivering lipophilic drugs which are poorly soluble in water (28, 29). Its ability to form oil-in-water (o/w) microemulsions under mild stirring after diluting with water is the basic principle of this system (30). In the gastrointestinal tract, the active ingredient is shown in a solubilized form, resulting in spontaneous microemulsion formation. For the drug absorption, a large interfacial surface area is provided by the small droplet size of the formed microemulsion (31). Numerous formulation-related specifications, for instance, oil/surfactant proportion, surfactant concentration, particle size, polarity, and charge of the microemulsion are the basis for the oral absorption efficiency of the active ingredient from the SMEDS, and the self-emulsification ability is also determined by those parameters (26). Thus, efficient self-emulsifying systems can only be obtained through the combination of very specific pharmaceutical excipients. The SMEDS formulation can successfully be optimized with the essential factors such as choice of the constituents, and properly

balanced proportion of the components. For the development of a suitable formulation, Design of Experimental (DOE) approaches have been widely utilized (32). According to traditional one-factor-at-a-time approaches, the proportions of SMEDS constituents have been optimized. Nevertheless, these methods are inefficient, time-consuming, and labor-intensive. Moreover, the effect of individual constituent and their interactions are analyzed with the insufficient data obtained from these methods (32, 33). Hence, DOE approaches such as mixture, central composite, factorial, and Box–Behnken designs have been suggested to examine the influences of independent variables (input variables) on dependent variables (responses) and the interaction between independent variables (34-36). The mixture design is a popular response surface methodology because of its minimal variance correlated with the interpretation of coefficients in a model (37). For optimization of the formulation, Bhattacharya et al. (38) successfully formulated docetaxel-loaded self-nanoemulsifying system by the use of mixture design. In this study, the independent variables were the concentration of oleic acid ( $X_1$ ), Tween<sup>®</sup> 80 ( $X_2$ ), and PEG 400 ( $X_3$ ) while the responses were emulsification time ( $Y_1$ ) and %drug release ( $Y_2$ ). Among total preparations, the optimized one consisted of oleic acid (42.37%), Tween<sup>®</sup> 80 (43.39%), and PEG 400 (14.21%). It was revealed that the best formulation showed 19.71s emulsification time and 95.21% of drug release. Sandhu *et al.* (39) well designed a tamoxifen-loaded SMEDS by a mixture design. The optimized formulation showed increased cellular uptake and enhanced bioavailability.

Self-emulsifying formulation has been prepared using materials which has been extensively researched. The transportation methods for

the lipids are different. The transportations of medium chain triglycerides (MCT) and long chain triglycerides (LCT) are via the portal blood to the systemic circulation and via the intestinal lymphatics respectively (40). Through the delivery systems of drug containing LCT, the first-pass metabolism of a compound may be diminished because the intestinal lymph travels directly to the systemic circulation without passing through the liver (41, 42). It was observed in the literature that MCT is better in solubility properties, higher in fluidity, and self-emulsification ability, than LCT, and so MCT has been preferred in SMEDS (30, 31). Moreover, an advanced chemical stability of compound in MCT is observed owing to the lack of double bonds and the purity of the lipid. SMEDS containing either medium chain or long chain triglyceride have been researched with danazol (43) and halofantrine (44). It was observed that the highest bioavailability was obtained by the use of LCT-SMEDS in both studies. Studies comparing LCT-SMEDS and MCT-SMEDS are still limited in number (45).

As a whole, the current study hypothesized that the solubility and dissolution rate of AST could be improved by SMEDS formulations containing either LCT or MCT. Regarding to this, the AST loaded SMEDS containing either LCT or MCT will be improved as a carrier for oral preparation for drug localization into brain tissues through this research. The AST loaded SMEDS formulations were prepared and the factors that influence the response variables by mixture design were optimized in order to prove this hypothesis. And then, the morphology and physicochemical properties were characterized. Therefore, the main objectives of this research work are as follows:

1. To carry out preformulation studies for choice of excipients in formulations/systems
2. To improve astaxanthin (AST)-loaded self-microemulsifying delivery system (SMEDS) formulations including medium and long chain fatty acids
3. To evaluate the effects of formulation variables on particle size, polydispersity index, zeta potential, active ingredient content, and percentage of transmittance of the formed microemulsions by using the design of experiment approach
4. To optimize the AST SMEDS products using mathematical models and balance the effects of formulation variables on the responses
5. To characterize the physicochemical properties of the optimized formulations
6. To perform *in vitro* release studies and determine release profiles of astaxanthin from the optimized formulations.

## **CHAPTER II**

### **REVIEW LITERATURE**

#### **1. Alzheimer's disease (AD)**

Alzheimer's disease (AD) is a common severe chronic neurodegenerative disorder which induces dementia in the elderly people. The people who suffer from AD shows gradual memory loss and other cognitive dysfunctions, which ultimately lead to integrated inability and eventually death. In 1906, Alois Alzheimer, a German physician firstly illustrated AD. In 1901, he studied on patient August D who suffered from signs and symptoms of hallucinations, cognition, and aggressive behavior. World Health Organization reported that there will be 71% of AD cases among 81.1 million dementia cases in 2040 (46, 47). The majority of AD patients are elderly people generally aged sixty-five or more. There are varieties of AD, namely, early-onset or late-onset form of AD. Early-onset form is sporadic or rare which occur in people who are younger than age sixty-five (48). These patients have autosomal dominant mutation on either one of the presenilin genes positioned on chromosomes 1 and 14 or in the amyloid precursor protein gene positioned on chromosome 21. Furthermore, there may be elevated prospect of progressing early-onset form of AD in the patients with Down's syndrome (49). The most common form of the disease is late-onset form, which develops in people age sixty-five and older. It may be genetic, but it is more likely a result of brain changes caused by lifestyle and environmental impacts (50).

The etiology of this disease is multifactorial. One of those factors is pathologically related with the accumulation of neurofibrillary tangles and amyloid beta (1). Oxidative stress is led by mitochondrial dysfunction and the accumulation of amyloid beta. Through many cellular molecular pathways, damage of tissue is followed as the result of oxidative stress, which is caused by the reactive oxygen species (ROS) formation. By different modes of necrosis or apoptosis, the cell components (proteins, nucleic acids, and lipids) can be damaged by ROS, which is then followed by cell death (2). Thus, it is crucial that the redox status is maintained in our body.

Two possible theoretical approaches are discovered for the treatment of AD while no drug has been found to effectively protect the nerve cells (3). The symptomatic treatment is observed as one approach to treat and reduce the cognitive symptoms. Another approach is for the prevention of the disease onset by sequestering the primary precursors and for reduction of the secondary pathologies of the disease. According to the specificity of each individual and the severity of the disease, the appropriate treatment strategies were selected. However, specific symptoms of AD are chiefly targeted by currently available therapeutic agents. These therapeutic agents include acetylcholinesterase inhibitors which suppress the acetylcholine degradation within the synapse and enhance the cholinergic neurotransmission. Other therapeutic strategies and agents such as immunotherapy, hormone replacement therapy, blocking of excitotoxicity, secretase effectors, the A $\beta$  vaccine trials, neurotrophins, statins, and nonsteroidal anti-inflammatory drugs (NSAIDs) have also been observed. However, their use remains questionable and all the treatments undergo various side effects. Hence,

further research studies are still required for the preventive and treatment of AD. The promising antioxidant therapy for the treatment of AD has been studied for years (4).

Regarding the pathophysiology of AD, currently there are numerous unknown aspects. For the initiation and progression of AD, the molecular mechanisms had been attempted to explain by the different theories. This complex neurodegenerative disease could not be fully explained by one of these hypotheses alone. The researchers considered that the initial causes of AD are the abnormal formation and accumulation of amyloid beta ( $A\beta$ ) plaques in the brain (51). Many researches have already described that an imbalance between synthesis and clearance of amyloid beta causes the formation of those plaques (52). In the brain of AD patients, oxidative stress and inflammation are induced by the accumulation of  $A\beta$  at the neurofibrillary tangle level, which causes the neuronal cell death (53, 54). Additionally, some studies have demonstrated that excessive numbers of damaged mitochondria are present in the neurons of AD patients, possibly because of the mitochondrial DNA mutations (55). In the early stages of AD, mitochondrial oxidative stress occurs, suggesting a major function of oxidative stress for the development of AD (56). Thus, natural compounds with anti-inflammatory and antioxidant properties have been suggested to prevent or reduce the AD development. The promising antioxidant therapy for the treatment of AD has been studied for years (4).



## 2. Astaxanthin (AST)

Carotenoids have attained commercial and scientific interest in recent decades, because of their vast chemical diversity and their beneficial effects on human health. These carotenoids have antioxidant, anti-inflammatory, antiproliferative, repairing, and antiaging effects. These bioactive compounds can be utilized either as cosmeceutical and nutraceutical ingredients for preventing chronic inflammation and oxidative stress-related diseases or as skin protection for inhibiting adverse effects of UV radiation (57-59).

In recent years, astaxanthin (AST) is a profitable carotenoid on the market because many researches have indicated its inhibitory effect on opposing inflammation and oxidative stress (7). In addition, AST has a powerful protective effect on human brain due to its chemical structure and can easily cross the blood-brain barrier (8). Therefore, the brain is regarded as an important target organ of AST. Nowadays, AST have gained much interest for its effect on the prevention or cotreatment of neurodegenerative diseases such as Parkinson and Alzheimer diseases.

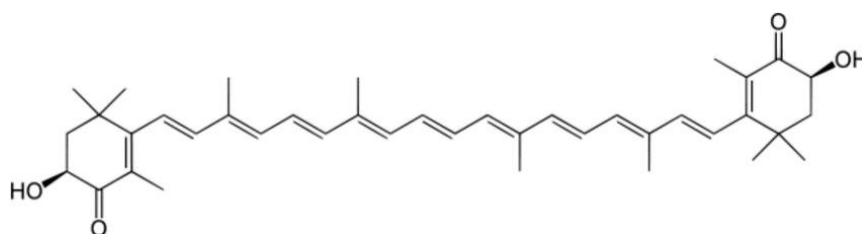


Figure 1. Chemical structure of astaxanthin (60)

AST can oppose oxidative injuries by scavenging of radicals, regulating gene expression, inhibiting lipid peroxidation, and quenching of singlet oxygen, (5, 6). AST is mainly present in the marine environment and microorganisms (6, 9, 10). AST exhibited strong anti-inflammatory effect by blocking nitric oxide production and the NF-KB-dependent signaling pathway and by inhibiting the inflammatory mediators expression (5, 12, 13). This finding validates the administration of AST as a cotreatment for AD. Unfortunately, astaxanthin is unstable during production and storage owing to its 3-hydroxy and 4-keto in the end of the molecule, and a chain of highly conjugated, double bond structure that is prone to chemical degradation (oxidation and isomerization) when exposed to light, oxygen, high temperature, and pH extremes (14). This causes color fading of AST and a loss of its biological activity. Moreover, the bioavailability of astaxanthin is greatly reduced owing to its poor solubility in water, resulting in negative effect on its practical applications (15). For the purpose of increasing the stability and bioavailability of AST, various approaches such as formulation of liposomes (15) and nanoparticles (16) have been examined.

Pan L, et al. (15) developed astaxanthin-loaded nanoliposomes by a film dispersion-ultrasonic technique. These formulations showed small droplet size with a uniform size distribution and high encapsulation efficiency. X-ray diffraction analysis and differential scanning calorimetry proved that AST is interacted with the lipid bilayer. It has been demonstrated that there could be remarkably enhancement of thermal stability of AST after encapsulation in nanoliposomes by the thermal gravimetric analysis. Moreover, the water dispersibility of

astaxanthin could be greatly enhanced by encapsulation. The measurements of steady-state fluorescence demonstrated that the incorporation of AST into the lipid bilayer increased micropolarity in the membrane, but reduced membrane fluidity. In addition, it confirmed that AST encapsulation in the lipid bilayer may be utilized for modulating the structural properties of membranes.

Guan L, et al.(16) prepared astaxanthin-loaded nanopowder to increase bioavailability and antioxidant activities. The nanoencapsulation and freeze-drying techniques were applied to formulate the nanopowder. The AST nanopowder showed AST content as high as 2.9% and the result of solubility with 230 mg/mL. The nanopowder showed a more powerful antioxidant effect compared with free AST. It was also observed that the nanopowder could deliver AST proficiently to the small intestine. Nanopowder having a unit dose of AST with 2.4 mg/kg exhibited no chronic toxicity to mice. Relative bioavailability and pharmacokinetics of the nanopowder confirmed that the AST delivery might be significantly enhanced by DNA/chitosan nanocarriers.

Shanmugapriya K, et al. (61) formulated emulsion-based delivery systems to increase the bioavailability of AST and alpha-tocopherol. Spontaneous and ultrasonication emulsification methods were used to formulate oil/ water microemulsion. The good stability of the microemulsion was confirmed by the use of dynamic light scattering and spherical-shaped was proved microemulsion transmission electron microscopy. Cytotoxicity studies confirmed that the microemulsion at lower concentrations could be less toxic than one at higher concentrations. Both minimum bactericidal concentrations and minimal

inhibitory concentration methods proved significant antibacterial activity to discompose the bacterial cell membrane integrity. This study demonstrated that emulsion-based delivery system act as a targeted drug delivery vehicle for cancer treatment applications.

Rodriguez-Ruiz V, et al. (62) designed a lipid carriers formulations to protect the antioxidant activity of astaxanthin. The antioxidant activity of the formulations was evaluated by  $\alpha$ -Tocopherol Equivalent Antioxidant Capacity assay. Atomic force microscopy, dynamic light scattering, and scattering electron microscopy techniques were characterized. These studies exhibited that spherical and negatively charged particles with the droplet size value of ~60 nm and the polydispersity index value of ~0.3. In the examination of AST loading, AST recovery of > 90% was observed. According to the results, the potential of the nanostructured lipid carriers has been described to improve the antioxidant activity and stabilize AST.

In these formulations, high expense of ingredients and complicated method of formulation are needed. Thus, suitable formulation with pharmaceutical approach is required to enhance its bioavailability.

### **3. Lipid-based formulations**

During recent times, the lipid-based formulations of the compounds with poorly water solubility have received much interest because these formulations have the ability to increase the solubility, dissolution, and oral bioavailability (18). Solubilizing or encapsulating

the drug in lipid excipients may improve the absorption of drug, thereby enhancement of bioavailability. The successful marketed lipid-based formulations introduce clofazimine (Lamprene<sup>®</sup>), saquinavir (Fortovase<sup>®</sup>), efavirenz (Sustiva<sup>®</sup>), and ritonavir (Norvir<sup>®</sup>) (19). Some examples of lipid-based formulations are oily liquids, liposomes, micelles, and self-emulsifying systems.

Some drugs (e.g. steroids) were formulated as simple lipid solutions by dissolving the drugs in oils (e.g., triacylglycerols). However, these formulations are limited because the quantity of oil needed to dissolve the required dose of active compound could be very high (19).

Liposomes are the vesicles used to transport drugs or genetic material into the cell. They consist of phospholipid bilayers enclosing an aqueous phase. According to their lamellarity, these vesicles can be classified from single lamellar with a size 50-250 nm to multilamellar with a size ranging between 1 and 5  $\mu\text{m}$ . They have ability to carry either hydrophobic compounds in their hydrophobic lipid bilayers or hydrophilic compounds in their inner aqueous phase. Because of the instability of the vesicles in the gastrointestinal tract, the oral delivery of liposomes is difficult and challenging. This may be due to the lipid bilayer structure can rapidly decompose in respect to van der Waals, electrostatic, and hydrophobic forces. Consequently, drug leakage, particle aggregation, and a reduced shelf life may be observed in the formulation of liposomes. Moreover, due to their poor control of drug release, the loaded drug is frequently dispersed in a rapid burst release. Additionally, owing to poor solubility of drugs in solution, liposomes may also show low efficiency of the drug encapsulation (22).

Micelles are aggregates of surfactant molecules dispersed in aqueous solution. The formation of micelles is provided by self-assembly of amphiphilic molecules. Micelles are usually spherical with a size 2-20 nm (20). These molecules consist of polar head and nonpolar tail. The molecules of micelles can deliver both hydrophilic and hydrophobic compounds. The difficulty in drug loading and high cost of preparation hinder the industrial growth of polymeric micelles (21). To obtain polymeric micelles containing the drug, the polymer can be solubilized directly with the drug when it is sufficiently hydrophilic. Although this technique is applicable for highly hydrophilic polymers, it is generally correlated with low capacity of drug loading. In micelles formulation, using an organic solvent is found to dissolve the polymers and drug with poorly water solubility which may cause safety and environmental concerns. Then, by dialysis or emulsification techniques, drug loaded polymeric micelles is prepared. However, for the efficient drug loading as well as the replenishment of water at regular intervals, dialysis system frequently requires more than 36 hours. Moreover, the emulsification process typically includes using chlorinated solvents that are unsafe. Additionally, disadvantages of micelles include poor physical stability *in vivo* and poor drug loading efficiency (22).

Self-microemulsifying delivery system (SMEDS) provides the microemulsions with a size ranging from 20 to 200 nm upon dilution (23, 24). Microemulsions (ME) are solution-like systems with an inner structure of nano droplets stabilized by a set of surfactants and co-surfactants (25). SMEDS preparation typically consists of a homogeneous mixture of an oil, a surfactant/co-surfactant, and an active compound, which is rapidly dispersed when introduced into the body.

Among various lipid-based formulations, SMEDS have gained much interest by the researchers due to their self-emulsification nature, ease of preparation, their stability, and scale-up (26). The oil presented in a SMEDS serve as the precursor for the lipoproteins and chylomicrons formation. This formation could enhance the absorption of drug through the intestinal lymphatics and hence increase the oral bioavailability of active compound with poorly water solubility by reducing the first-pass effect of drug metabolism. Moreover, the presence of surfactant in SMEDS might alter the cell membrane permeability and thereby enhance permeability of drug. Additionally, due to their amphiphilic nature, the absorption of surfactants is observed at the interface between oil and water phases, that may decrease the interfacial tension and increase the drug penetration into the epithelial cells. Moreover, the drug also presents in dissolved form, resulting in increasing absorption of drug. Owing to its reproducible drug release, SMEDS has also attracted attention because it is less dependent on the physiological conditions typically found in the gastrointestinal tract.



#### **4. Self-microemulsifying delivery system (SMEDS)**

SMEDS is a simple formulation produced by a simple technique method as well as required less time of formulation and available cheap excipients (27). Owing to small droplet sizes upon dispersion and their behavior of self-dispersion that has been shown to enhance drug absorption, SMEDS is a beneficial approach in delivering lipophilic drugs (28, 29). Its ability to form oil-in-water microemulsions by mild stirring

after diluting with water is the basic principle of SMEDS (30). The active ingredient is shown in a solubilized form, resulting in spontaneous microemulsion formation in the gastrointestinal tract. A large interfacial surface area for the absorption of drug, is provided by the small droplet size of the formed microemulsion (31). Numerous formulation-related specifications such as oil/surfactant ratio, surfactant concentration, particle size, polarity, and charge of the microemulsion systems are the basis for the oral absorption efficiency of the active ingredient from the SMEDS, and the self-emulsification ability is also determined by those parameters (26). Thus, efficient self-emulsifying systems can only be obtained through the combination of very specific pharmaceutical excipients. The SMEDS formulation can successfully be optimized with the essential factors such as choice of the constituents, and properly balanced proportion of the components.

The increase of the drug absorption and oral bioavailability is due to low interfacial tension and the increment of solubilization for the drugs with poorly water solubility (30, 63). In some cases, the emulsification and dispersion efficiency are improved by using lipophilic surfactants and co-solvents (64-66). Moreover, the advantages of SMEDS include the reduction of dose, the prevention of gastric irritation, the improved stability in contrast to emulsions, the reduced production time and the protection of the drugs from the chemical and enzymatic degradation (67, 68).

Although SMEDS formulation has several advantages, certain limitations are found in this system. Due to the change of pH, the drugs may precipitate in vivo (69). In addition, when SMEDS formulations are encapsulated in soft gelatin capsules, the volatile solvents in



formulations may travel to the shells of gelatin capsules, with the result of the precipitation of the drugs (70). Another challenges to develop SMEDS formulation are the oxidation of lipid excipients and the lack of useful predicative in vitro models (27, 71). Moreover, problems in handling, stability, and storage are also occurred in liquid SMEDS (71).

Self-emulsifying formulation has been prepared using materials which has been extensively researched. The transportation methods for the lipids are different. The transportations of medium chain triglycerides (MCT) are via the portal blood to the systemic circulation, while long chain triglycerides (LCT) are via the intestinal lymphatics (40). Through drug delivery systems containing LCT, the first-pass metabolism of an active compound may be diminished because the intestinal lymphatics travels directly to the systemic circulation without passing through the liver (41, 42). It was observed in the literature that MCT is better in solubility properties, higher in fluidity, and self-emulsification ability, than LCT, and so MCT has been preferred in SMEDS (30, 31). Moreover, an advanced chemical stability of compound in MCT is observed owing to the lack of double bonds and the purity of the lipid. SMEDS incorporating either medium chain or long chain triglycerides (LCT-SMEDS or MCT-SMEDS) have been researched with danazol (43) and halofantrine (44). It was observed that the highest bioavailability was obtained by the use of LCT-SMEDS in both studies. Studies comparing LCT-SMEDS and MCT-SMEDS are still limited in number (45).

Like lipids, carotenoids are absorbed into the body and transported through the lymphatic system into the liver. Depending on the accompanying dietary constituents, carotenoids absorption may be increased or decreased. The carotenoid absorption may be enhanced by

a high fat diet while its absorption reduced by a low cholesterol diet. After ingestion, AST mixes with bile acid and make micelles in the small intestine. The micelles containing AST are partially absorbed by intestinal cells. These cells assimilate AST into chylomicra. In the systemic circulation, the digestion of these chylomicra containing AST are carried out by lipoprotein lipase after releasing into the lymph. The liver and other tissues remove chylomicron remnants rapidly. AST is incorporated with lipoproteins and transported into the tissues (60).

#### **4.1. Components of SMEDS formulation**

##### **4.1.1. Oil**

Oil is a relevant ingredient in SMEDS formulation because it has the ability for solubilizing the drug, for facilitating the process of self-microemulsification, and for increasing the delivery of hydrophobic compound through the intestinal lymphatics, resulting in enhancement of the drug absorption in the gastrointestinal tract (72). Both long chain triglycerides (LCT) and medium chain triglycerides (MCT) with different saturation degree have been utilized for the development of SMEDS formulations (68). Since hydrolyzed or modified vegetable oils have better emulsification and drug solubility properties, these excipients have been used (73).

The fatty acid chains with 14-20 carbons are included in the long chain triglycerides (74). A mixture of glyceride esters of unsaturated long chain fatty acids is comprised in vegetable oils. Since these are often

found in daily food and are easily digestible, they are considered as safe products (75). Although it is difficult to emulsify, the drug transport can be improved by oils composed of long chain triglycerides through the lymphatic system in gastrointestinal tract (76). The stimulation of lymphatic transport of drugs has proved by using LCT (soybean oil and cottonseed oil) for improving the bioavailability of drugs with poorly water solubility (77). Both the type and the concentration of lipids have effect on lymphatic transport. Fatty acid chains of 6-12 carbons are contained in medium chain triglycerides (75). Comparing to LCT, MCT has the ability to get digested efficiently (78, 79). Moreover, it indicates enhanced solubility properties, greater fluidity, and good emulsifying ability having less oxidation tendency. Thus, the common use of MCTs are occurred comparing to LCTs (75, 78).

#### 4.1.2. Surfactants

The performance of surfactant in SMEDS formulation is for decreasing the interfacial tension and adjusting the spontaneous curvature of the interface (80). The required low interfacial tension can be provided by choosing appropriate surfactant. The selection of surfactant basically depends on the efficiency and rapidity to microemulsify the oil, solubilizing ability for the drug, safety, and emulsion type to be formulated (81). For the formulations of self-emulsification, a variety of compounds which describes surfactant properties may be applied but oral administration can accept only very few surfactants. An important determining factor in selecting a surfactant is safety. Less toxic are

included in non-ionic surfactants comparing to ionic surfactants (82). Surfactants can dissolve high concentrations of drugs with poorly water solubility as they are amphiphilic in nature.

#### **4.1.3. Co-surfactants**

Usually, high surfactant concentrations and addition of co-surfactants are necessary in the formulation of a successful SMEDS. With the purposes to decrease the interfacial surface tension of oil and water phases, to fluidize the hydrocarbon region of interfacial film, to enhance the loading efficiency of drug, and to form the spontaneous microemulsion, co-surfactant with hydrophilic-lipophilic balance (HLB) value 10-14 has been generally utilized along with surfactant (48). In SMEDS formulations, both concentration and type of co-surfactant are important. For example, SMEDS with low molecular weight co-surfactants should not be added into gelatin capsules because they may be absorbed into capsule shells which may cause drug precipitation (75). Similarly, the precipitation of drug upon dilution of SMEDS are formed by the higher co-surfactant concentration resulting from partitioning of co-surfactant into aqueous phase (83).

## 5. The process of emulsification

### 5.1. Mechanism of self-emulsification

As reported by 'Reiss', the process of self-emulsification is found when the change of entropy that prefers dispersion is greater than the energy necessary to enhance the surface area of the dispersion. The free energy of the typical emulsion is a direct function of the energy needed for a new surface area formation between the lipid and aqueous phases and its equation could be presented by:

$$\Delta G = \sum N\pi r^2 \sigma$$

Where,  $\Delta G$  refers to the free energy of the process, N represents the number of droplets with radius r and  $\sigma$  stands for the interfacial energy. The stable emulsion is produced by emulsifiers which create a monolayer on the droplets of emulsion and thus decrease the interfacial energy. In the self-emulsifying systems, the free energy needed for the emulsion formation may be either very poor or positive or negative. After that, the process of spontaneous emulsification takes place (84).

### 5.2. Dilution phases

The spontaneous curvature of the surfactant layer ranges through a number of feasible liquid crystalline phases during dilution of a SMEDS formulation. After appropriate dilution, the structure of droplet can move from a reversed spherical droplet to a reversed rod-shaped droplet, hexagonal phase, lamellar phase, cubic phase and various other structures until the formation of a spherical droplet again (84).

## 6. Design of Experimental (DOE) approaches

For the development of a suitable formulation, Design of Experimental (DOE) approaches have been widely utilized (32). DOE is a systematic method to determine the relationships between factors affecting a process and the output of that process (85). According to traditional one-factor-at-a-time approaches, the proportions of SMEDS constituents have been optimized. Nevertheless, these methods are inefficient, time-consuming, and labor-intensive. Moreover, the effect of individual constituent and their interactions are analyzed with the insufficient data obtained from these methods (32, 33). Hence, DOE approaches such as mixture, central composite, factorial, and Box–Behnken designs have been suggested to examine the influence of independent variables (input variables) on dependent variables (responses) as well as the interaction between independent variables (34–36). The mixture design is a popular response surface methodology because of its minimal variance correlated with the interpretation of coefficients in a model (37).

For formulation characterization and optimization, mixture designs are utilized when the overall amount of a composition is determined. The application of each component and its ratio in the formulation are rationalized in their scope (86, 87). The determination of suitable solvent–cosolvent combinations in liquid forms, the selection of diluent proportions in solid formulations, etc. are included in the common applications of mixture design in pharmaceutical technology. There are several various models of mixture experimental designs. The most commonly used ones include simplex centroid, simplex axial, extreme

vertex designs, and simplex lattice. Each of which is applied for a different purpose.

- Simplex centroid and simplex axial designs are used for the purpose of screening out the most important components among many different ones in a mixture.
- For the cases with constraints on one or more components, extreme vertex designs are selected to be used.
- A simplex lattice design can be useful when there are not such a large number of components, but a high order polynomial equation is required so that the response surface can be accurately described.

In the mixture experimental designs, the independent variables are the mixture components. Therefore, their levels are not independent. For example, if  $x_1, x_2, \dots, x_q$  indicate the proportions of  $q$  components of a mixture, then

$$0 \leq x_i \leq 1 \quad i = 1, 2, \dots, q \quad \sum_{i=1}^q x_i = 1 \quad (1)$$

These constraints are represented graphically in Figure 2 for  $q = 3$  components. With three components, the mixture space is a triangle with vertices correlating with formulations. The mixtures are 100 percent of a single component.

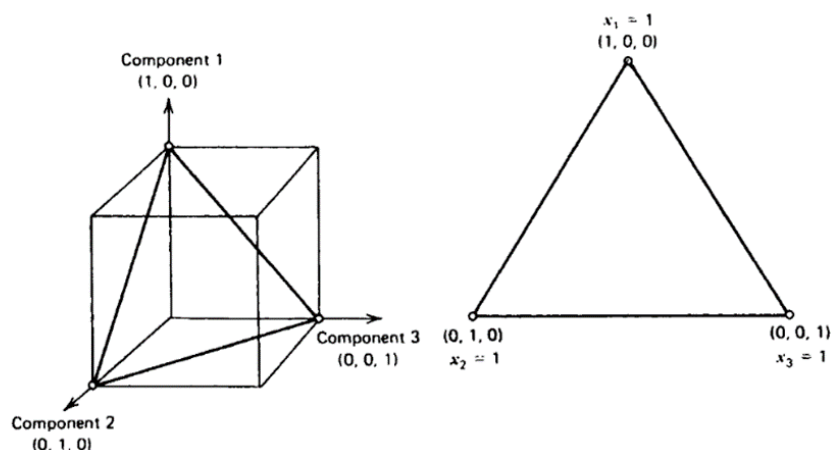


Figure 2. Three-component simplex region (88)

For optimization of the formulation, Bhattacharya et al. (38) successfully formulated docetaxel-loaded self-nanoemulsifying drug delivery system by the use of the mixture design. In this study, the independent variables were the concentration of oleic acid ( $X_1$ ), Tween<sup>®</sup> 80 ( $X_2$ ), and PEG 400 ( $X_3$ ) while the responses were emulsification time ( $Y_1$ ) and %drug release ( $Y_2$ ). Among total formulations, the optimized formulation was composed of oleic acid (42.37%), Tween<sup>®</sup> 80 (43.39%), and PEG 400 (14.21%). It was observed that the best formulation exhibited 19.71s emulsification time and 95.21% of drug release. Sandhu *et al.* (39) well designed a tamoxifen-loaded SMEDS by a mixture design. The optimized formulation showed increased cellular uptake and enhanced bioavailability.



## CHAPTER III

### MATERIALS AND METHODS

#### Materials

All chemicals and reagents used in this research work were of analytical grade purity.

- Astaxanthin (pharmacoepial grade), Hangzhou DayangChem Co., Ltd. (Hangzhou, P. R. China), Lot No. 20190625
- Medium chain triglyceride (MCT), Mead Johnson (Evansville, IN, USA), Lot No.02723
- Castor oil, United Dispensary, Co., Ltd. (Bangkok, Thailand), Lot No.100740
- Olive oil, United Dispensary, Co., Ltd. (Bangkok, Thailand), Lot No. 691383
- Soybean oil, United Dispensary, Co., Ltd. (Bangkok, Thailand), Lot No.990273
- Cremophor<sup>®</sup> RH 40, United Dispensary, Co., Ltd. (Bangkok, Thailand), Lot No. 497867
- Cremophor<sup>®</sup> EL, United Dispensary, Co., Ltd. (Bangkok, Thailand), Lot No. 849861
- Labrafil<sup>®</sup>, United Dispensary, Co., Ltd. (Bangkok, Thailand), Lot No. 161499
- Labrasol<sup>®</sup>, United Dispensary, Co., Ltd. (Bangkok, Thailand), Lot No. 32623
- Tween<sup>®</sup> 80, United Dispensary, Co., Ltd. (Bangkok, Thailand), Lot No. 809861

- Tween<sup>®</sup> 60, United Dispensary, Co., Ltd. (Bangkok, Thailand), Lot No. 708843
- Tween<sup>®</sup> 20, United Dispensary, Co., Ltd. (Bangkok, Thailand), Lot No. 769557
- Miglyol<sup>®</sup> 812, Sasol (Witten, Germany), Lot No. 070318
- Commercial astaxanthin soft gelatin capsule, Nutrex Hawaii, Co., Ltd. (Kailua-Kona, USA), Lot No. 03513

### **Equipment**

- 4-digital Analytical balance (A200S, Sartorius, Germany)
- 5-digital Analytical balance (X205T, Mettler-Toledo, Switzerland)
- Centrifuge (5810, Eppendorf, Germany)
- Shaking incubator (LSI-3016A, LabTech, Korea)
- Zetasizer (Nano-ZS, Malvern, UK)
- Transmission Electron Microscope (JEM-2100, JEOL, Japan)
- Ultraviolet-visible spectrophotometer (Cary 60, Agilent, US)

## Methods

### 1. Screening of the excipients

#### 1.1. Solubility studies of oils, surfactants, and co-surfactants

The test of AST solubility was completed in various oils (castor oil, olive oil, sunflower oil, medium chain triglyceride (MCT), Captex<sup>®</sup>, and Miglyol<sup>®</sup> 812) and surfactants (Cremophor<sup>®</sup> RH 40, Cremophor<sup>®</sup> EL, Labrafil<sup>®</sup>, Labrasol<sup>®</sup>, Tween<sup>®</sup> 80, Tween<sup>®</sup> 60, and Tween<sup>®</sup> 20). The solubility of astaxanthin was examined by the use of shake flask method in various excipient vehicles (89). An excess amount of astaxanthin was filled in each glass vial which comprised the amount of 5 ml of each vehicle. Then, in order to enhance the solubilizing of AST, vortex mixer was utilized to combine the resulted mixtures for 3 minutes. After that, a temperature-controlled shaking incubator (LSI-3016A, Lab Tech, Korea) was applied to achieve the equilibrium of the mixtures by keeping the mixtures at 150 revolutions per minute (rpm) for 72 hrs at  $37 \pm 0.5$  °C temperature. After that, the usage of the centrifuge at 5,000 rpm for 10 min leads to the removal of the insoluble precipitates. The filtration of the supernatant solution was then completed on the use of a 0.45  $\mu$ m nylon filter. Lastly, an ultraviolet-visible (UV–VIS) spectrophotometer was utilized at  $\lambda_{\text{max}}$  of 490 nm in order to accomplish the spectrophotometric analysis of all solutions.

## 1.2. Emulsification studies for selection of surfactants and co-surfactants

Depending on the percent transmittance, the screening of surfactants and co-surfactants was performed. 300 mg of each of the surfactants was added to 300 mg of chosen oil in order to assess emulsification ability of the surfactants. Then, homogenization was attained as a result of gently heating the mixture at 40-45 °C for 30 s. After that, distilled water was utilized to dilute 50 mg out of this mixture up to 50 mL so that fine emulsion was produced. Next in order, the resultant mixtures were allowed to stand for 2 hrs and the visual observation was done for the relative turbidity. By the use of distilled water as blank, the assessment of transmittance was also completed with the help of UV-VIS spectrophotometer at 650 nm. In the same way as mentioned in the screening process of surfactant, co-surfactant mixtures (100 mg), specific surfactant (200 mg) and chosen oil (300 mg) were then prepared and examined (90).



## 2. Construction of pseudoternary phase diagram

At ambient temperature, pseudoternary phase diagram was created by using the water-titration method to figure out the concentration of constituents for the predominant range of microemulsion (91). The chosen surfactant and co-surfactant were combined at five fixed proportions (1:1, 2:1, 3:1, 4:1, and 5:1 w/w) to set up various surfactant/co-surfactant mixtures ( $S_{\text{mix}}$ ). Then, it was followed by the addition of the selected oil to each  $S_{\text{mix}}$  at separate proportions (9:1, 8:2,

7:3, 6:4, 5:5, 4:6, 3:7, 2:8, and 1:9 w/w). Gentle swirling of the mixture was formed as a result of the incorporation of water to each mixture in 5% stepwise increments. For the transparency and turbidity, the visual observation of the mixture was started and recorded after every dropwise addition of water. At this stage, the proportions of oil,  $S_{\text{mix}}$ , and water were calculated in percentage. Pseudoternary phase diagrams were designed according to the microemulsion region, and these percentages by using Chemix School™ software. Pseudoternary phase diagrams were also constructed with AST by applying AST-oil mixture to examine the effect of AST addition on the microemulsion area.

### **3. Design of Experiment for optimization of AST-loaded SMEDS**

The compositions of AST-loaded SMEDS formulations were optimized by using the mixture design with the help of Minitab software (version 17.0; Minitab™ Inc., State College, PA, USA). The optimization of formulations is usually aimed for determining the levels of the variable that affect the selected responses from which a high-quality product may be developed. The three components were used as independent variables. The amount of oil ( $X_1$ ), surfactant ( $X_2$ ), and co-surfactant ( $X_3$ ) were set based on the results of the pseudoternary phase diagram. The sum of the amount of  $X_1$ ,  $X_2$ ,  $X_3$ , and AST were 100% for any experiment. Droplet size ( $Y_1$ ; nm), polydispersity index ( $Y_2$ ), zeta potential ( $Y_3$ ; mV), active ingredient content ( $Y_4$ ; %), and percentage of transmittance ( $Y_5$ ; %) were examined as the response variables to optimize the formulation. The independent variables and responses are shown in Table 1.

Table 1. Independent variables and responses in the mixture design.

<b>Independent variables</b>		
X <sub>1</sub>	Oil (LCT or MCT) content (%)	
X <sub>2</sub>	Surfactant content (%)	
X <sub>3</sub>	Co-surfactant content (%)	
<b>Responses</b>		<b>Acceptable range</b>
Y <sub>1</sub>	Droplet size (nm)	20-200 nm
Y <sub>2</sub>	PDI	0-1
Y <sub>3</sub>	Zeta potential (mV)	± 30 mV
Y <sub>4</sub>	Active ingredient content (%)	90-110%
Y <sub>5</sub>	Transmittance (%)	98-100%

The LCT-SMEDS region was designated at a boundary of 10-40% castor oil, 48-72% Cremophor<sup>®</sup> RH 40, and 12-18% Tween<sup>®</sup> 80. The MCT-SMEDS region was designated at a boundary of 10-30% castor oil, 35-45% Cremophor<sup>®</sup> RH 40, and 35-45% Tween<sup>®</sup> 80. For the experimental design studies, these ranges were considered the testing ranges. Appropriate design spaces were evolved by Minitab<sup>™</sup> Software version 17 shown in Table 2 and Table 3. After that, the experiments were performed, and the data were collected. The next step was the analysis of the data and interpretation of the results. Some responses have to be minimized or maximized to provide a product with desired characteristics.

Table 2. Formulation table for AST-loaded SMEDS containing castor oil.

Formulations	Components (%)			
	castor oil	Cremophor <sup>®</sup> RH 40	Tween <sup>®</sup> 80	AST
LCT-SMEDS <sub>1</sub>	33.9864	47.9808	17.9928	0.0400
LCT-SMEDS <sub>2</sub>	15.9936	71.9712	11.9952	0.0400
LCT-SMEDS <sub>3</sub>	9.9960	71.9712	17.9928	0.0400
LCT-SMEDS <sub>4</sub>	39.9840	47.9808	11.9952	0.0400
LCT-SMEDS <sub>5</sub>	36.9852	47.9808	14.9940	0.0400
LCT-SMEDS <sub>6</sub>	27.9888	59.9760	11.9952	0.0400
LCT-SMEDS <sub>7</sub>	12.9948	71.9712	14.9940	0.0400
LCT-SMEDS <sub>8</sub>	21.9912	59.9760	17.9928	0.0400
LCT-SMEDS <sub>9</sub>	24.9900	59.9760	14.9940	0.0400
LCT-SMEDS <sub>10</sub>	29.4882	53.9784	16.4934	0.0400
LCT-SMEDS <sub>11</sub>	20.4918	65.9736	13.4946	0.0400
LCT-SMEDS <sub>12</sub>	17.4930	65.9736	16.4934	0.0400
LCT-SMEDS <sub>13</sub>	32.4870	53.9784	13.4946	0.0400



Table 3. Formulation table for AST-loaded SMEDS containing MCT oil.

Formulations	Components (%)			
	MCT	Cremophor <sup>®</sup> RH 40	Tween <sup>®</sup> 80	AST
MCT-SMEDS <sub>1</sub>	29.9880	34.9860	34.9860	0.0400
MCT-SMEDS <sub>2</sub>	19.9920	34.9860	44.9820	0.0400
MCT-SMEDS <sub>3</sub>	9.9960	44.9820	44.9820	0.0400
MCT-SMEDS <sub>4</sub>	19.9920	44.9820	34.9860	0.0400
MCT-SMEDS <sub>5</sub>	24.9900	34.9860	39.9840	0.0400
MCT-SMEDS <sub>6</sub>	24.9900	39.9840	34.9860	0.0400
MCT-SMEDS <sub>7</sub>	14.9940	44.9820	39.9840	0.0400
MCT-SMEDS <sub>8</sub>	14.9940	39.9840	44.9820	0.0400
MCT-SMEDS <sub>9</sub>	19.9920	39.9840	39.9840	0.0400
MCT-SMEDS <sub>10</sub>	24.9900	37.4850	37.4850	0.0400
MCT-SMEDS <sub>11</sub>	19.9920	37.4850	42.4830	0.0400
MCT-SMEDS <sub>12</sub>	14.9940	42.4830	42.4830	0.0400
MCT-SMEDS <sub>13</sub>	19.9920	42.4830	37.4850	0.0400

All the responses were fitted to various models such as linear, quadratic, full cubic, and full quartic models. For the suggested models from the program, the results of goodness-of-fit statistical measures were then examined. The variation in a response variable was represented by  $R^2$  value. A greater  $R^2$  value demonstrates that all the variability of the dependent variables could be explained by the model. The average vertical distance of data values from the fitted regression line was indicated by the standard error (SE) of regression. To determine how well a given model fits the data, the predicted residual error sum of squares (PRESS) was used. A lower PRESS value indicated that the model has the better ability of the prediction level. Based on the values of  $R^2$ , SE,



and PRESS, the best fitted model was selected for each dependent variable.

For optimization, a target value and a limit value (upper or lower) were needed (92). When a response variable is set to be minimized, a value for the upper bound was required. In contrast, a value for the lower bound was necessary when a response variable is set to be maximized. Several researches on microemulsions as well as SMEDS recommended that the ideal diameter of a stable microemulsion should be 20-200 nm (23, 24). The smaller microemulsion particle size was followed by a larger interfacial surface area, which leads to promoting rapid absorption and enhanced bioavailability. The minimum experimental value of droplet size was obtained from our experimental run of mixture design. Therefore, for the optimization, both the target value and upper bound of droplet size ( $Y_1$ ) were the minimum experimental value (nm) and 200 nm, respectively. The numerical value of poly dispersity ranges from 0 to 1 (93). The uniform and narrow size distribution is provided by the low PDI value. Poly dispersity index ( $Y_2$ ) was set to be minimized, and a target value and upper bound of the minimum experimental value and 1, respectively, were selected. Zeta potential is important to measure because it governs the stability of microemulsion. For a better physical colloidal stability, a zeta potential value -30 mV or +30 mV is generally considered to have sufficient repulsive force (94). The electrostatic repulsion between the droplets was indicated by the high zeta potential value. Therefore, zeta potential ( $Y_3$ ) was set to be maximized. Active ingredient content ( $Y_4$ ) was set to be maximized. The selection of lower bound was performed depending on the lowest percentage of active ingredient content from our experimental run. USP has established that

the acceptable range of most compounded preparations is typically  $\pm 10\%$ , or within the range of 90% - 110% (95). Transparency of formulation was determined in the termed of percent transmittance (%T) greater than or equal to 98% indicates the high clarity of microemulsion (96). The value %transmittance ( $Y_5$ ) was set to be maximized, and a target value of 98% was selected. The lower bound was selected based on the lowest percentage of %transmittance from our experimental run.

After optimizing each response, the combination of all the defined dependent variables can be performed into one overall response by using the desirability function. In practice, the desirability function approach is a multi-response optimization technique. The desirability value lies between 0 and 1 and it represents the closeness of a response to its ideal value. From the program, the optimized formulation ratios of independent variables and the predicted values of responses were provided. These values were supported by a desirability function value.

To validate the mixture design model, the SMEDS of the optimized formulations were then prepared, and the values of experimentally measured response were compared with the values predicted from the program. The reliability and accuracy of the estimation by using desirability functions were evaluated by calculating the values of prediction errors. If the measured values were close to their predicted values, the prediction error (%) are small, suggesting that the mixture experimental design successfully optimized the SMEDS formulation. The prediction errors (%) were calculated by using the following equation:

$$\text{Prediction error (\%)} = \frac{\text{measured value} - \text{predicted value}}{\text{measured value}} \times 100 (\%)$$

### 3.2. Preparation of SMEDS

Thirteen formulations for each oil were prepared. The determination upon the quantity to be taken for excipients rely on the microemulsification area in the phase diagram. AST was precisely measured in weight and dissolved in oil. Then, using a water bath, the mixture was warmed at 37 °C. The mixture was later combined with surfactant and co-surfactant and then stirred with a magnetic bar for 10 min. Furthermore, the sonication of the formulations was done at 40 °C for 15 min (91).

### 3.3. Droplet size and poly dispersity index (PDI)

The performance of emulsion was determined by the emulsion droplet size in terms of rate and extent of drug release, as well as absorption. The information about size distribution can be provided by the examination of PDI. The uniform and narrow size distribution is suggested by the low value of PDI. In a glass beaker, about 0.1 ml of each SMEDS formulation and 25 ml of distilled water was constantly stirred for dilution (1:250) (38). The resultant emulsion was then subjected to particle size analysis. The droplet size distribution, polydispersity index of the resultant microemulsion were determined by dynamic light scattering (Malvern Zetasizer™, UK). The preparation was transferred to a cuvette and measured with a fixed angle of 90°. After equilibrium, the particle (droplet) size was recorded. All studies were repeated in triplicate.

### 3.4. Zeta-potential

The zeta potential value specifies the physical stability of diluted emulsion. It is the measurement of the electric charge at the surface of the particles. The values were examined by determining the electrophoretic mobility of the particle. It was determined by using Zetasizer™ (Malvern Zetasizer™, UK). The suitable dilution of the sample was performed with distilled water (1:250) and the diluted preparation was placed in a disposable zeta cell (38). All samples were measured in triplicate. The results were indicated as mean  $\pm$  SD.

### 3.5. Active ingredient content

Solvent was used to extract AST in emulsion samples. The samples were appropriately diluted with organic solvent (dichloromethane: methanol = 1:4 v/v). The preparation of samples was performed in triplicate and absorbances were measured after suitably diluting the samples. An ultraviolet-visible spectrophotometer was utilized in the quantification of astaxanthin at 480 nm (61). The solvent mixture of dichloromethane and methanol was used as a blank. From a calibration plot, the calculation of AST content in each formulation was performed.

### **3.6. %Transmittance**

When the value of percentage transmittance is near to 100%, the clear and transparent microemulsion formation is provided (97). The transparency of SMEDS formulation was examined spectrophotometrically at the wavelength of 650 nm after appropriate dilution of formulation with distilled water (1:250). The water was kept as blank.

## **4. Characterization of the optimized formulations**

### **4.1. Visual observation**

For self-microemulsifying properties, the visual determination of the optimized formulations was completed. The formulations were subjected to dilute with distilled water (1:250) and followed by stirring diluted microemulsions for 1 min and stored up to 24 hrs. After that, any signs of precipitation and phase separation were visually detected (44).

### **4.2. Self-emulsification time**

To examine the effectiveness of self-microemulsification, each optimized formulation was subjected to dilute with distilled water (1:250) and stirred constantly at 100 rpm and at  $37 \pm 0.5^\circ\text{C}$  (98). After that the time taken which is needed to form microemulsion was recorded.

#### **4.3. Refractive index measurement**

The value of refractive index demonstrated that the formulation is transparent in nature. If refractive index value of the formulation is similar to that of water (1.333), then formulation have transparency. This measurement was done by using refractometer (Mettler Toledo, Thailand). The dilution of the optimized formulations was performed with distilled water (1:250). One drop of the diluted formulation was placed on the slide and compared with the refractive index value of water (99).

#### **4.4. Transmission electron microscopy (TEM)**

The optimized SMEDS formulations were determined for morphological analysis by using TEM (TEM; JEOL USA JSM-6700F) as an imaging aid. The formulations were diluted and a single drop of diluted sample was placed on the holey film grid and stained with a 2% aqueous solution of phosphotungstic acid, and allowed to dry before being observed under the electron microscope (99). The digital microscopic camera recorded the micrographs.

#### **4.5. Freeze-thaw stability studies**

The dilution of optimized formulations was performed with distilled water (1: 250). The droplet size, PDI, zeta potential, and the active ingredient content of the diluted microemulsions were examined for instability problems (100, 101). The freeze-thaw test was performed

three cycles in a temperature range of  $-20\text{ }^{\circ}\text{C}$  to  $25\text{ }^{\circ}\text{C}$ . For each temperature, the self-microemulsion samples were stored at least 48 hrs.

#### 4.6. *In vitro* release studies

With the use of a dialysis bag diffusion technique, *in vitro* AST release study was conducted (102). HCl/NaCl buffer pH 1.2, acetate buffer pH 4.5, and phosphate buffer pH 7.4 were used as the dissolution media. Before the experiment, the dialysis bags were hydrated overnight. In dialysis bags, the optimized formulations were positioned. The dialysis bags were immersed in 900 mL of medium, maintained at  $37\text{ }^{\circ}\text{C}$  and at 100 rpm. The sample (10 mL) was collected at predetermined time intervals of 5 mins, 10 mins, 15 mins, 30 mins, 1 hr, 2 hrs, 4 hrs, and 8 hrs. Then, it was refilled with similar volume of tested medium. The ultraviolet-visible spectrophotometer was used for the analysis of the AST content in the aliquots.

#### Statistical Analysis

All quantitative data was expressed as means  $\pm$  standard deviation (SD). The p-values were calculated with one-way ANOVA using statistical software (SPSS<sup>TM</sup>, version 16.0) with  $p < 0.05$  considered statistically significant. The results obtained from the *in vitro* dissolution experiment were analyzed statistically by using *t*-test.

## CHAPTER IV

### RESULTS AND DISCUSSION

#### 1. Screening of the excipients

##### 1.1. Solubility studies of oils, surfactants, and co-surfactants

For successful formulations, proper solubility of active substance in SMEDS excipients is crucial so that active compound precipitation can be avoided before undergoing self-emulsification in the gut (103-105). The capability of the active substance loading of the oil phase is the consideration aspect concerning the choice of excipients for the SMEDS formulation (103). The increase in active compound (AST) solubility in the oil leads to the lowering in the requirements of surfactant and co-surfactant in the SMEDS formulation, leading to minimization of their toxic effects (105). The most common oil used in lipid-based formulations to dissolve hydrophobic drugs or substances are vegetable oils because they are safe, digestible, and absorbable (106). In our work, the test of AST solubility was completed in different oils including castor oil, sunflower oil, olive oil, medium chain triglyceride (MCT), Captex<sup>®</sup>, and Miglyol<sup>®</sup> 812. Figures 3 and 4 displayed the solubility of AST in different oils and surfactants/co-surfactants, respectively. In Figure 3, compared to other oils, castor oil pointed out the greatest solubilizing capacity for astaxanthin. Data also suggest that AST has more solubility in medium chain triglycerides (MCT, Captex<sup>®</sup>, and Miglyol<sup>®</sup> 812) rather than long chain triglycerides (sunflower oil and olive oil except castor oil). This may be due to LCT have lesser ester content per gram than MCT (107). Moreover, greater solubility of the active substance in MCT than in LCT may be related to the shorter chain length of MCT, which



allocates ease of solubilizing capacity of the lipophilic compounds, because of higher surface area (30). In contrast, some studies reported that LCT possess greater solubilization than MCT for particularly lipophilic compounds (108-110). This is because the solubilization of oil for lipophilic compounds rises with the chain length of oil (111). Among various long chain triglycerides used, castor oil ( $155.87 \pm 1.63 \mu\text{g/ml}$ ) exhibited highest AST solubilization capacity, while among medium chain triglycerides, the highest solubility of the AST was observed in MCT ( $91.1 \pm 1.98 \mu\text{g/ml}$ ). Based on the solubility data of AST, one medium (MCT oil) and one long chain triglyceride (castor oil) which has the highest solubility result were selected for further investigation.

In this study, all tested surfactants were non-ionic ones; therefore, they are considered safe and biocompatible (112). All the surfactants selected for solubility determination in this research have being commonly used in lipid-based formulations. Compared to other surfactants investigated in this study, astaxanthin has the highest solubility in Tween<sup>®</sup> 80 (HLB 15), secondly in Cremophor<sup>®</sup> RH 40 (HLB 15), and then followed by Tween<sup>®</sup> 20 (HLB 16.7), Labrafil<sup>®</sup> (HLB 4), and Cremophor<sup>®</sup> EL (HLB 13.5) as presented in Figure 4. According to their efficiency of emulsification, the ultimate selection of different surfactants was further assured.

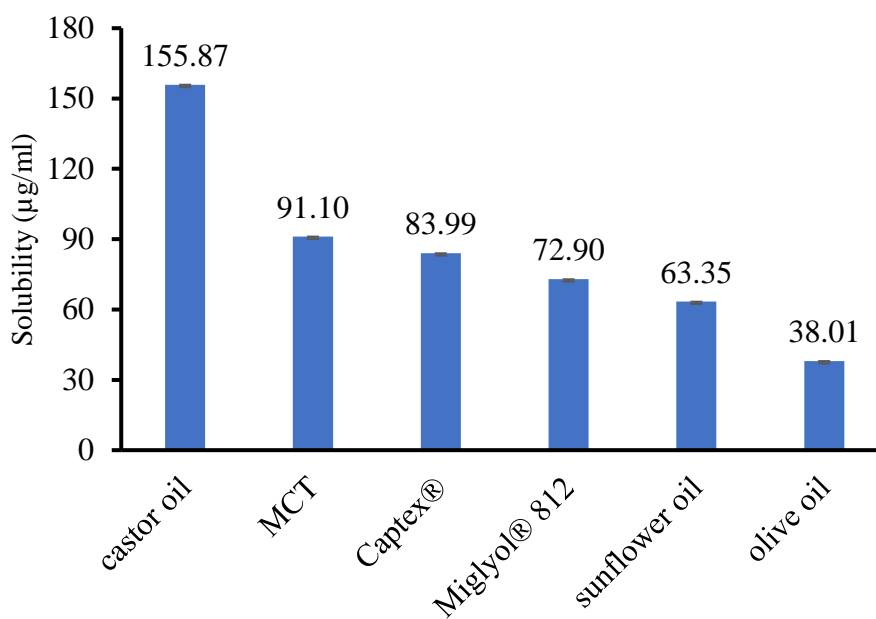


Figure 3. Solubility of astaxanthin in different oils

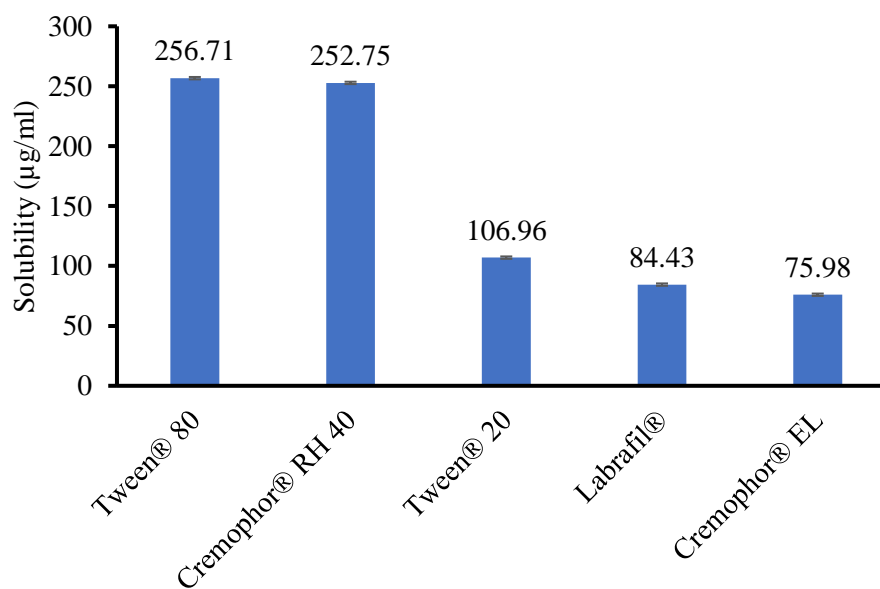


Figure 4. Solubility of astaxanthin in different surfactants

## 1.2. Emulsification studies for selection of surfactants and co-surfactants

The emulsifying efficiency of the surfactant is an important factor although the active ingredient solubility is a major standard in the selection of the SMEDS ingredients (113). Hence, regarding the chosen oil, the test on the emulsifying efficiency of different surfactants was performed. Grading standards were introduced to determine the capacity for self-microemulsification (114), as shown in Table 4. Emulsifying activity is revealed with the capacity of surfactants to protect the oil-water interface produced by homogenization, thus lowering the interfacial tension (115). Therefore, the more active the surfactants, the more the interfacial tension is reduced. The assessment of the emulsification efficiency was done by the help of its percentage UV transmittance. Optical clarity is similar to high transmittance because the scattering of opalescent dispersions may direct towards incident radiation to greater degree by comparison with transparent dispersions. The scattering of light is the attribute of the light intensity passing through such dispersion because optical homogeneities are absent in the medium (116). Therefore, for prediction of a relative droplet size, percentage transmittance may be applied. Table 5 shows the list of the percentage transmittance values. Although, hydrophilic-lipophilic balance (HLB) value of the surfactants utilized in this research were  $\geq 4$ , there were significant variation in their capacity to emulsify oils. Among all tested surfactants, highest %transmittance as shown in Table 5 was reported for Cremophor<sup>®</sup> RH 40 with both the castor oil and MCT showing the highest emulsification efficiency. This may be due to the distinction in the structure and chain length of the surfactant (117). Cremophor<sup>®</sup> RH 40 has branched alkyl

structures which enhance the penetration capacity into the oil phase than the linear chain alkyl structures, so leading to the formation of self-microemulsion efficiently (118). Moreover, it was observed that Cremophor<sup>®</sup> EL showed lower emulsifying efficiency than Cremophor<sup>®</sup> RH 40. This is because the ethoxy content per mole of castor oil is different. 35 moles of ethoxy content are present in Cremophor<sup>®</sup> EL, while 40 moles of ethoxy content are present in Cremophor<sup>®</sup> RH 40 (119). Owing to the better emulsification efficiency, Cremophor<sup>®</sup> RH 40 which also has higher solubility of AST was selected as a surfactant for next investigation.

Table 4. Evaluation standard for self-microemulsification efficiency.

Grade	Emulsification capacity	% Transmittance	Appearance
A	Excellent	>90	clear and transparent
B	Good	80–90	Slightly less clear and bluish white
C	Fair	50–80	Milky or grayish white
D	Poor	<50	No homogeneity

Table 5. Emulsification Efficiency of Various Surfactants.

Oil	Surfactant	%Transmittance	Emulsification activity
castor oil	Tween <sup>®</sup> 80	49.09 ± 0.75	D
	Cremophor <sup>®</sup> RH 40	93.21 ± 0.11	A
	Tween <sup>®</sup> 20	66.83 ± 0.48	C
	Labrafil <sup>®</sup>	64.20 ± 1.70	C
	Cremophor <sup>®</sup> EL	87.79 ± 0.06	B
MCT	Tween <sup>®</sup> 80	62.61 ± 1.02	C
	Cremophor <sup>®</sup> RH 40	96.81 ± 1.04	A
	Tween <sup>®</sup> 20	51.84 ± 1.45	C
	Labrafil <sup>®</sup>	13.03 ± 1.74	D
	Cremophor <sup>®</sup> EL	50.39 ± 1.14	C

\* Values are expressed as mean ± S.D., n = 3.

To enhance the absorption, dispersibility, and stability of the formulation, co-surfactant was added to the surfactant-containing formulations (120). Co-surfactants are utilized in SMEDS formulations for increasing the solubility of active substances and promoting the dispersibility of the surfactants in the oil, so enhancing the uniformity and stability of the formulations (121). Surfactants and co-surfactant molecules are dominantly adsorbed at the interfaces. Therefore, the interfacial surface tension is decreased and a mechanical barrier is provided to prevent coalescence and the stability of the formulations is improved (122). Table 6 presents relative capacity of co-surfactants to enhance emulsification efficiency of surfactants. Tween<sup>®</sup> 20 and Labrafil<sup>®</sup> have very less %transmittance and could not also form clear solution with chosen oils and surfactant. Compared to other tested co-surfactants, Tween<sup>®</sup> 80 exhibited good emulsification efficiency (99.80% ± 0.06%) with castor oil and Cremophor<sup>®</sup> RH 40 mixture, while it also

increased spontaneity of microemulsion formation and exhibited clear solution along with good water uptake capacity, with MCT and Cremophor<sup>®</sup> RH 40 mixture, showing maximum transmittance ( $99.82\% \pm 1.13\%$ ). This may be due to penetration of the oils to a greater extent into the hydrocarbon chain of Tween<sup>®</sup> 80 resulting in reduction of the interfacial surface tension and enhancement of microemulsification spontaneously. Moreover, Tween<sup>®</sup> 80 also showed the highest solubility (Figure 4) for astaxanthin. Therefore, for both oils, Tween<sup>®</sup> 80 was selected as co-surfactant for next studies.

Table 6. Emulsification Efficiency of Various Co-surfactants.

Oil	Surfactant	Cosurfactant	% Transmittance	Emulsifying activity
castor oil	Cremophor <sup>®</sup> RH 40	Tween <sup>®</sup> 80	$99.80 \pm 0.06$	A
		Tween <sup>®</sup> 20	$59.14 \pm 0.09$	C
		Labrafil <sup>®</sup>	$44.96 \pm 0.33$	D
MCT	Cremophor <sup>®</sup> RH 40	Tween <sup>®</sup> 80	$99.82 \pm 1.13$	A
		Tween <sup>®</sup> 20	$49.57 \pm 1.20$	D
		Labrafil <sup>®</sup>	$64.48 \pm 1.25$	C

\* Values are expressed as mean  $\pm$  S.D, n = 3.

## 2. Pseudoternary phase diagram

In stomach, there is differing liquid volume at various times. Therefore, there should be a formation of emulsion, preferably microemulsion, without precipitation of drug, when the formulation is diluted with distilled water. It was observed that emulsification capacity is constantly related to the amount of oil, water, surfactant, and/or co-surfactant (123). The pseudoternary phase diagram was developed for

determining the self-microemulsifying area and for calculating the concentrations of oil, surfactant, and co-surfactant which leads to stable SMEDS. In order to create the phase diagram, the castor oil or MCT oil, Cremophor® RH 40, and Tween® 80 were defined as oil, surfactant, and co-surfactant, respectively, depending on the solubility and emulsification studies. When titrated with water under mild agitation, SMEDS forms microemulsion with less than 200 nm. It is a thermodynamic spontaneous emulsification process as the energy needed for the formation of microemulsion is very low (124). The surfactant facilitates this process. A layer was formed around the oil globule by the presence of surfactant in such a way polar head pull out the water phase and nonpolar tail lies toward lipid phase, resulting in reducing the surface energy between the oil-water interface (125). Moreover, the mixture of surfactant and co-surfactant ( $S_{\text{mix}}$ ) ratio is an another important factor in the microemulsion formation because mechanical barrier to coalescence is provided by adsorbing the surfactant and co-surfactant at interface (126). The co-surfactant is also important for the formation of microemulsion with an appropriate concentration range. Due to its high-water solubility, becoming less stable system of microemulsion will be caused by an excess amount of co-surfactant. This may lead to increasing the droplet size owing to the expanding interfacial film (103). Therefore, the pseudoternary phase diagrams at five various  $S_{\text{mix}}$  ratios (1:1, 2:1, 3:1, 4:1, and 5:1) were developed for each oil by using water-titration method. The visual observation was performed and recorded after each 5% increment of the water to the mixture of oil and  $S_{\text{mix}}$ . At the same time, the proportions of oil and  $S_{\text{mix}}$  were also calculated. By using Chemix School™ software, a separate

diagram was developed for each  $S_{\text{mix}}$  ratio and visual observation was also recorded for each diagram (APPENDIX A). Based on the visual observations, only microemulsion points were plotted by using Chemix School™ software because only microemulsion region is of interest for the development of SMEDS formulations. In the pseudoternary phase diagram, the black region represented the self-microemulsification area.

Comparing to the other ratios for the SMEDS containing castor oil (LCT-SMEDS), a comparatively largest microemulsion region was produced by the  $S_{\text{mix}}$  proportion of 4:1 as presented in Figure 5 a-e. According to Figure 6 a-e, for the SMEDS formulations containing MCT (MCT-SMEDS), microemulsion formation was highest at  $S_{\text{mix}}$  1:1 ratio. It was also showed that the enhancement of  $S_{\text{mix}}$  ratio lead to the increase in the microemulsion formation area for LCT-SMEDS except 5:1 ratio. Moreover, phase separation was detected after several hours at a 5:1 ratio of LCT-SMEDS. In contrast, for MCT-SMEDS, it was also observed that the enhancement of  $S_{\text{mix}}$  ratio lead to the decrease in the microemulsion formation area. Another observation was that poor microemulsion was formed with high concentration of oil in all cases. This may be due to very less amount of water entrapment capacity upon dilution (127).

The effect of active substance addition was examined on the boundaries of microemulsion region by the repetition of the water-titration procedure in the presence of AST for the best ratio of 4:1 for LCT-SMEDS and 1:1 for MCT-SMEDS. According to Figure 7 a-b and Figure 8 a-b, it was mentioned that the addition of the AST into the blank SMEDS formulation presented no significant effect on the microemulsion regions of both LCT-SMEDS and MCT-SMEDS.



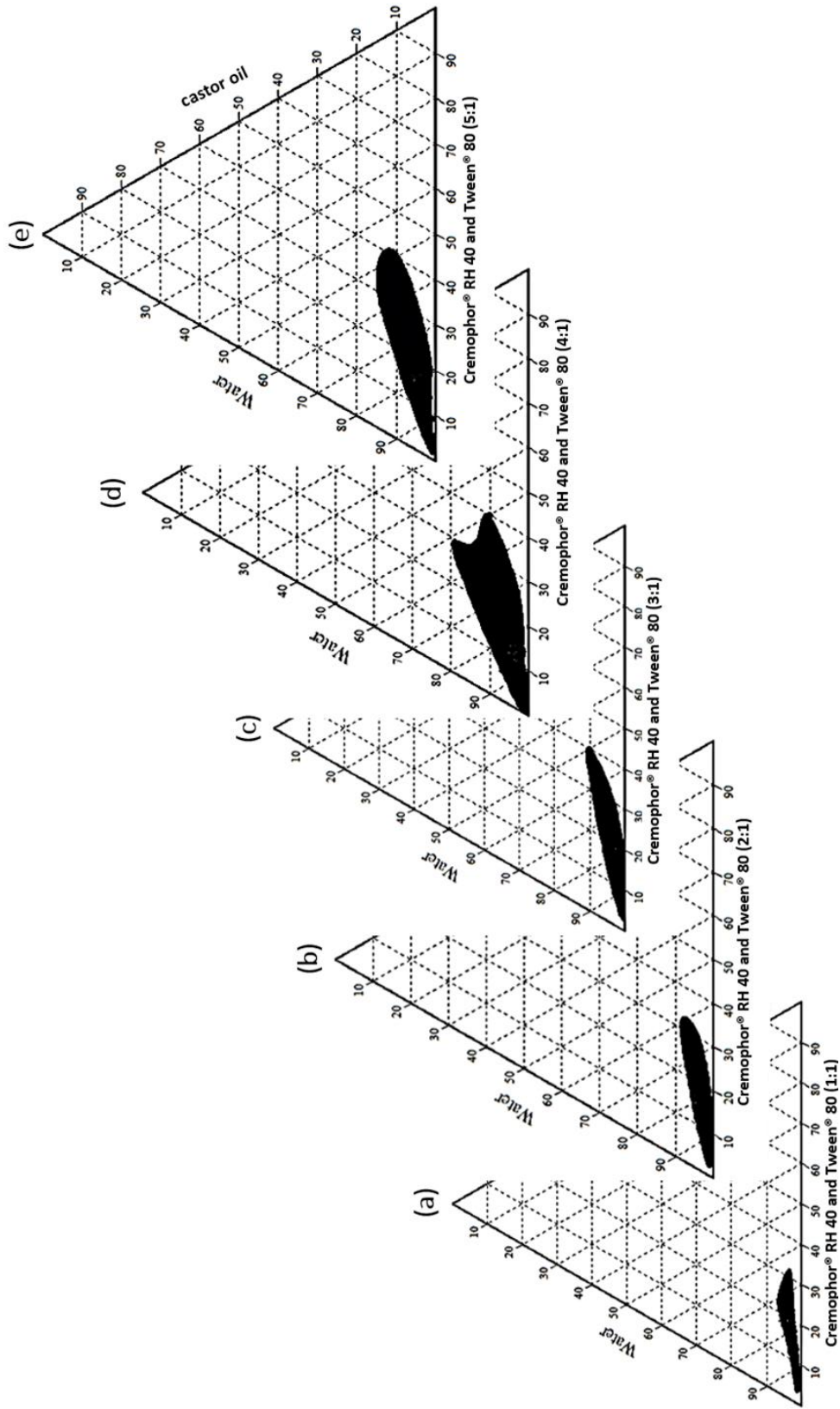


Figure 5. Pseudoternary phase diagram with the following components: castor oil, Cremophor® RH 40, and Tween® 80. Surfactant and cosurfactant ratio of (a) 1:1, (b) 2:1, (c) 3:1, (d) 4:1, and (e) 5:1

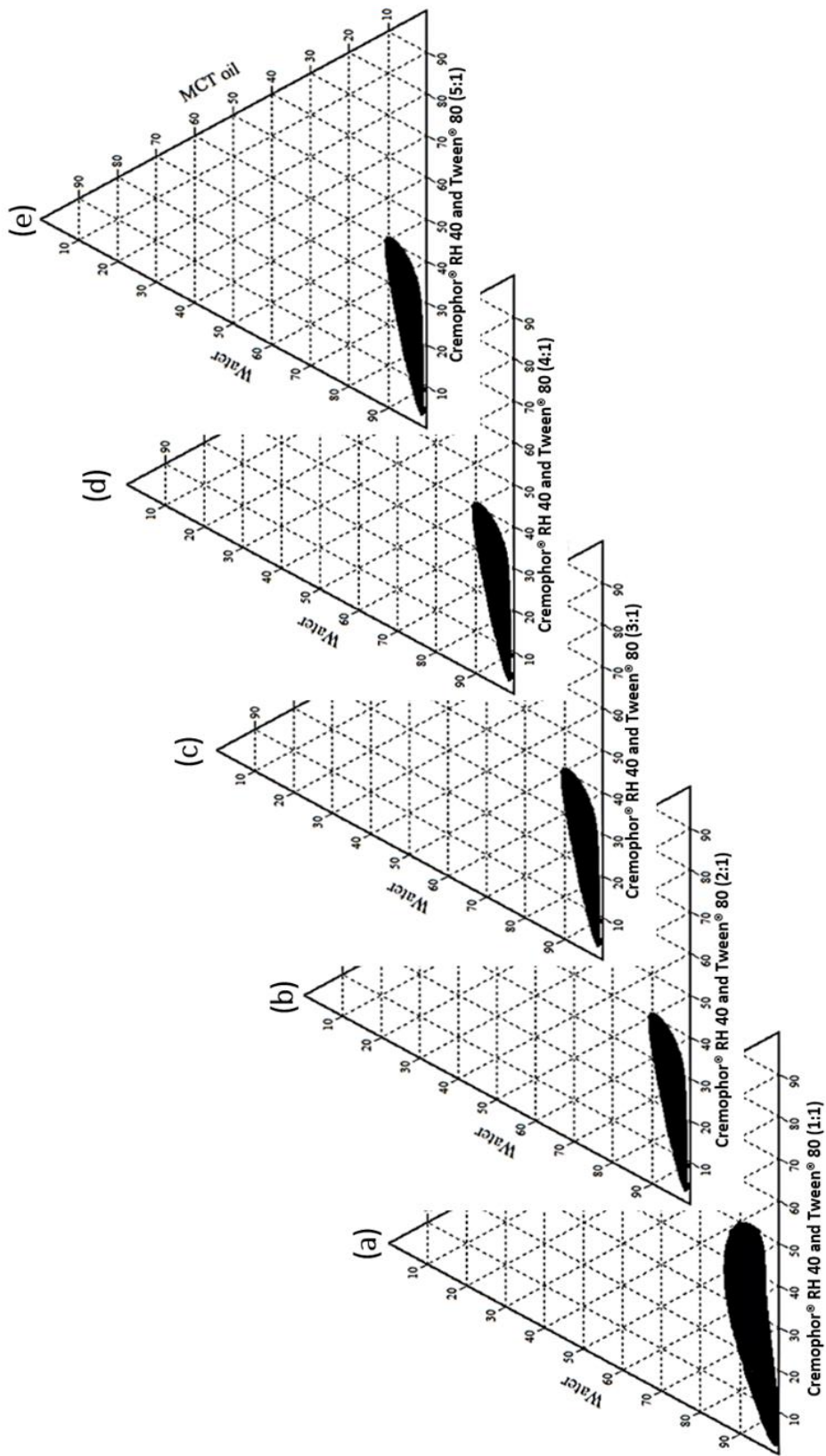


Figure 6. Pseudoternary phase diagram with the following components: MCT oil, Cremophor® RH 40, and Tween® 80. Surfactant and cosurfactant ratio of (a) 1:1, (b) 2:1, (c) 3:1, (d) 4:1, and (e) 5:1

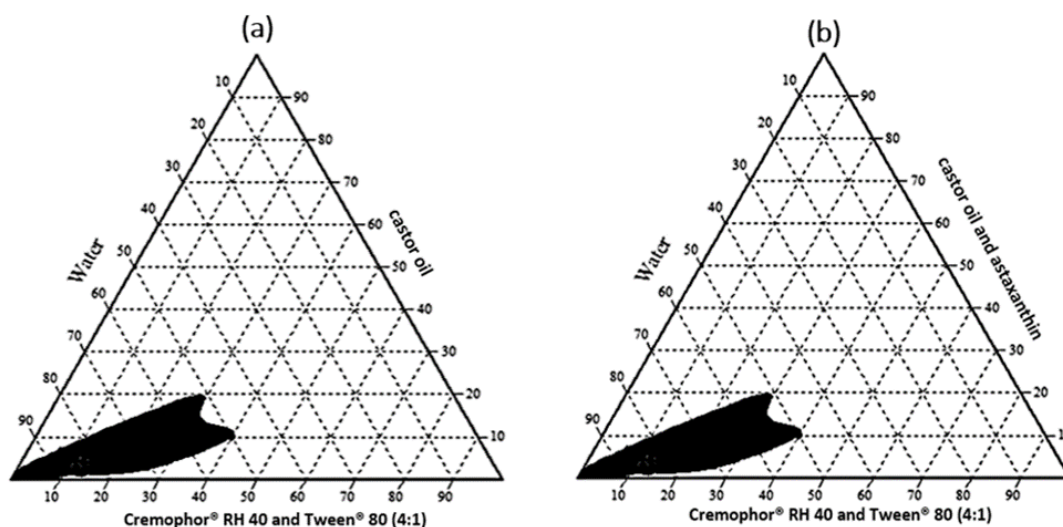


Figure 7. Pseudoternary phase diagrams constructed (a) in absence and (b) in presence of astaxanthin respectively using castor oil as the lipid phase.

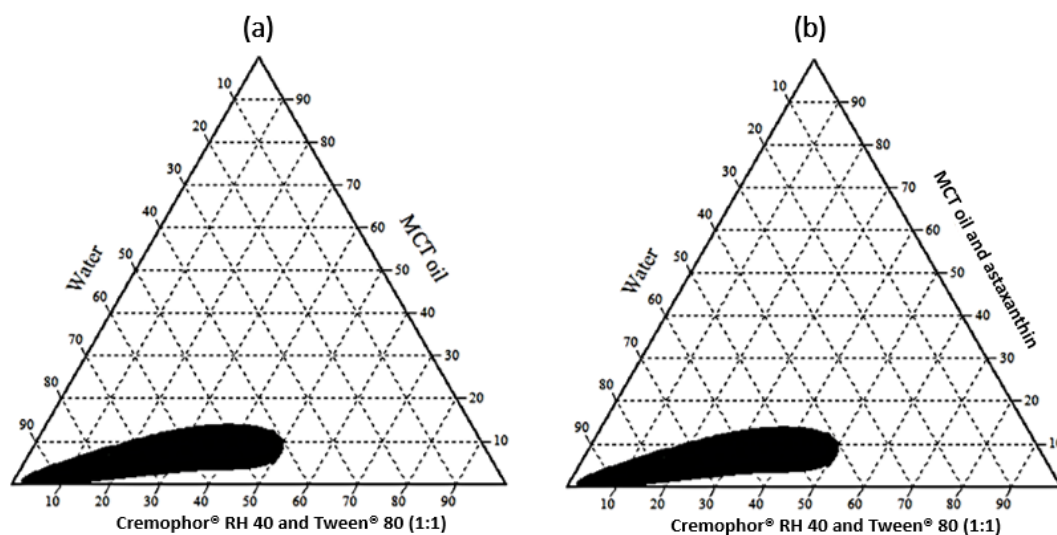


Figure 8. Pseudoternary phase diagrams constructed (a) in absence and (b) in presence of astaxanthin respectively using MCT oil as the lipid phase.

### **3. Design of Experiment for optimization of AST-loaded SMEDS**

#### **3.1. Statistical analysis by using mixture experimental design**

By the use of Minitab software (Minitab Inc, State College, PA, USA), a mixture design technique was applied for the optimization of the AST-loaded SMEDS composition. In the mixture design, the responses (dependent variables) were expected to rely on the ratios of the formulation excipients. It was also observed that the primary factors effecting the *in vitro* dispersion of SMEDS preparations were considered to be the quantity of oil, surfactant, and co-surfactant (128, 129). Hence, the input variables were defined by these factors, and their experimental design space was chosen depending on the results of pseudoternary phase diagram. For the input variables  $X_1$ ,  $X_2$ , and  $X_3$  respectively, castor oil, Cremophor<sup>®</sup> RH 40, and Tween<sup>®</sup> 80 were stated for LCT-SMEDS, while MCT, Cremophor<sup>®</sup> RH 40, and Tween<sup>®</sup> 80 were specified for MCT-SMEDS. A separate experimental design space was developed for each SMEDS. In order to enhance the oral absorption of poorly water-soluble AST, five response factors, which are critical properties of SMEDS, were selected: droplet size ( $Y_1$ ; nm), PDI ( $Y_2$ ), zeta potential ( $Y_3$ ; mV), active ingredient content ( $Y_4$ ; %), and percentage of transmittance ( $Y_5$ ; %). As shown in Table 7 and Table 8, the range of independent variables used to develop design space were summarized.

Table 7. Range of independent variables of LCT-SMEDS in the mixture design.

Independent variables		Range (%)	
		Minimum	Maximum
X <sub>1</sub>	castor oil (% oil)	10	40
X <sub>2</sub>	Cremophor® RH 40 (% surfactant)	48	72
X <sub>3</sub>	Tween® 80 (% co-surfactant)	12	18

Table 8. Range of independent variables of MCT-SMEDS in the mixture design.

Independent variables		Range (%)	
		Minimum	Maximum
X <sub>1</sub>	MCT (% oil)	10	30
X <sub>2</sub>	Cremophor® RH 40 (% surfactant)	35	45
X <sub>3</sub>	Tween® 80 (% co-surfactant)	35	45

As stated in the mixture design, thirteen experimental runs were developed for each SMEDS containing the castor or MCT oil. As shown in Table 9, for LCT-SMEDS, Y<sub>1</sub> ranged from 20.17 to 128.74 nm, Y<sub>2</sub> from 0.20 to 0.37, and Y<sub>3</sub> from -8.34 to -12.90 mV, Y<sub>4</sub> from 84.55 to 99.71 %, and Y<sub>5</sub> from 75.72 to 98.57 %. For MCT-SMEDS, Y<sub>1</sub> ranged from 22.01 to 33.2 nm, Y<sub>2</sub> from 0.09 to 0.43, and Y<sub>3</sub> from -9.91 to 14.9 mV, Y<sub>4</sub> from 90.11 to 96.69 %, and Y<sub>5</sub> from 97.43 to 98.8 % as mentioned in Table 10. The various models were used to be fitted all the responses. Table 11 and Table 12 demonstrated the outcomes of goodness-of-fit for these models of LCT-SMEDS and MCT-SMEDS.

The average vertical distance of the data from the fitted regression line was pointed out by the standard error (SE) of regression. The data fitting capacity of a given model was determined by the predicted residual error sum of squares (PRESS). The lower value of PRESS leads to the better ability of the model prediction. The variation in a response variable was represented by  $R^2$  value. The model with higher  $R^2$  value explained all the variability of the response. According to SE, PRESS, and  $R^2$  values, the selection of the best fitted model was performed for each of the five responses.

According to Table 11,  $Y_1$ ,  $Y_2$ ,  $Y_3$ ,  $Y_4$ , and  $Y_5$  of LCT-SMEDS were stated to be fitted by quadratic, linear, quadratic, linear, and full cubic mathematical models respectively. The linear, quadratic, linear, linear, and full cubic mathematical models were recommended from the program to fit  $Y_1$ ,  $Y_2$ ,  $Y_3$ ,  $Y_4$ , and  $Y_5$  of MCT-SMEDS respectively as shown in Table 12. Due to the indication of a sequential p value of  $< 0.05$ , the model terms of LCT-SMEDS and MCT-SMEDS were significant. In addition, the model fitting was also indicated by a lack of fit p-value which is greater than 0.1. For each model,  $R^2$  and adjusted  $R^2$  values revealed the multiple regression and analysis of the regression. In this study, the values of  $R^2$  for all responses were higher than 90%. Furthermore, the fit was sufficient in this research as adjusted  $R^2$  values were similar to  $R^2$  values.

Table 9. Mixture experimental design for optimizing LCT-SMEDS formulation and the associated response data.

Formulation	Independent variables (%)				Dependent variables (Responses)				
	castor oil (%; X <sub>1</sub> )	Cremophor® RH 40 (%; X <sub>2</sub> )	Tween®80 (%; X <sub>3</sub> )	Droplet size (nm; Y <sub>1</sub> )	PDI (Y <sub>2</sub> )	Zeta potential (mV; Y <sub>3</sub> )	Active ingredient content (%; Y <sub>4</sub> )	% Transmittance (%; Y <sub>5</sub> )	
LCT-SMEDS <sub>1</sub>	33.9864	47.9808	17.9928	99.93 ± 1.88	0.36 ± 0.07	-11.51 ± 2.96	86.97 ± 0.58	81.67 ± 4.03	
LCT-SMEDS <sub>2</sub>	15.9936	71.9712	11.9952	24.36 ± 0.18	0.29 ± 0.10	-10.41 ± 3.47	97.47 ± 2.27	98.35 ± 0.08	
LCT-SMEDS <sub>3</sub>	9.9960	71.9712	17.9928	20.17 ± 0.37	0.22 ± 0.01	-9.45 ± 0.77	99.71 ± 0.37	98.57 ± 0.15	
LCT-SMEDS <sub>4</sub>	39.9840	47.9808	11.9952	128.74 ± 4.82	0.28 ± 0.01	-11.43 ± 1.62	84.55 ± 0.49	75.72 ± 1.04	
LCT-SMEDS <sub>5</sub>	36.9852	47.9808	14.9940	122.09 ± 3.31	0.32 ± 0.08	-11.17 ± 1.42	85.27 ± 0.92	78.48 ± 0.57	
LCT-SMEDS <sub>6</sub>	27.9888	59.9760	11.9952	35.00 ± 1.64	0.23 ± 0.04	-12.90 ± 1.48	92.23 ± 0.88	97.41 ± 0.50	
LCT-SMEDS <sub>7</sub>	12.9948	71.9712	14.9940	22.91 ± 0.12	0.34 ± 0.01	-12.33 ± 2.03	98.14 ± 0.98	98.50 ± 0.36	
LCT-SMEDS <sub>8</sub>	21.9912	59.9760	17.9928	27.70 ± 0.47	0.20 ± 0.07	-11.30 ± 1.91	94.48 ± 0.72	98.11 ± 0.12	
LCT-SMEDS <sub>9</sub>	24.9900	59.9760	14.9940	25.57 ± 4.95	0.37 ± 0.03	-11.17 ± 0.98	93.45 ± 1.98	98.07 ± 0.19	
LCT-SMEDS <sub>10</sub>	29.4882	53.9784	16.4934	65.21 ± 3.2	0.34 ± 0.05	-9.19 ± 3.13	90.09 ± 1.16	94.88 ± 1.39	
LCT-SMEDS <sub>11</sub>	20.4918	65.9736	13.4946	26.96 ± 0.61	0.31 ± 0.02	-9.06 ± 0.94	95.58 ± 1.71	98.15 ± 0.40	
LCT-SMEDS <sub>12</sub>	17.4930	65.9736	16.4934	26.07 ± 0.96	0.33 ± 0.01	-8.34 ± 2.14	96.17 ± 0.82	98.31 ± 0.53	
LCT-SMEDS <sub>13</sub>	32.4870	53.9784	13.4946	76.04 ± 2.12	0.30 ± 0.02	-8.51 ± 1.17	87.73 ± 1.16	92.28 ± 2.16	

Table 10. Mixture experimental design for optimizing of MCT-SMEDS formulation and the associated response data.

Formulation	Independent variables (%)			Dependent variables (Responses)				
	MCT (%; X <sub>1</sub> )	Cremophor® RH 40 (%; X <sub>2</sub> )	Tween® 80 (%; X <sub>3</sub> )	Droplet size (nm; Y <sub>1</sub> )	PDI (Y <sub>2</sub> )	Zeta potential (mV; Y <sub>3</sub> )	Active ingredient content (%; Y <sub>4</sub> )	% Transmittance (%; Y <sub>5</sub> )
MCT-SMEDS <sub>1</sub>	29.9880	34.9860	34.9860	33.20 ± 0.54	0.09 ± 0.00	-14.90 ± 0.76	90.11 ± 1.77	97.43 ± 0.45
MCT-SMEDS <sub>2</sub>	19.9920	34.9860	44.9820	28.67 ± 0.15	0.34 ± 0.04	-13.29 ± 2.29	91.19 ± 1.51	98.29 ± 0.16
MCT-SMEDS <sub>3</sub>	9.9960	44.9820	44.9820	22.01 ± 0.75	0.15 ± 0.03	-9.91 ± 1.75	96.69 ± 0.82	98.07 ± 0.15
MCT-SMEDS <sub>4</sub>	19.9920	44.9820	34.9860	26.42 ± 0.19	0.43 ± 0.11	-12.37 ± 0.98	95.16 ± 0.81	98.80 ± 0.01
MCT-SMEDS <sub>5</sub>	24.9900	34.9860	39.9840	32.19 ± 0.37	0.30 ± 0.02	-14.17 ± 1.21	90.16 ± 0.80	97.69 ± 0.19
MCT-SMEDS <sub>6</sub>	24.9900	39.9840	34.9860	30.50 ± 0.21	0.41 ± 0.07	-14.13 ± 1.94	90.26 ± 0.88	98.53 ± 0.07
MCT-SMEDS <sub>7</sub>	14.9940	44.9820	39.9840	22.45 ± 0.38	0.38 ± 0.08	-11.57 ± 2.22	96.61 ± 1.12	98.77 ± 0.05
MCT-SMEDS <sub>8</sub>	14.9940	39.9840	44.9820	23.37 ± 0.17	0.32 ± 0.04	-11.84 ± 1.41	96.24 ± 1.26	97.77 ± 0.03
MCT-SMEDS <sub>9</sub>	19.9920	39.9840	39.9840	24.75 ± 0.01	0.39 ± 0.02	-12.25 ± 0.91	93.69 ± 1.84	98.50 ± 0.01
MCT-SMEDS <sub>10</sub>	24.9900	37.4850	37.4850	29.61 ± 0.16	0.27 ± 0.07	-13.42 ± 1.93	90.25 ± 1.66	98.30 ± 0.14
MCT-SMEDS <sub>11</sub>	19.9920	37.4850	42.4830	27.43 ± 0.25	0.28 ± 0.07	-13.26 ± 1.52	92.35 ± 1.17	98.27 ± 0.25
MCT-SMEDS <sub>12</sub>	14.9940	42.4830	42.4830	22.30 ± 0.35	0.42 ± 0.08	-10.30 ± 0.60	96.34 ± 1.31	98.63 ± 0.09
MCT-SMEDS <sub>13</sub>	19.9920	42.4830	37.4850	25.43 ± 0.09	0.39 ± 0.09	-11.92 ± 1.95	94.01 ± 1.52	98.59 ± 0.07



Table 11. Summary of results of statistical analysis and model equations for the measured responses of LCT-SMEDS.

Models	SE	PRESS	R <sup>2</sup>	R <sup>2</sup> (adj)	Remark
<b>Droplet size</b>					
Linear	17.6952	1311.24	80.39%	79.31%	
Quadratic	10.0087	4312.41	93.90%	92.98%	suggested
Full cubic	10.7533	4335.33	93.17%	92.36%	
Full quartic	10.0203	5873.82	93.46%	93.30%	
<b>PDI</b>					
Linear	0.0460777	0.0907071	92.02%	90.63%	suggested
Quadratic	0.0471451	0.1007071	91.11%	90.46%	
Full cubic	0.0482528	0.127091	91.03%	90.25%	
Full quartic	0.0508643	0.15135	82.17%	81.72%	
<b>Zeta potential</b>					
Linear	2.37366	302.915	82.44%	81.02%	
Quadratic	2.02908	212.683	98.15%	95.22%	suggested
Full cubic	2.24052	240.854	91.79%	91.03%	
Full quartic	2.28664	246.138	92.21%	88.54%	
<b>Active ingredient content</b>					
Linear	1.14904	59.8364	94.44%	94.13%	suggested
Quadratic	1.22456	73.3972	93.52%	92.84%	
Full cubic	1.21462	62.3793	93.62%	92.26%	
Full quartic	1.21111	86.3057	93.05%	92.23%	
<b>% Transmittance</b>					
Linear	4.79487	983.071	68.44%	66.69%	
Quadratic	1.97902	178.68	95.07%	94.33%	suggested
Full cubic	1.337	103.393	93.02%	92.41%	
Full quartic	1.38986	113.005	93.56%	92.72%	

Note: SE, Standard error of the regression, represents the standard distance between the data values and fitted regression line.

PRESS, Prediction error sum of squares, the smaller the PRESS value, the better the model predictive ability.

R<sup>2</sup>, Percentage of response variable variation; the higher the value, the better the model fits the data.

R<sup>2</sup> (adj), Percentage of response variable variation based on its relationship with one or more predictor variables

Table 12. Summary of results of statistical analysis and model equations for the measured responses of MCT-SMEDS.

Models	SE	PRESS	R <sup>2</sup>	R <sup>2</sup> (adj)	Remark
<b>Droplet size</b>					
Linear	1.32082	70.4879	90.05%	89.20%	suggested
Quadratic	1.37072	75.9915	88.98%	88.36%	
Full cubic	1.37072	75.9915	88.98%	88.36%	
Full quartic	1.37072	75.9915	88.98%	88.36%	
<b>PDI</b>					
Linear	0.11177	0.5583	92.39%	91.53%	
Quadratic	0.07	0.20091	97.55%	96.73%	suggested
Full cubic	0.06959	0.20418	66.99%	64.16%	
Full quartic	0.06947	0.2019	67.10%	64.27%	
<b>Zeta potential</b>					
Linear	1.4284	86.5063	99.12%	96.44%	suggested
Quadratic	2.2689	88.1534	94.48%	92.67%	
Full cubic	2.2689	88.1534	94.48%	92.67%	
Full quartic	2.2689	88.1534	94.48%	92.67%	
<b>Active ingredient content</b>					
Linear	1.12636	70.6528	96.41%	95.23%	suggested
Quadratic	1.42795	88.6952	76.34%	75.03%	
Full cubic	1.42795	86.9951	79.17%	76.82%	
Full quartic	1.21384	79.5072	84.80%	81.95%	
<b>% Transmittance</b>					
Linear	0.35166	5.50457	40.05%	36.72%	
Quadratic	0.15803	1.5682	91.83%	89.52%	suggested
Full cubic	0.19745	1.89542	82.68%	80.05%	
Full quartic	0.1899	1.92286	84.46%	81.55%	

Note: SE, Standard error of the regression, represents the standard distance between the data values and fitted regression line.

PRESS, Prediction error sum of squares, the smaller the PRESS value, the better the model predictive ability.

R<sup>2</sup>, Percentage of response variable variation; the higher the value, the better the model fits the data.

R<sup>2</sup> (adj), Percentage of response variable variation based on its relationship with one or more predictor variables

Table 13. Analysis of variance of measured responses for LCT-SMEDS.

Response	Source	DF	Seq SS	Adj SS	Adj MS	F-value	P-value
Droplet size ( $Y_1$ )	Regression	5	53988.600	53988.600	10797.700	101.610	< 0.0001
	Linear	2	46223.200	7527.500	3763.700	35.420	< 0.0001
	Quadratic	3	7765.400	7765.400	2588.500	24.360	< 0.0001
	$X_1X_2$	1	7083.100	7068.400	7068.400	66.510	< 0.0001
	$X_1X_3$	1	47.300	679.000	679.000	6.390	0.016
	$X_2X_3$	1	635.000	635.000	635.000	5.980	0.020
	Residual Error	33	3506.900	3506.900	106.300		
	Lack-of-Fit	7	896.300	896.300	128.000	1.280	0.301
	Pure Error	26	2610.600	2610.600	100.400		
Total	38	57495.500	0.650				
PDI ( $Y_2$ )	Regression	2	0.006	0.006	0.003	0.650	0.030
	Linear	2	0.006	0.006	0.003	0.650	0.030
	Residual Error	36	0.171	0.171	0.004		
	Lack-of-Fit	10	0.104	0.104	0.010	4.040	0.102
	Pure Error	26	0.067	0.067	0.002		
	Total	38	0.177				
Zeta potential ( $Y_3$ )	Regression	2	4.515	4.515	2.257	0.450	0.041
	Linear	2	4.515	4.515	2.257	0.450	0.041
	Residual Error	36	180.718	180.718	5.020		
	Lack-of-Fit	10	73.671	73.671	7.367	1.790	0.113
	Pure Error	26	107.046	107.046	4.117		
	Total	38	185.233				
Active ingredient content ( $Y_4$ )	Regression	2	917.520	917.520	458.762	305.930	< 0.0001
	Linear	2	917.520	917.520	458.762	305.930	< 0.0001
	Residual Error	36	53.980	53.980	1.500		
	Lack-of-Fit	10	15.630	15.630	1.563	1.060	0.426
	Pure Error	26	38.360	38.360	1.475		
	Total	38	971.510				
% Transmittance ( $Y_5$ )	Regression	5	2493.44	2493.44	623.360	163.68	< 0.0001
	Linear	2	1795.25	1270.62	635.309	166.82	< 0.0001
	Quadratic	3	698.19	698.19	349.093	91.67	< 0.0001
	$X_1X_2$	1	344.66	344.66	344.665	175.86	< 0.0001
	$X_1X_3$	1	344.66	344.66	344.665	175.86	< 0.0001
	$X_2X_3$	1	8.86	8.86	8.863	2.33	0.136
	Residual Error	34	129.48	129.48	3.808		
	Lack-of-Fit	8	79.26	79.26	9.907	5.13	0.001
	Pure Error	26	50.22	50.22	1.932		
	Total	38	2622.92				

Note: DF, degrees of freedom.

Seq SS, sequential sums of squares

Adj SS, adjusted sums of squares

Adj MS, adjusted mean square

Table 14. Analysis of variance of measured responses for MCT-SMEDS.

Response	Source	DF	Seq SS	Adj SS	Adj MS	F-value	P-value
Droplet size ( $Y_1$ )	Regression	2	545.940	545.940	272.971	145.280	< 0.0001
	Linear	2	545.940	545.940	272.971	145.280	< 0.0001
	Residual Error	36	67.640	67.640	1.879		
	Lack-of-Fit	10	28.800	28.800	2.880	1.930	0.187
	Pure Error	26	38.840	38.840	1.494		
	Total	38	613.580				
PDI ( $Y_2$ )	Regression	5	0.347	0.347	0.087	17.690	< 0.0001
	Linear	2	0.064	0.292	0.146	29.780	< 0.0001
	Quadratic	3	0.283	0.283	0.142	28.890	< 0.0001
	$X_1X_2$	1	0.197	0.064	0.064	12.970	0.001
	$X_1X_3$	1	0.024	0.024	0.024	4.980	0.032
	$X_2X_3$	1	0.024	0.024	0.024	4.980	0.032
	Residual Error	34	0.167	0.167	0.005		
	Lack-of-Fit	8	0.060	0.060	0.008	1.840	0.114
	Pure Error	26	0.106	0.106	0.004		
Total	38	0.513					
Zeta potential ( $Y_3$ )	Regression	2	71.936	71.936	35.968	17.630	< 0.0001
	Linear	2	71.936	71.936	35.968	17.630	< 0.0001
	Residual Error	36	73.451	73.451	2.040		
	Lack-of-Fit	10	7.387	7.387	0.739	0.290	0.977
	Pure Error	26	66.064	66.064	2.541		
	Total	38	145.387				
Active ingredient content ( $Y_4$ )	Regression	2	236.860	236.860	118.428	58.080	< 0.0001
	Linear	2	236.860	236.860	118.428	58.080	< 0.0001
	Residual Error	36	73.410	73.410	2.039		
	Lack-of-Fit	10	28.440	28.440	2.844	1.640	0.149
	Pure Error	26	44.970	44.970	1.730		
	Total	38	310.260				
% Transmittance ( $Y_5$ )	Regression	5	5.335	5.335	1.334	21.680	< 0.0001
	Linear	2	5.335	5.335	1.334	21.680	< 0.0001
	Quadratic	3	2.360	2.360	1.180	19.180	< 0.0001
	$X_1X_2$	1	1.308	0.206	0.206	3.340	0.006
	$X_1X_3$	1	0.526	0.526	0.526	8.550	0.006
	$X_2X_3$	1	0.526	0.526	0.526	8.550	0.006
	Residual Error	34	2.092	2.092	0.062		
	Lack-of-Fit	8	1.318	1.318	0.165	5.540	0.101
	Pure Error	26	0.773	0.773	0.030		
	Total	38	7.426				

Note: DF, degrees of freedom.

Seq SS, sequential sums of squares

Adj SS, adjusted sums of squares

Adj MS, adjusted mean square

## 3.2. Influence of independent variables on responses in experimental designs

### 3.2.1. Influence on droplet size ( $Y_1$ )

The performance of emulsion was determined by the emulsion droplet size (130). Where the smaller the microemulsion droplet size, the larger the interfacial surface area, hence rapid absorption is promoted, and bioavailability is improved. In this research, the droplet size of SMEDS after dilution was selected as one of the responses because it is important for *in vitro* evaluation. In the preparation of SMEDS, the lesser the droplet size of SMEDS, the better the result of the release of drug with higher bioavailability. Hence, for having a minimized droplet size ( $Y_1$ ) value, the SMEDS formulations were optimized.

According to Table 9, the lowest ( $20.17 \pm 0.37$  nm) and the highest ( $128.74 \pm 4.82$  nm) values were resulted respectively from formulation LCT-SMEDS<sub>3</sub> and LCT-SMEDS<sub>4</sub>. The quadratic model (Table 11) statistically fitted well to the data. According to the results of analysis of variance, the program produced the following polynomial equation (1). The increase in amount of castor oil may direct towards the enhancement in the mean droplet size, and its fall may be resulted by increasing the amount of Cremophor<sup>®</sup> RH 40 and Tween<sup>®</sup> 80. It can be concluded from the P value of  $<0.05$  (Table 13) that the droplet size was significantly influenced by all the individual term and the interaction terms. The droplet size was positively, synergistically, and significantly influenced by the interaction term  $X_1X_2$  and  $X_1X_3$ , and significantly and antagonistically affected by the term  $X_1X_2$ , indicated by the negative value of the coefficient. Hence, it can be summarized that the increase in the amount of oil and the decrease in the amount of surfactant mixture

lead to the increasement of droplet size. The value of the coefficient, that expresses the effect of the dependent variable, was in the order  $X_3 > X_1 > X_2$ .

As shown in Table 10, formulations MCT-SMEDS<sub>1</sub> and MCT-SMEDS<sub>3</sub> showed the highest ( $33.2 \pm 0.54$  nm) and the lowest ( $19.67 \pm 4.82$  nm) values, respectively. The linear model (Table 12) statistically fitted well to the data. According to the results of variance analysis, the program produced the following polynomial equation (2). The order of the coefficient value was  $X_1 > X_3 > X_2$ . It was detected that the increase in amount of MCT oil and Tween<sup>®</sup> 80 may yield the increasing droplet size, whereas the increase in the amount of Cremophor<sup>®</sup> RH 40 may lead to the decreasing droplet size. It was inferred from the P value of  $< 0.05$  (Table 14) that all the individual term could significantly affect the droplet size. The relationship of the input variables and droplet size ( $Y_1$ ) for LCT-SMEDS and MCT-SMEDS was shown in Figure 9-12.

$$\text{Droplet size } (Y_1) = 1022 X_1 - 87 X_2 - 7902 X_3 - 2182 X_1 X_2 + 10818 X_1 X_3 + 10539 X_2 X_3 \quad (1)$$

$$\text{Droplet size } (Y_1) = 83.5020 X_1 - 0.507786 X_2 + 25.6265 X_3 \quad (2)$$

### 3.2.2. Influence on PDI ( $Y_2$ )

The polydispersity index (PDI) was selected as another response. The test of PDI provided the details about the distribution of particle size. The uniform and narrow microemulsion droplet size distribution is

implied by the low value of PDI (131). Table 9 and Table 10 respectively showed the outcomes of PDI measurements for LCT-SMEDS and MCT-SMEDS. The PDI of LCT-SMEDS and MCT-SMEDS was ranged between 0.2 to 0.37 and between 0.09 to 0.43, respectively. After dilution with water, all the polydispersity values were below 0.6, suggesting good uniformity in the droplet size distribution (107).

As mentioned in Table 9, the following equation (3) was to be developed for the PDI of LCT-SMEDS by the linear model. The order of the coefficient value was  $X_3 > X_2 > X_1$ . According to the indication of the positive coefficient values, the higher in the oil, surfactant, and co-surfactant contents would increase PDI of LCT-SMEDS. In Figure 9 and 10, the response surface and contour plots of PDI ( $Y_2$ ) for LCT-SMEDS were individually presented.

For the PDI of MCT-SMEDS, the following equation (4) was developed by the use of the suggested quadratic model as shown in Table 12. With the decrease in concentrations of the oil, surfactant, and co-surfactant, PDI of MCT-SMEDS formulations may enhance. It can be concluded that PDI was significantly, positively, and synergistically affected by the interaction term  $X_1X_2$ ,  $X_1X_3$ , and  $X_2X_3$ . The effect of the corresponding factor on the PDI ( $Y_2$ ) was significantly indicated by the P value of  $<0.05$  as presented in Table 14. The response surface and contour plots of PDI ( $Y_2$ ) for MCT-SMEDS were individually shown in Figure 11 and 12.

$$\text{PDI } (Y_2) = 0.2844 X_1 + 0.3416 X_2 + 0.3944 X_3 \quad (3)$$

$$\text{PDI (Y}_2\text{)} = -16.27 X_1 - 1.08 X_2 - 0.03 X_3 + 31.54 X_1 X_2 + 19.54 X_1 X_3 + 28.67 X_2 X_3 \quad (4)$$

### 3.2.3. Influence on zeta potential (Y<sub>3</sub>)

The surface charge of microemulsion droplet may be described by the value of zeta potential. Owing to deflocculation of microemulsion particles, the theory mentions that system remains stable, and the zeta potential value should be in the ranges of +30 to -30 mV for identical system (94). It was observed that the negative surface charge of microemulsion droplets was found in conventional SMEDS formulation as free fatty acids were present in the oils. Non-ionic surfactants were widely utilized because of their minimal toxicity. Table 9 and 10 describes the zeta potential results of diluted LCT-SMEDS and MCT-SMEDS formulations respectively. For diluted LCT-SMEDS formulations, the values of zeta potential were ranged from -8.34 to -12.9 mV. On the other hand, the zeta potential values were ranged between -9.91 and -14.9 mV for diluted MCT-SMEDS formulations.

According to Table 11 and 12, the linear model was suggested to the zeta potential data of both LCT-SMEDS and MCT-SMEDS. For LCT-SMEDS (equation 5), the order of the coefficient value was  $X_1 > X_2 > X_3$ , whereas the order of the coefficient value was  $X_1 > X_3 > X_2$  for MCT-SMEDS (equation 6). According to the observations from the equations, the decrease in the quantity of the oil, surfactant, and co-surfactant may direct towards the increase in zeta potential. It can be summarized from the P value of  $< 0.05$  (Table 13 and Table 14) that zeta potential was significantly affected by all the individual term. The plots in



Figure 9-12 presented the relationship between the independent variables and zeta potential ( $Y_3$ ).

$$\text{Zeta potential } (Y_3) = -13.79 X_1 - 11.32 X_2 - 1.88 X_3 \quad (5)$$

$$\text{Zeta potential } (Y_3) = -33.12 X_1 - 2.44 X_2 - 12.41 X_3 \quad (6)$$

#### **3.2.4. Influence on active ingredient content ( $Y_4$ )**

Since final dose of the active ingredient is decreased by the higher drug loading in SMEDS formulation, active ingredient content is a critical parameter. With lower amount of oils and surfactants, an equivalent dose of active ingredient requires to be delivered at a higher drug loading. It was observed that large quantity of the surfactants causes the irritation on GIT, however, the amount of surfactants incorporated in the SMEDS preparation may be lessened at maximum active ingredient loading (132). Hence, as criteria for the optimization, active ingredient content was selected.

While the active ingredient content of LCT-SMEDS formulations ranged from 84.55 to 99.71% as mentioned in Table 9, the active ingredient content of MCT-SMEDS ranged from 90.11 to 96.69% as shown in Table 10. According to the statistically fitted data, the program suggested the linear model for both LCT-SMEDS and MCT-SMEDS (Table 11 and 12). To confirm the relationship between independent variables and active ingredient content of LCT-SMEDS and MCT-SMEDS, the equation 7 and 8 were respectively generated on the basis of the outcomes of analysis of variance (Table 13 and 14). As presented in

equation 7, the order of the coefficient value was  $X_2 > X_3 > X_1$ , while in equation 8, the order of the coefficient value was  $X_1 > X_3 > X_2$ . The increase of the oil, surfactant, and co-surfactant contents would improve active ingredient content according to the positive value of all coefficients. In Figure 9-12, the further support of 3D contour and response surfaces plots were shown for the obtained polynomial equations.

$$\text{Active ingredient content (Y}_4\text{)} = 53.96 X_1 + 108.13 X_2 + 93.89 X_3 \quad (7)$$

$$\text{Active ingredient content (Y}_4\text{)} = 33.12 X_1 + 2.44 X_2 + 12.41 X_3 \quad (8)$$

### 3.2.5. Influence on %transmittance (Y<sub>5</sub>)

The microemulsion formation was confirmed through transparency, and hence transmittance was selected as another response. The high clarity of microemulsion is indicated by transmittance value greater than or equal to 98% (133). The transparency of microemulsion, which may be reduced by the large particle size, results in higher values of %transmittance. The %transmittance of LCT-SMEDS ranged from 75.72-98.57 % as shown in Table 9, and in contrast, the %transmittance of MCT-SMEDS ranged from 97.43 to 98.8 % as indicated in Table 10.

The quadratic model, as shown in Table 11 and 12, was to be statistically fitted well to the %transmittance data of both LCT-SMEDS and MCT-SMEDS. The effect of independent variables on %transmittance of LCT-SMEDS and MCT-SMEDS was reflected by the following equations 9 and 10. In equation 9, the order of the coefficient

value was  $X_1 > X_3 > X_2$ , while on the contrary, the order of the coefficient value was  $X_2 > X_3 > X_1$  as mentioned in equation 10. According to the observations from equation 9, %transmittance may reduce with the enhancement in amount of the oil and may improve with the increasing the quantity of the surfactant and co-surfactant. In equation 10, the increasing the quantity of the oil, surfactant, and co-surfactant may enhance %transmittance. The effect of the related factor on %transmittance ( $Y_5$ ) was significantly found in the P value of  $< 0.05$  as shown in Table 13 and 14. It can be summarized from equation 9 and 10 that the interaction term  $X_1X_2$ ,  $X_1X_3$ , and  $X_2X_3$  have significant synergistic effect on %transmittance as expressed by the positive coefficient value. Figure 9-12 presented the 3D plots of LCT-SMEDS and MCT-SMEDS which indicate the effect of independent variables on %transmittance ( $Y_5$ ).

$$\begin{aligned} \% \text{Transmittance } (Y_5) = & -228.2 X_1 + 42.3 X_2 + 60.1 X_3 + 658.8 X_1 X_2 + \\ & 354.8 X_1 X_3 + 243.7 X_2 X_3 \end{aligned} \quad (9)$$

$$\begin{aligned} \% \text{Transmittance } (Y_5) = & 49.05 X_1 + 104.02 X_2 + 88.15 X_3 + 56.76 X_1 X_2 + \\ & 90.76 X_1 X_3 + 98.13 X_2 X_3 \end{aligned} \quad (10)$$

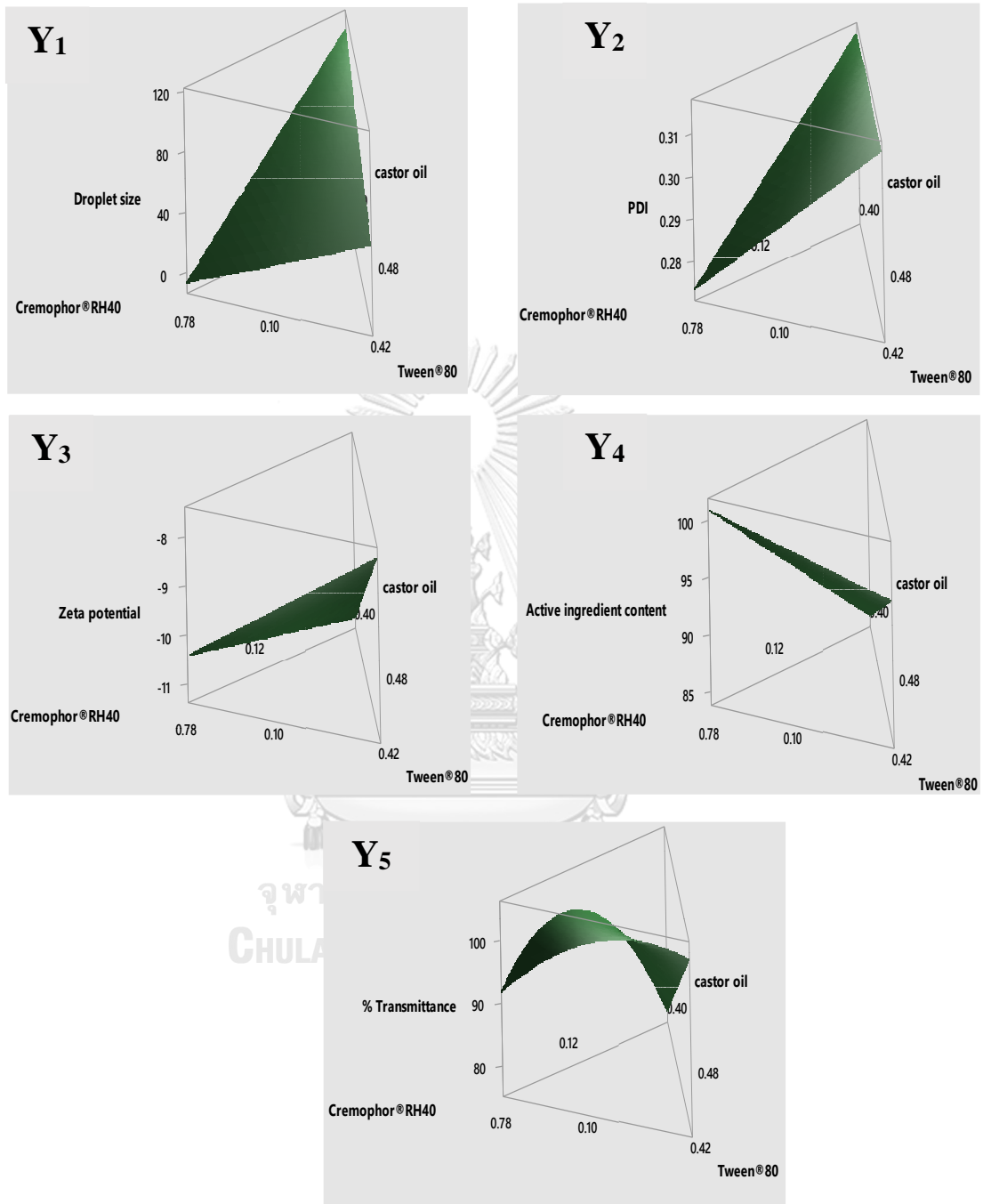


Figure 9. Three-dimensional response surface plot for the effects of the independent variables on the responses, Y<sub>1</sub>, Y<sub>2</sub>, Y<sub>3</sub>, Y<sub>4</sub>, and Y<sub>5</sub> of LCT-SMEDS

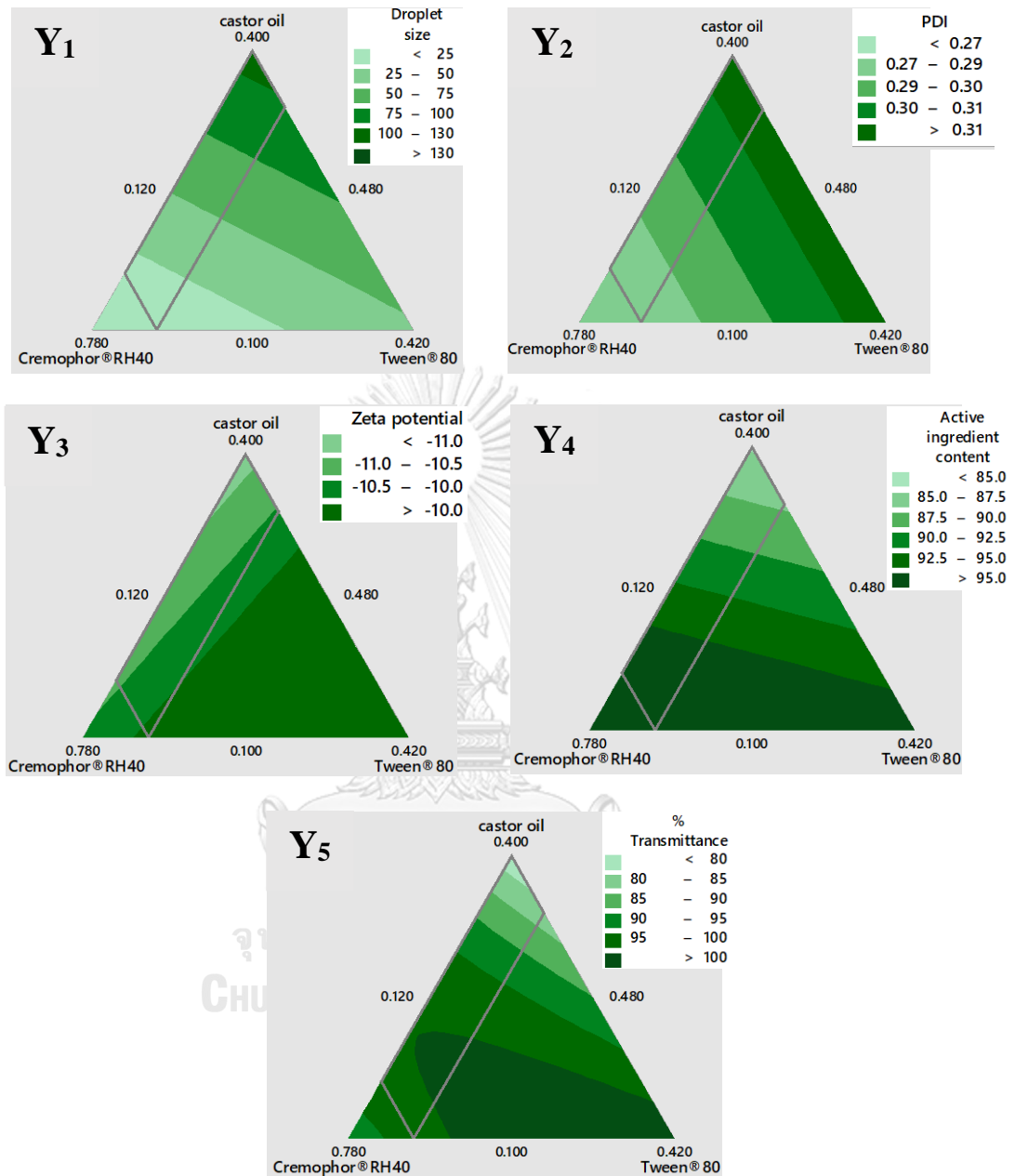


Figure 10. Contour plots for the effects of the independent variables on the responses, Y<sub>1</sub>, Y<sub>2</sub>, Y<sub>3</sub>, Y<sub>4</sub>, and Y<sub>5</sub> of LCT-SMEDS

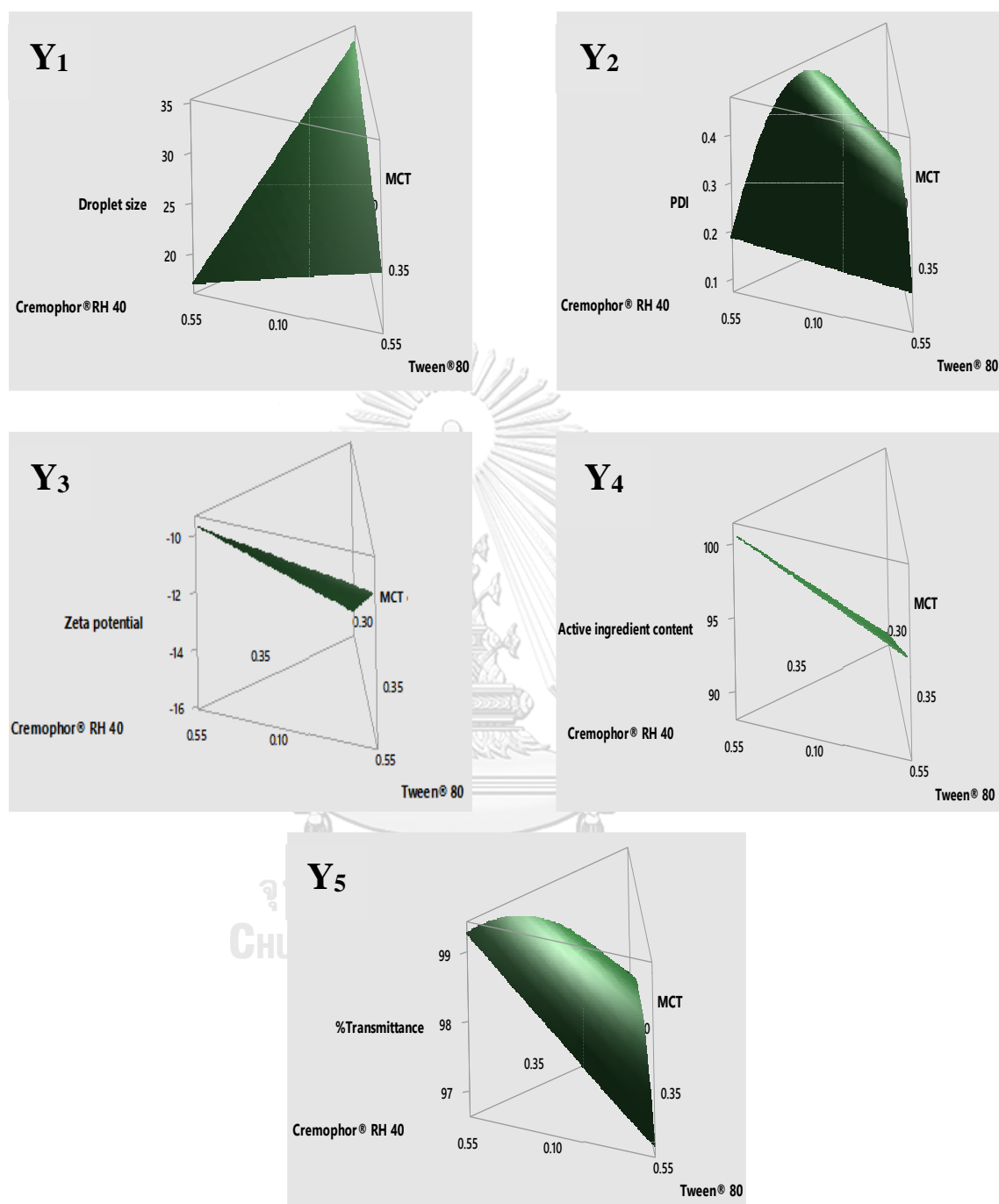


Figure 11. Three-dimensional response surface plot for the effects of the independent variables on the responses, Y<sub>1</sub>, Y<sub>2</sub>, Y<sub>3</sub>, Y<sub>4</sub>, and Y<sub>5</sub> of MCT-SMEDS

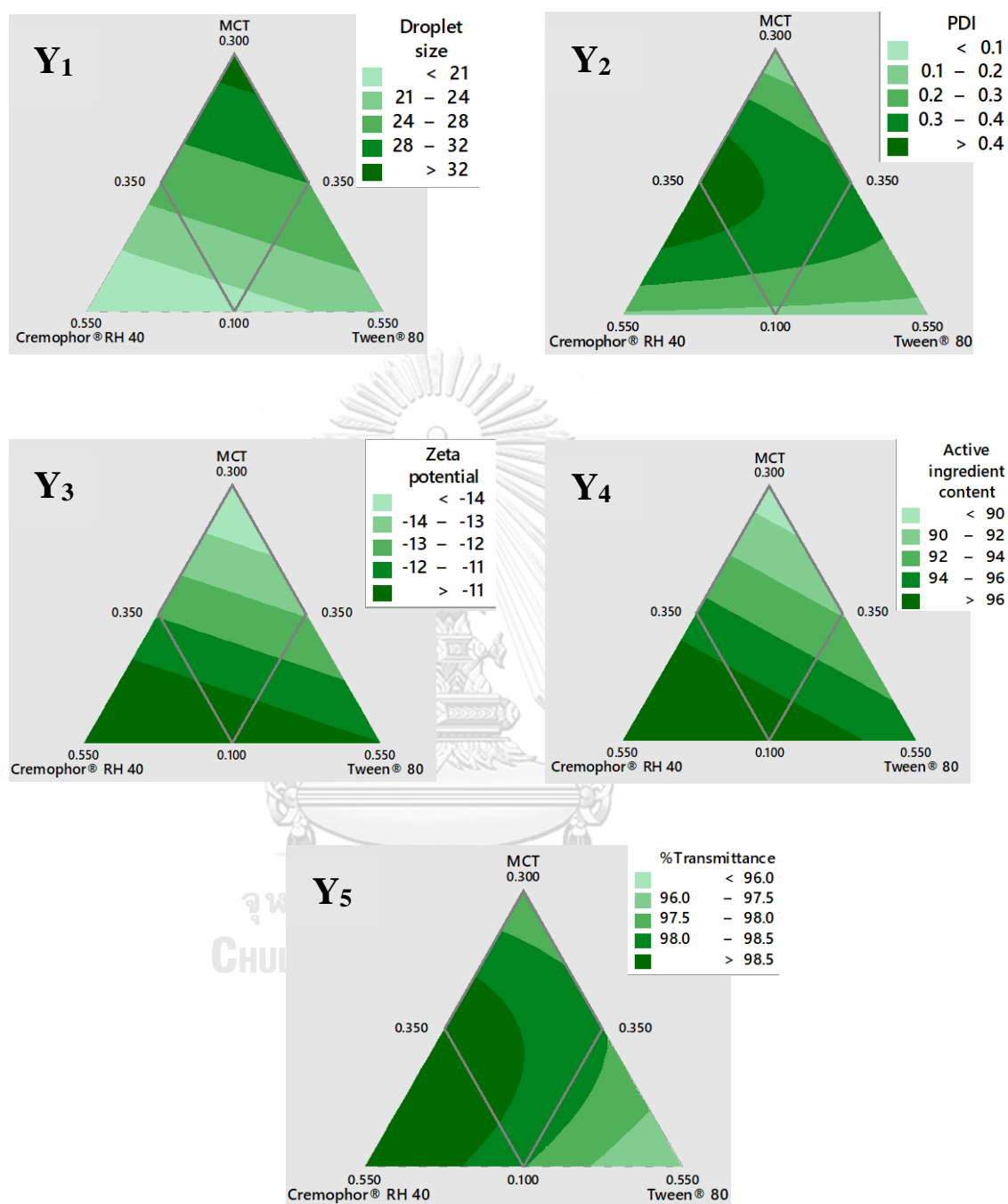


Figure 12. Contour plots for the effects of the independent variables on the responses, Y<sub>1</sub>, Y<sub>2</sub>, Y<sub>3</sub>, Y<sub>4</sub>, and Y<sub>5</sub> of MCT-SMEDS

### 3.3. Optimization and Validation of the formulations

The degree of the input or independent variables that provides the optimum responses were examined, after the influence of the independent variables has been studied on the responses. The formulations were optimized to determine the degree of independent variables ( $X_1$ ,  $X_2$  and  $X_3$ ) that would provide a minimum value of droplet size ( $Y_1$ ), PDI ( $Y_2$ ) with maximum value of zeta potential ( $Y_3$ ), active ingredient content ( $Y_4$ ), and %transmittance ( $Y_5$ ). The observation of the influence of independent variables on responses were performed from the polynomial equations, response surface plots, and 3D contour plots.

By the use of desirability function, the optimization of independent variables were performed for the values of responses, where  $Y_1$  and  $Y_2$  were fixed to be minimized, and  $Y_3$ ,  $Y_4$ , and  $Y_5$  were fixed to be maximized for both LCT-SMEDS and MCT-SMEDS. After calculating by the consolidation of all the equations presented above, with a desirability value of 0.807 (Figure 13) and of 0.794 (Figure 14), the levels of independent variables of LCT-SMEDS and MCT-SMEDS were suggested respectively by the program as the optimized formulations. The overlaid contour plots of the optimized SMEDS formulations were presented in Figure 15 and 16.

Regarding the influence of the input variables on all five response variables, the optimization plots of LCT-SMEDS and MCT-SMEDS were presented in Figure 13 and 14. The optimized formulation ratios of  $X_1$ ,  $X_2$ , and  $X_3$  for LCT-SMEDS were 19.59 %, 62.34 %, and 18.03 %, respectively, which provide theoretically the values of 22.71 nm, 0.28, -9.70 mV, 97.87 %, and 98.38 % for  $Y_1$ ,  $Y_2$ ,  $Y_3$ ,  $Y_4$ , and  $Y_5$ , respectively, while that of  $X_1$ ,  $X_2$ , and  $X_3$  for MCT-SMEDS were 12.39 %, 44.98 %, and 42.63 %, respectively.



and 42.59 %, respectively which provide theoretical values of 22.02 nm, 0.17, -10.69 mV, 98.72 %, and 97.09 % for  $Y_1$ ,  $Y_2$ ,  $Y_3$ ,  $Y_4$ , and  $Y_5$ , respectively.

For validation of these mixture design models, three different batches of LCT-SMEDS and MCT-SMEDS were prepared and the responses were measured. Table 15 and 16 represented the predicted and measured values of  $Y_1$ ,  $Y_2$ ,  $Y_3$ ,  $Y_4$ , and  $Y_5$  for the best LCT-SMEDS and MCT-SMEDS, respectively. For both LCT-SMEDS and MCT-SMEDS, the actual values of responses were in close agreement to expected values. In order to measure the reliability and accuracy, values of prediction errors were determined. The prediction errors of all responses were small and desirable as shown in Table 15 and 16. Thus, it can be concluded from the results of these observations that the mixture design method applied for the optimization of LCT-SMEDS and MCT-SMEDS in our research was reliable and accurate. These optimized formulations were subjected to further studies.

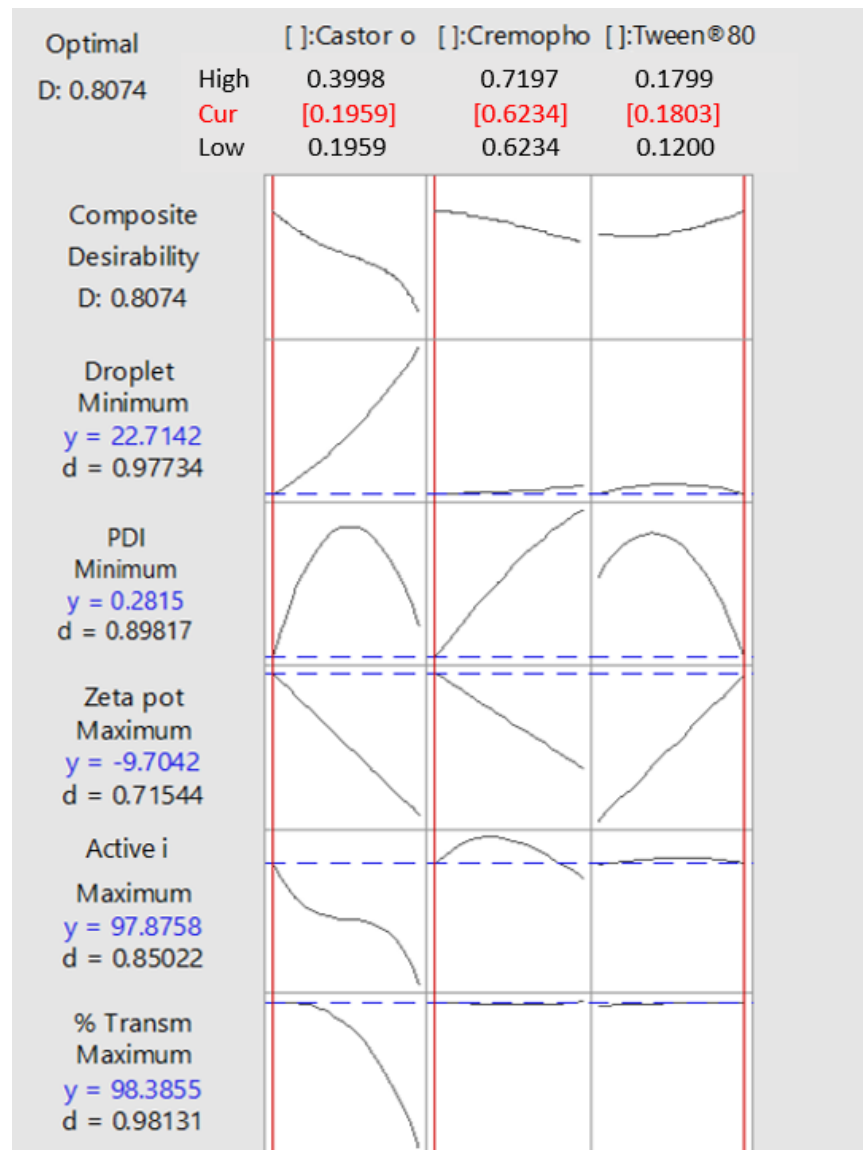


Figure 13. Response optimizer plot for LCT-SMEDS

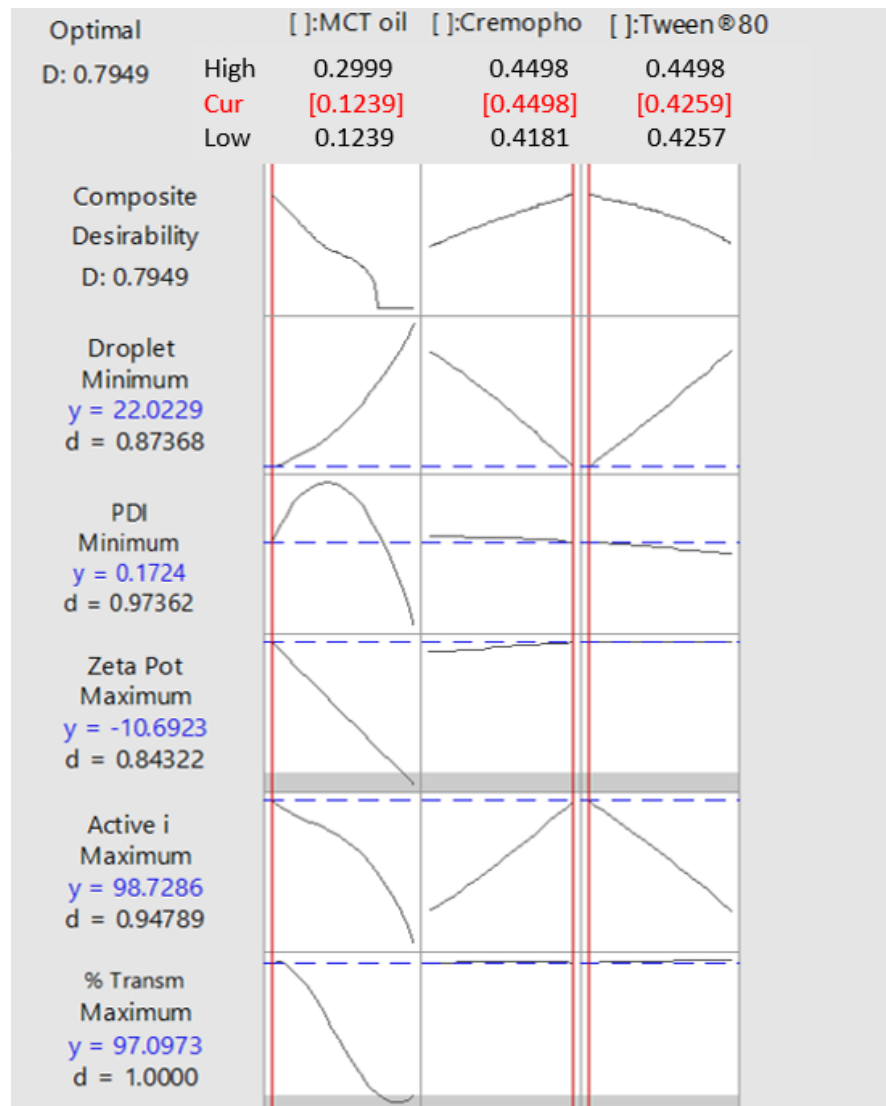


Figure 14. Response optimizer plot for MCT-SMEDS

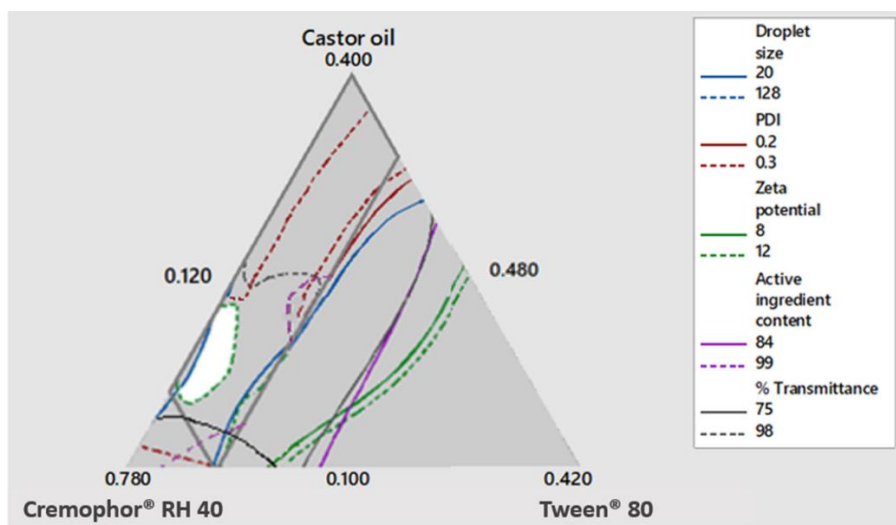


Figure 15. Overlaid contour plot for LCT-SMEDS

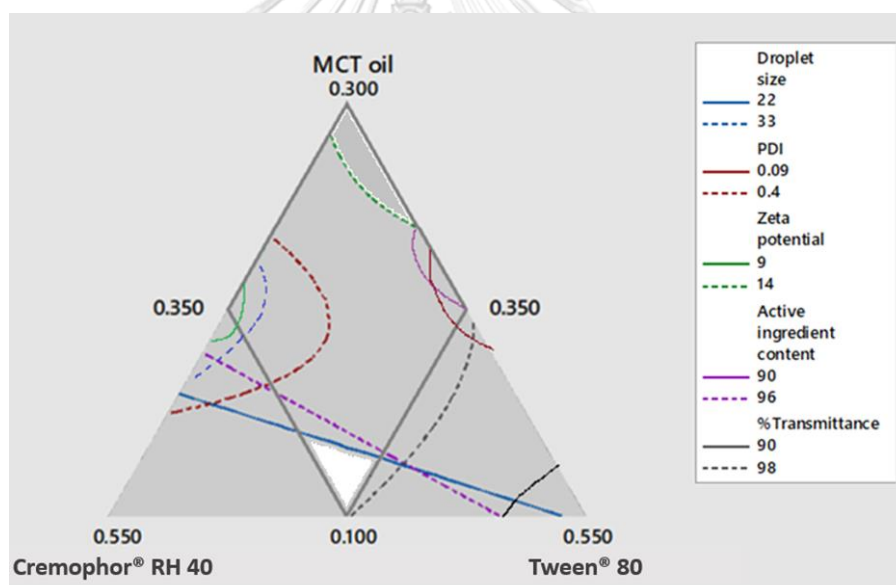


Figure 16. Overlaid contour plot for MCT-SMEDS

Table 15. Predicted and measured values of optimized LCT-SMEDS formulation.

Responses	Predicted value	Measured value	Prediction error (%)
Droplet size (nm; Y1)	22.71	22.55 ± 0.96	- 0.70
PDI (Y2)	0.28	0.27 ± 0.02	-3.70
Zeta potential (mV; Y3)	-9.70	-9.35 ± 1.75	-3.74
Active ingredient content (%; Y4)	97.87	96.49 ± 0.60	-1.43
Transmittance (%; Y5)	98.38	98.80 ± 0.11	0.42

Table 16. Predicted and measured values of optimized MCT-SMEDS formulation.

Responses	Predicted value	Measured value	Prediction error (%)
Droplet size (nm; Y1)	22.02	23.10 ± 0.72	4.67
PDI (Y2)	0.17	0.18 ± 0.06	5.55
Zeta potential (mV; Y3)	-10.69	-10.62 ± 1.77	-0.65
Active ingredient content (%; Y4)	98.72	96.37 ± 1.03	-2.43
Transmittance (%; Y5)	97.09	99.15 ± 0.17	2.07

#### 4. Characterization of the optimized formulations

##### 4.1. Visual observation

The identification of any signs of phase separation and precipitation of the optimized formulations was visually performed after dilution. With the help of visibility grading criteria, formulations examined were graded from A to E (134). When SMEDS was dispersed in aqueous phase,  $S_{mix}$  was assumed to penetrate the aqueous phase and redistribute between the oil-water interface (126). As shown in Table 17,

the optimized formulations were found with no indications of precipitation and phase separation. Clear and transparent microemulsions were rapidly formed through these optimized formulations. Hence, they were classified with the value A.

Table 17. Results of visibility grade, precipitation, and phase separation.

Formulations	Visibility grade*	Precipitation	Phase separation	Emulsification time (s)	Refractive index
LCT-SMEDS <sub>OTM</sub>	A	No	No	44 ± 1	1.4222 ± 0.07
MCT-SMEDS <sub>OTM</sub>	A	No	No	58 ± 2	1.4501 ± 0.02

\*Visual grading system: (A) denoting a rapidly forming (within 1 min) microemulsion that was clear or slightly bluish in appearance; (B) denoting a rapidly forming, slightly less clear emulsion that had a bluish white appearance; (C) denoting a bright white emulsion (similar in appearance to milk) that formed within 2 min; (D) denoting a dull, grayish white emulsion with a slightly oily appearance that was slow to emulsify (longer than 2 min); and (E) denoting a formulation that exhibited either poor or minimal emulsification with large oil droplets present on the surface.

จุฬาลงกรณ์มหาวิทยาลัย  
CHULALONGKORN UNIVERSITY

#### 4.2. Emulsification time

Emulsification timing was determined for the optimized formulations. “Self-emulsification” means that a SMEDS formulation has to be rapidly dispersed by a gentle agitation when diluted with the water. Determining the emulsification rate could estimate the efficiency of self-emulsification. The optimized formulations MCT-SMEDS and LCT-SMEDS<sub>OTM</sub> indicated emulsification time of below 1 min with good

emulsification as reported in Table 17. It was observed that MCT-SMEDS<sub>OTM</sub> was taken a few more emulsification time although the results of emulsification time were not considerable different between LCT-SMEDS<sub>OTM</sub> and MCT-SMEDS<sub>OTM</sub>. Lower quantity of Cremophor<sup>®</sup> RH 40 in MCT-SMEDS<sub>OTM</sub> may be the reason behind this. Owing to a less quantity of surfactant, the interfacial tension may be increased which ultimately leads to the fall of the emulsification rate (135).

#### **4.3. Refractive index**

When the refractive index value of the formulation is similar to that of water (1.333), a transparent nature of the formulation is observed (136). The results of refractive index were shown in Table 17. It was indicated that there were no significant differences in the refractive index data of the optimized formulations measured. The results of refractive index were close to that of water showing the optimized formulations were transparent in nature.

#### **4.4. Transmission electron microscopy (TEM)**

The appearance of the optimized SMEDS formulations was homogeneous and transparent liquid. The morphology of the optimized LCT-SMEDS and MCT-SMEDS of AST formulations was observed by using TEM. The morphology of the diluted LCT-SMEDS<sub>OTM</sub> and MCT-SMEDS<sub>OTM</sub> was shown in Figure 17. It can be observed that oil droplets

were homogenous with good integrity. Moreover, it was indicated that no signs of AST precipitation in LCT-SMEDS<sub>OTM</sub> were showed concluding the good stability of diluted LCT-SMEDS<sub>OTM</sub> formulation. In contrast, it was observed that AST seem to be precipitated in MCT-SMEDS<sub>OTM</sub> formulation. Therefore, LCT-SMEDS<sub>OTM</sub> may be the most stable formulation as inter particulate repulsion of the long chain triglycerides allow them to disperse for a longer period of time (137).

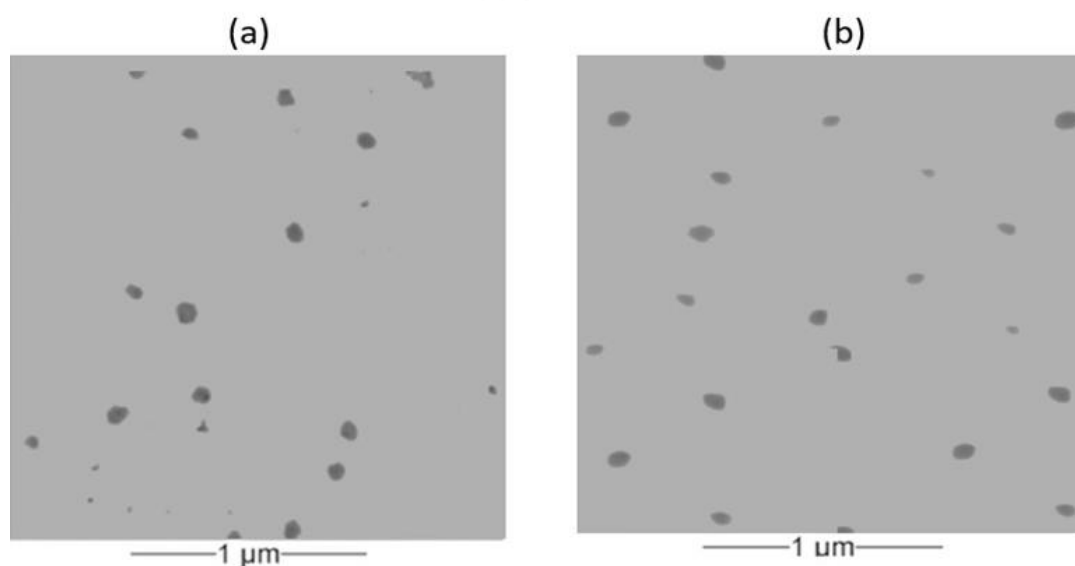


Figure 17. TEM images (a) LCT-SMEDS and (b) MCT-SMEDS of AST

#### 4.5. Freeze-thaw stability studies

The optimized LCT-SMEDS and MCT-SMEDS of AST formulations were performed freezing–thawing cycles from  $-20^{\circ}\text{C}$  to  $25^{\circ}\text{C}$ . The droplet size, PDI, zeta potential, and the content in formulations were determined before and after the study. As shown in Table 18, the data obtained after freezing–thawing cycles were almost close to that of the formulations before the cycles. Any significant



changes in physical appearance of the diluted formulations were not observed after freeze-thaw stability studies. Moreover, the diluted microemulsions indicated no signs of drug precipitation, phase separation, cracking, and creaming after subjected to freezing-thawing cycles, which suggests the formation of stable microemulsions.

Table 18. Stability profile of optimized SMEDS formulations.

Formulation	Treatment	Droplet size (nm)	PDI	Zeta potential (mV)	Content (%)
LCT-SMEDS <sub>OTM</sub>	before test	22.55 ± 0.96	0.25 ± 0.02	-11.35 ± 1.75	96.49 ± 0.6
	freeze-thaw (1 <sup>st</sup> cycle)	22.96 ± 0.84	0.27 ± 0.02	-12.37 ± 1.49	96.00 ± 0.56
	freeze-thaw (2 <sup>nd</sup> cycle)	23.50 ± 0.63	0.28 ± 0.02	-12.55 ± 1.59	95.82 ± 0.71
	freeze-thaw (3 <sup>rd</sup> cycle)	23.67 ± 0.67	0.29 ± 0.02	-13.19 ± 1.27	95.54 ± 0.69
MCT-SMEDS <sub>OTM</sub>	before test	23.40 ± 0.72	0.38 ± 0.06	-12.62 ± 3.17	96.37 ± 1.03
	freeze-thaw (1 <sup>st</sup> cycle)	23.67 ± 0.58	0.41 ± 0.06	-13.38 ± 2.75	96.23 ± 1.02
	freeze-thaw (2 <sup>nd</sup> cycle)	24.42 ± 0.26	0.43 ± 0.05	-13.82 ± 2.55	96.11 ± 0.99
	freeze-thaw (3 <sup>rd</sup> cycle)	24.55 ± 0.32	0.43 ± 0.05	-13.87 ± 2.52	95.93 ± 1.18

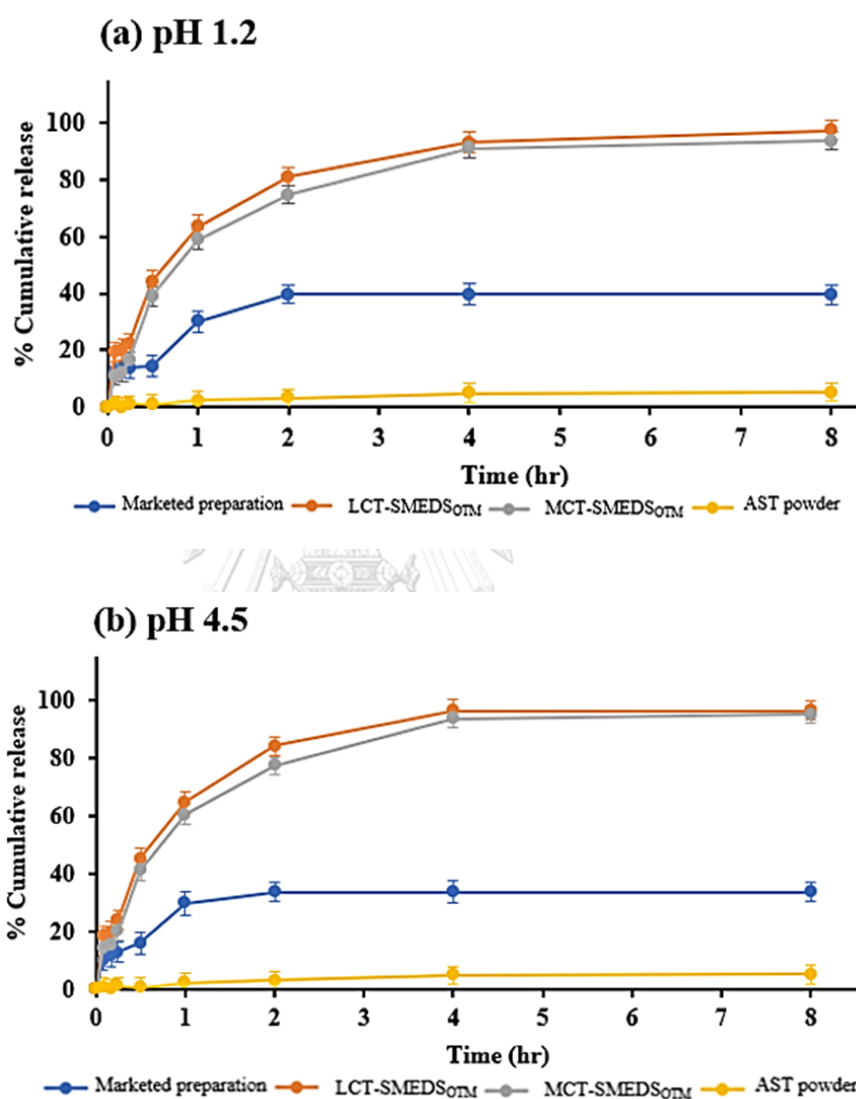
#### 4.6. *In vitro* release studies

The evaluation of active ingredient release studies was performed for optimized LCT-SMEDS and MCT-SMEDS compared to one marketed preparation and raw AST with the use of dialysis bag method. Marketed preparation (soft capsule) contains 4 mg AST which is suspended in oleic safflower oil. HCl/NaCl buffer pH 1.2, acetate buffer pH 4.5, and phosphate buffer pH 7.4 were used as the dissolution media.

The *in vitro* dissolution comparison of the formulations in different media were exhibited in Figure 18 a-c. In all media, the AST releases were examined, and the resultant data indicated the highest percentage of release with the use of LCT-SMEDS. The release profiles showed that the AST release from the LCT-SMEDS<sub>OTM</sub> formulation was higher than from the MCT-SMEDS<sub>OTM</sub> formulation and significantly increased compared to the marketed preparation and raw AST.

As demonstrated in Figure 18 a-c, the release of AST from LCT-SMEDS<sub>OTM</sub> and MCT-SMEDS<sub>OTM</sub> were not quite different in all media. Therefore, it can be concluded that the release of AST from SMEDS was independent of all pH media. Moreover, the data showed that the AST release rate was distinctly reduced on the usage of marketed product as the cumulative AST release was very low with about 30% even after about 8 hours was consumed in all media. In contrast, the SMEDS formulations indicated a significantly enhanced drug release rate as around 40% of cumulative AST release was achieved after 0.5 hour, also about 60% after 1 hr, and about 80% after 2 hrs respectively in all media. Within 4 hrs, the SMEDS formulations reached the maximum percentage of released AST. The final release percentage of both SMEDS formulations were over 90%. Therefore, it is apparent from the profiles of AST release that both SMEDS formulations are relatively faster in the release of drug, as compared to marketed product and raw AST. In contrast to marketed preparation and raw AST, SMEDS formulations produced small droplet size and showed better release rate because they have greater solubility of AST in the excipients of SMEDS (138, 139). In addition, the oil phase of SMEDS may be the factor affecting the release

because it may serve as carrier molecules for active compound molecules to diffuse from dialysis membrane (127, 140).



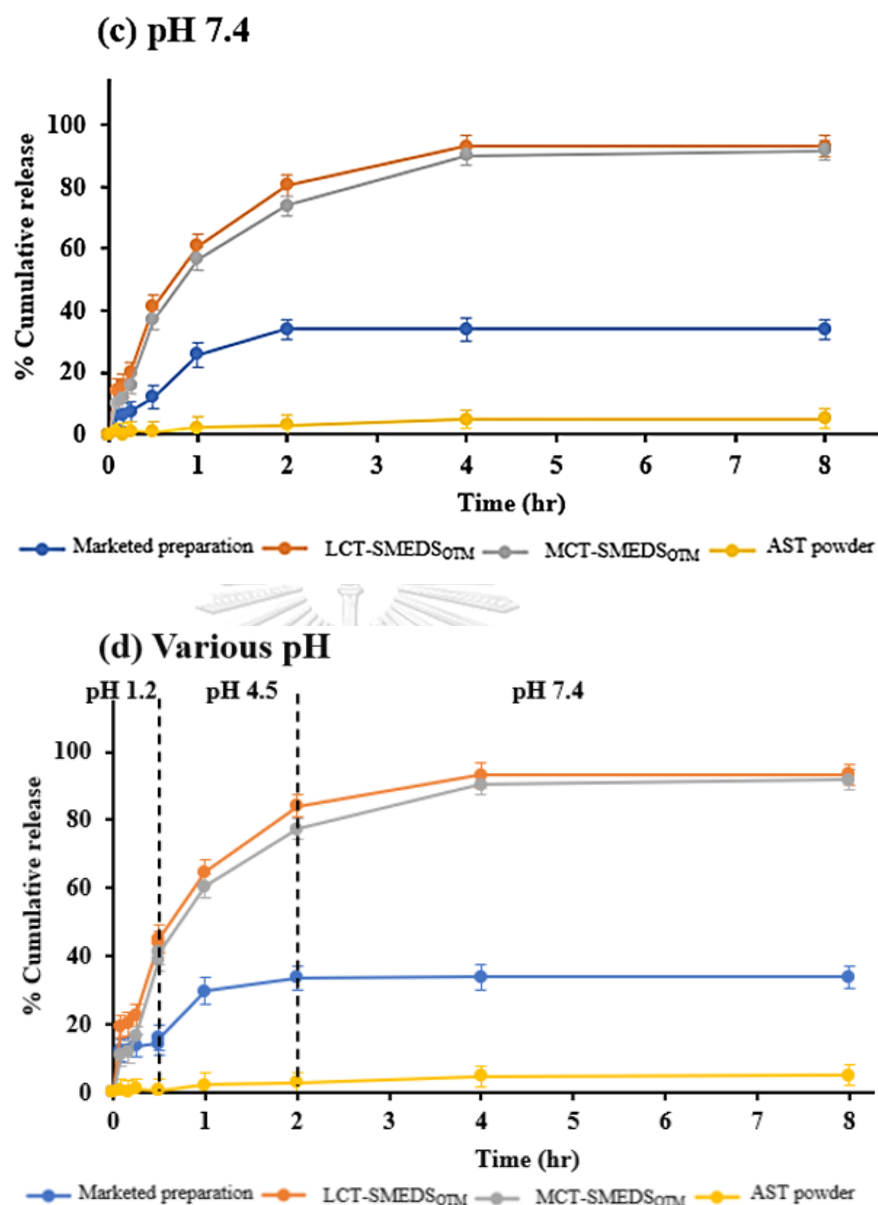


Figure 18. The AST release profiles of LCT-SMEDS, MCT-SMEDS, marketed preparation, and raw AST in different dissolution media (n = 3). (a) pH 1.2, (b) pH 4.5, (c) pH 7.4, and (d) various pH.

Moreover, another dissolution profile was developed by using the data of AST release in various pH to further study the effect of pH on the rate of astaxanthin release. The *in vitro* release profile of AST from

SMEDS formulation over time in different media were shown in Figure 18(d). At pH 1.2, the amount of AST released of both LCT-SMEDS and MCT-SMEDS was about 40% at first 30 min, while at pH 4.5, about 80% of AST was released after 2 hrs. The dissolution rate of AST was more than 90% after 8 hrs. AST release was complete and approached a plateau level within 4 hrs, resulting the values of 93.09 % and 90.24% for LCT-SMEDS and MCT-SMEDS, respectively. It can be observed that the dissolution of optimized LCT-SMEDS and MCT-SMEDS showed good dissolution profiles in all pH media. The overall dissolution rate of all these optimized formulations indicating > 90 % of AST releases indicated the availability of AST at the site of absorption. The results showed that AST-SMEDS could significantly enhance the rapid release of AST and increase the dissolution rate compared with the marketed preparation and untreated AST powder. This might be related to the formation of small droplets and their rapid dispersion. Besides, it was also concluded that the release of AST from the SMEDS formulation was independent of pH.

Furthermore, for better understanding the dissolution behavior of AST in the gastrointestinal tract, the release of AST from the optimized SMEDS formulations was studied by changing the pH continuously (141). The media used in the tests were pH 1.2 HCl buffer for the first 30 min, pH 4.5 acetate buffer for the next 1.5 hrs, and pH 7.4 phosphate buffer for the last 6 hrs. The similar trends as demonstrated in previous dissolution profile (Figure 18(d)) were found for the tested formulations.

## CHAPTER V

### CONCLUSION

Currently, various routes of administration have been studied so that the delivery of the drug can be effective. For the administration of drugs to patients, the most convenient way is considered to be the oral route. Poor oral absorption of many new compounds is caused mainly due to their poor water solubility. For improving oral absorption of poorly soluble compounds, conventional solubilization approaches such as salt formation, cosolvents, and surfactant-based micellar formation are commonly applied in the present.

In the current research, self-microemulsifying astaxanthin delivery systems were developed and optimized for the prevention and cotreatment of Alzheimer disease. A homogenous mixture of the oils, surfactants, and/or co-solvents/surfactants with a fine oil-in-water (o/w) microemulsions formation upon gentle agitation, after dilution with water, are called self-microemulsifying system.

In preformulation study, according to the solubility data of AST, the selection of one medium (MCT) and one long chain triglyceride (castor) which has the highest solubility result was performed for further studies. From the results emulsification efficiency, due to their better emulsification efficiency, Cremophor<sup>®</sup> RH 40 and Tween<sup>®</sup> 80 were used as a surfactant and co-surfactant, respectively, for both oils.

After selection of the excipients, the construction of pseudoternary phase diagram was completed at different surfactant and co-surfactant ratios 1:1, 2:1, 3:1, 4:1, and 5:1 for both the oils. From ternary phase diagram, 4:1 surfactant to co-surfactant ratio was selected for LCT-

SMEDS preparation, while 1:1 surfactant to co-surfactant ratio was selected for MCT-SMEDS.

In this thesis study, one of the aims was to determine the influence of input variables on important characteristics of the formed microemulsions by using the design of experiment approach. The optimization of formulations is usually aimed for determining the amount of the variable that affect the selected responses from which a high-quality product may be developed. The use of statistical experimental design methods makes it possible to experiment with a number of different factors at the same time and gives a clear picture to understand how the factors behave separately and together. Mixture experimental design was utilized in order to evaluate the influence of the microemulsion components on the response variables and optimize the responses simultaneously to determine the most appropriate combination of component proportions. The levels of oil ( $X_1$ ), surfactant ( $X_2$ ), and co-surfactant ( $X_3$ ) were set according to the results of the pseudoternary phase diagram. The droplet size ( $Y_1$ ; nm), PDI ( $Y_2$ ), zeta potential ( $Y_3$ ; mV), active ingredient content ( $Y_4$ ; %), and percentage of transmittance ( $Y_5$ ; %) were examined as the response variables to optimize the formulation. Appropriate design spaces were evolved by Minitab™ Software version 17.

The triglycerides were used to study the influence of AST solubility because they are freely picked up by the chylomicrons and travel through lymphatic system. With two different triglycerides, SMEDS formulations were prepared. The castor oil was selected as long chain triglyceride, while MCT was selected as medium chain triglyceride. As shown in Tables 2 and 3, thirteen SMEDS formulations of each of

these LCT, and MCT were developed using mixture experimental design. Among these formulations, the selection of only the formulation from each batch (LCT-SMEDS<sub>OTM</sub> and MCT-SMEDS<sub>OTM</sub>) that exhibited the required features, was performed.

Droplet size and zeta potential values of LCT-SMEDS were found to be in between 20.17 nm to 128.74 nm and -8.34 mV to -12.9 mV, respectively, while that of MCT-SMEDS formulations were to be from 22.01 nm to 33.2 nm and -9.91 mV to -14.9 mV, respectively. Polydispersity index of all formulations was found to be less than 1 which suggests that uniform distribution of globules throughout formulation. The AST content of LCT-SMEDS and MCT formulations was in the 84.55-99.71% range and in the 90.11-96.69 % range respectively, which points out the uniform dispersion of the active ingredient in formulations. %transmittance of all formulations of LCT-SMEDS of AST was found to be in the range of 75.72 to 98.57%, while %transmittance of all formulations of MCT-SMEDS of AST was found in between 97.43 to 98.8%. This indicates that prepared liquid SMEDS are clearer when the less oil was used in the formulation.

By using the desirability function, the optimization of independent variables was performed. The optimized formulation ratios of  $X_1$ ,  $X_2$ , and  $X_3$  for LCT-SMEDS were 19.59 %, 62.34 %, and 18.03 %, respectively, which provide theoretically the values of 22.71 nm, 0.28, -9.70 mV, 97.87 %, and 98.38 % for  $Y_1$ ,  $Y_2$ ,  $Y_3$ ,  $Y_4$ , and  $Y_5$ , respectively, while that of  $X_1$ ,  $X_2$ , and  $X_3$  for MCT-SMEDS were 12.39 %, 44.98 %, and 42.59 %, respectively which provide theoretical values of 22.02 nm, 0.17, -10.69 mV, 98.72 %, and 97.09 % for  $Y_1$ ,  $Y_2$ ,  $Y_3$ ,  $Y_4$ , and  $Y_5$ , respectively. For confirmation of this experimental design values, three different



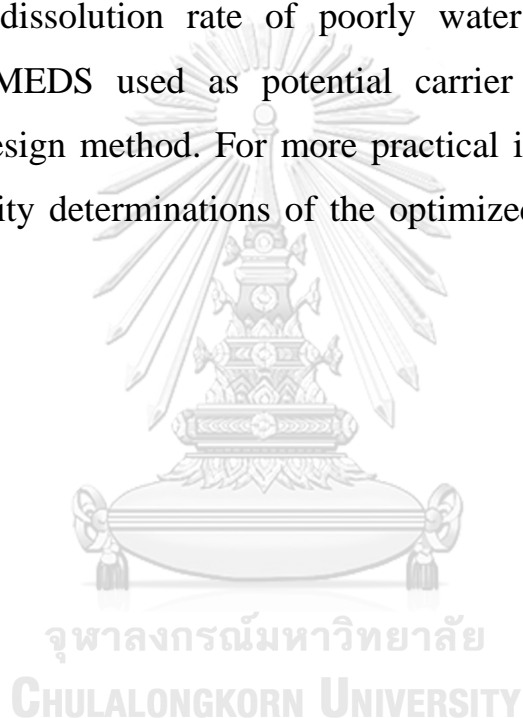
batches of the optimized LCT-SMEDS and MCT-SMEDS formulations were prepared and the responses were measured. The actual values of responses for both LCT-SMEDS and MCT-SMEDS were in close agreement to predicted values. Therefore, the mixture experimental design method used for optimizing LCT-SMEDS and MCT-SMEDS in this research was reliable and accurate.

Moreover, from results of visual observation, emulsification time, and refractive index studies, it was found that optimized formulations of LCT-SMEDS and MCT-SMEDS of AST rapidly formed microemulsion which was clear red solution with no indications of precipitation and phase separation. From the results of characterization of TEM, it was found that oil droplets were homogenous with good integrity. After three cycles of freeze-thaw stability study, all the optimized formulations were found to be stable. Moreover, the diluted microemulsions indicated no signs of drug precipitation, phase separation, creaming, and cracking after subjected to freeze-thaw cycles. Therefore, based on the above evaluation of the optimized formulations, it could be concluded that rapid microemulsion with good physicochemical properties and stability were generated by LCT-SMEDDS and MCT-SMEDS formulations.

According to the above-mentioned results, LCT-SMEDS<sub>OTM</sub> and MCT-SMEDS<sub>OTM</sub> results were found not to be significantly different. However, LCT-SMEDS<sub>OTM</sub> may be the most stable formulation as the inter particulate repulsion of long chain triglycerides allowed them to disperse for a longer period of time.

In addition, by comparison with marketed preparation and raw AST powder, remarkable enhancement of *in vitro* release profile was

indicated in percentage with the use of the optimized LCT-SMEDS and MCT-SMEDS formulations. Thus, mixture experimental design is an effective tool for the optimization of AST-SMEDS formulation. Moreover, SMEDS could be a promising way in order to enhance the oral bioavailability of a poorly water-soluble AST. Current study showed the effectiveness of SMEDS formulation in solubility and dissolution improvement of AST. Therefore, it comes to conclusion that the solubility and dissolution rate of poorly water-soluble AST can be resolved by SMEDS used as potential carrier system with mixture experimental design method. For more practical improvement in future, the bioavailability determinations of the optimized AST-SMEDS would be required.



## REFERENCES



จุฬาลงกรณ์มหาวิทยาลัย  
**CHULALONGKORN UNIVERSITY**

1. Wojsiat J, Zoltowska KM, Laskowska-Kaszub K, Wojda U. Oxidant/antioxidant imbalance in Alzheimer's disease: therapeutic and diagnostic prospects. *Oxidative Medicine and Cellular Longevity*. 2018;28:16-32.
2. Llanos-Gonzalez E, Henares-Chavarino A, Pedrero-Prieto CM, Garcia-Carpintero S, Frontinan-Rubio J, Sancho-Bielsa FJ, Alcain FJ, Peinado JR, Rabanal-Ruiz Y, Duran-Prado M. Interplay between mitochondrial oxidative disorders and proteostasis in Alzheimer's Disease. *Frontiers in Neuroscience*. 2020;13:1444-1453.
3. Feng Y, Wang X. Antioxidant therapies for Alzheimer's disease. *Oxidative Medicine and Cellular Longevity*. 2012;22:17-34.
4. Rottkamp CA, Nunomura A, Raina AK, Sayre LM, Perry G, Smith MA. Oxidative stress, antioxidants, and Alzheimer disease. *Alzheimer Disease & Associated Disorders*. 2000;14(1):62-66.
5. Dose J, Matsugo S, Yokokawa H, Koshida Y, Okazaki S, Seidel U, Eggersdorfer M, Rimbach G, Esatbeyoglu T. Free radical scavenging and cellular antioxidant properties of astaxanthin. *International Journal of Molecular Sciences*. 2016;17(1):103-117.
6. Galasso C, Corinaldesi C, Sansone C. Carotenoids from marine organisms: biological functions and industrial applications. *Antioxidants*. 2017;6(4):96-129.
7. Galasso C, Orefice I, Pellone P, Cirino P, Miele R, Ianora A, Brunet C, Sansone C. On the neuroprotective role of astaxanthin: new perspectives?. *Marine Drugs*. 2018;16(8):247-262.
8. Grimmig B, Kim SH, Nash K, Bickford PC, Shytle RD. Neuroprotective mechanisms of astaxanthin: a potential therapeutic role in preserving cognitive function in age and neurodegeneration. *Geroscience*. 2017;39(1):19-32.
9. Yuan JP, Peng J, Yin K, Wang JH. Potential health-promoting effects of astaxanthin: a high-value carotenoid mostly from microalgae. *Molecular Nutrition & Food Research*. 2011;55(1):150-65.
10. Cirino P, Brunet C, Ciaravolo M, Galasso C, Musco L, Vega Fernandez T, Sansone C, Toscano A. The sea urchin *Arbacia lixula*: a novel natural source of astaxanthin. *Marine Drugs*. 2017;15(6):187-197.
11. Galasso C, Orefice I, Toscano A, Vega Fernandez T, Musco L, Brunet C, Sansone C, Cirino P. Food modulation controls astaxanthin accumulation in eggs of the sea urchin *Arbacia lixula*. *Marine Drugs*. 2018;16(6):186-195.

12. Ohgami K, Shiratori K, Kotake S, Nishida T, Mizuki N, Yazawa K, Ohno S. Effects of astaxanthin on lipopolysaccharide-induced inflammation *in vitro* and *in vivo*. *Investigative Ophthalmology & Visual Science*. 2003;44(6):2694-701.
13. Solomonov Y, Hadad N, Levy R. The combined anti-Inflammatory effect of astaxanthin, Lyc-O-Mato and carnosic acid. *Marine Drugs*. 2018;8(1):653-660.
14. Lin SF, Chen YC, Chen RN, Chen LC, Ho HO, Tsung YH, Sheu MT, Liu DZ. Improving the stability of astaxanthin by microencapsulation in calcium alginate beads. *Marine Drugs*. 2016;11(4):132-144.
15. Pan L, Wang H, Gu K. Nanoliposomes as vehicles for astaxanthin: characterization, *in vitro* release evaluation and structure. *Molecules*. 2018;23(11):2822-2833.
16. Guan L, Liu J, Yu H, Tian H, Wu G, Liu B, Dong P, Li J, Liang X. Water-dispersible astaxanthin-rich nanopowder: preparation, oral safety and antioxidant activity *in vivo*. *Food & Function*. 2019;10(3):1386-97.
17. Tonda-Turo C, Origlia N, Mattu C, Accorroni A, Chiono V. Current limitations in the treatment of Parkinson's and Alzheimer's diseases: state-of-the-art and future perspective of polymeric carriers. *Current Medicinal Chemistry*. 2018;25(41):5755-71.
18. Jannin V, Musakhanian J, Marchaud D. Approaches for the development of solid and semi-solid lipid-based formulations. *Advanced Drug Delivery Reviews*. 2008;60(6):734-46.
19. Kalepu S, Manthina M, Padavala V. Oral lipid-based drug delivery systems—an overview. *Acta Pharmaceutica Sinica B*. 2013;3(6):361-72.
20. Xu W, Ling P, Zhang T. Polymeric micelles, a promising drug delivery system to enhance bioavailability of poorly water-soluble drugs. *Journal of Drug Delivery*. 2013;13:112-119.
21. Jiang GB, Quan D, Liao K, Wang H. Novel polymer micelles prepared from chitosan grafted hydrophobic palmitoyl groups for drug delivery. *Molecular Pharmaceutics*. 2006;3(2):152-60.
22. Alexander-Bryant AA, Berg-Foels WS, Wen X. Bioengineering strategies for designing targeted cancer therapies. *Advances in Cancer Research* 2013;118:1-59.
23. Basalious EB, Shawky N, Badr-Eldin SM. SNEDDS containing bioenhancers for improvement of dissolution and oral absorption of

- lacidipine. I: development and optimization. *International Journal of Pharmaceutics*. 2010;391(1-2):203-11.
24. Ansari KA, Pagar KP, Anwar S, Vavia PR. Design and optimization of self-microemulsifying drug delivery system (SMEDDS) of felodipine for chronotherapeutic application. *Brazilian Journal of Pharmaceutical Sciences*. 2014;50(1):203-12.
  25. Spornath A, Aserin A. Microemulsions as carriers for drugs and nutraceuticals. *Advances in Colloid and Interface Science*. 2006;128:47-64.
  26. Akula S, Gurram AK, Devireddy SR. Self-microemulsifying drug delivery systems: an attractive strategy for enhanced therapeutic profile. *International Scholarly Research Notices*. 2014;24:11-23.
  27. Zhang P, Liu Y, Feng N, Xu J. Preparation and evaluation of self-microemulsifying drug delivery system of oridonin. *International Journal of Pharmaceutics*. 2008;355(1-2):269-276.
  28. Larsen A, Holm R, Pedersen ML, Müllertz A. Lipid-based formulations for danazol containing a digestible surfactant, Labrafil M2125CS: *in vivo* bioavailability and dynamic *in vitro* lipolysis. *Pharmaceutical Research*. 2008;25(12):2769-77.
  29. Singh B, Bandopadhyay S, Kapil R, Singh R, Katare OP. Self-emulsifying drug delivery systems (SEDDS): formulation development, characterization, and applications. *Critical Reviews™ in Therapeutic Drug Carrier Systems*. 2009;26(5):427-451.
  30. Shah NH, Carvajal MT, Patel CI, Infeld MH, Malick AW. Self-emulsifying drug delivery systems (SEDDS) with polyglycolized glycerides for improving *in vitro* dissolution and oral absorption of lipophilic drugs. *International Journal of Pharmaceutics*. 1994;106(1):15-23.
  31. Charman SA, Charman WN, Rogge MC, Wilson TD, Dutko FJ, Pouton CW. Self-emulsifying drug delivery systems: formulation and biopharmaceutic evaluation of an investigational lipophilic compound. *Pharmaceutical Research*. 1992;9(1):87-93.
  32. Holm R, Jensen IH, Sonnergaard J. Optimization of self-microemulsifying drug delivery systems (SMEDDS) using a D-optimal design and the desirability function. *Drug Development and Industrial Pharmacy*. 2006;32(9):1025-32.
  33. Tran T, Rades T, Mullertz A. Formulation of self-nanoemulsifying drug delivery systems containing monoacyl phosphatidylcholine

- and Kolliphor® RH40 using experimental design. *Asian Journal of Pharmaceutical Sciences*. 2018;13(6):536-45.
34. Liu Y, Zhang P, Feng N, Zhang X, Wu S, Zhao J. Optimization and *in situ* intestinal absorption of self-microemulsifying drug delivery system of oridonin. *International Journal of Pharmaceutics*. 2009;365(1-2):136-42.
  35. Marasini N, Yan YD, Poudel BK, Choi HG, Yong CS, Kim JO. Development and optimization of self-nanoemulsifying drug delivery system with enhanced bioavailability by Box–Behnken design and desirability function. *Journal of Pharmaceutical Sciences*. 2012;101(12):4584-96.
  36. Yeom DW, Chae BR, Son HY, Kim JH, Chae JS, Song SH, Oh D, Choi YW. Enhanced oral bioavailability of valsartan using a polymer-based supersaturable self-microemulsifying drug delivery system. *International Journal of Nanomedicine*. 2017;12:3533-3545.
  37. Mura P, Furlanetto S, Cirri M, Maestrelli F, Marras AM, Pinzauti S. Optimization of glibenclamide tablet composition through the combined use of differential scanning calorimetry and D-optimal mixture experimental design. *Journal of Pharmaceutical and Biomedical Analysis*. 2005;37(1):65-71.
  38. Bhattacharya S. Design and development of docetaxel solid self-microemulsifying drug delivery system using principal component analysis and D-optimal design. *Asian Journal of Pharmaceutics*. 2018;12(01):73-81.
  39. Sandhu PS, Kumar R, Beg S, Jain S, Kushwah V, Katare OP, Singh B. Natural lipids enriched self-nano-emulsifying systems for effective co-delivery of tamoxifen and naringenin: Systematic approach for improved breast cancer therapeutics. *Nanomedicine: Nanotechnology, Biology and Medicine*. 2017;13(5):1703-13.
  40. Porter CJ, Charman WN. Uptake of drugs into the intestinal lymphatics after oral administration. *Advanced Drug Delivery Reviews*. 1997;25(1):71-89.
  41. Caliph SM, Charman WN, Porter CJ. Effect of short-, medium-, and long-chain fatty acid-based vehicles on the absolute oral bioavailability and intestinal lymphatic transport of halofantrine and assessment of mass balance in lymph-cannulated and non-cannulated rats. *Journal of Pharmaceutical Sciences*. 2000;89(8):1073-84.

42. Palin KJ, Wilson CG. The effect of different oils on the absorption of probucol in the rat. *Journal of Pharmacy and Pharmacology*. 1984;36(9):641-3.
43. Porter CJ, Kaukonen AM, Boyd BJ, Edwards GA, Charman WN. Susceptibility to lipase-mediated digestion reduces the oral bioavailability of danazol after administration as a medium-chain lipid-based microemulsion formulation. *Pharmaceutical Research*. 2004;21(8):1405-12.
44. Khoo SM, Humberstone AJ, Porter CJ, Edwards GA, Charman WN. Formulation design and bioavailability assessment of lipidic self-emulsifying formulations of halofantrine. *International Journal of Pharmaceutics*. 1998;167(1-2):155-64.
45. Grove M, Müllertz A, Nielsen JL, Pedersen GP. Bioavailability of seocalcitol: II: development and characterisation of self-microemulsifying drug delivery systems (SMEDDS) for oral administration containing medium and long chain triglycerides. *European Journal of Pharmaceutical Sciences*. 2006;28(3):233-42.
46. Ferri CP, Prince M, Brayne C, Brodaty H, Fratiglioni L, Ganguli M, Hall K, Hasegawa K, Hendrie H, Huang Y, Jorm A. Global prevalence of dementia: a Delphi consensus study. *The Lancet*. 2005;366(9503):2112-7.
47. Kalaria RN, Maestre GE, Arizaga R, Friedland RP, Galasko D, Hall K, Luchsinger JA, Ogunniyi A, Perry EK, Potocnik F, Prince M. Alzheimer's disease and vascular dementia in developing countries: prevalence, management, and risk factors. *The Lancet Neurology*. 2008;7(9):812-26.
48. Van Cauwenberghe C, Van Broeckhoven C, Sleegers K. The genetic landscape of Alzheimer disease: clinical implications and perspectives. *Genetics in Medicine*. 2016;18(5):421-30.
49. Bekris LM, Yu CE, Bird TD, Tsuang DW. Genetics of Alzheimer disease. *Journal of Geriatric Psychiatry and Neurology*. 2010;23(4):213-27.
50. Isik AT. Late onset Alzheimer's disease in older people. *Clinical Interventions in Aging*. 2010;5(2):307-311.
51. Irvine GB, El-Agnaf OM, Shankar GM, Walsh DM. Protein aggregation in the brain: the molecular basis for Alzheimer's and Parkinson's diseases. *Molecular Medicine*. 2008;14(7):451-64.



52. Wildsmith KR, Holley M, Savage JC, Skerrett R, Landreth GE. Evidence for impaired amyloid  $\beta$  clearance in Alzheimer's disease. *Alzheimer's Research & Therapy*. 2013;5(4):1-6.
53. Manczak M, Anekonda TS, Henson E, Park BS, Quinn J, Reddy PH. Mitochondria are a direct site of A $\beta$  accumulation in Alzheimer's disease neurons: implications for free radical generation and oxidative damage in disease progression. *Human Molecular Genetics*. 2006;15(9):1437-49.
54. Hanzel CE, Pichet-Binette A, Pimentel LS, Iulita MF, Allard S, Ducatzenzeiler A, Do Carmo S, Cuellar AC. Neuronal driven pre-plaque inflammation in a transgenic rat model of Alzheimer's disease. *Neurobiology of Aging*. 2014;35(10):2249-62.
55. de la Monte SM, Wands JR. Molecular indices of oxidative stress and mitochondrial dysfunction occur early and often progress with severity of Alzheimer's disease. *Journal of Alzheimer's Disease*. 2006;9(2):167-81.
56. Nunomura A, Perry G, Aliev G, Hirai K, Takeda A, Balraj EK, Jones PK, Ghanbari H, Wataya T, Shimohama S, Chiba S. Oxidative damage is the earliest event in Alzheimer disease. *Journal of Neuropathology & Experimental Neurology*. 2001;60(8):759-67.
57. Nichols JA, Katiyar SK. Skin photoprotection by natural polyphenols: anti-inflammatory, antioxidant and DNA repair mechanisms. *Archives of Dermatological research*. 2010;302(2):71-83.
58. Berthon JY, Nachat-Kappes R, Bey M, Cadoret JP, Renimel I, Filaire E. Marine algae as attractive source to skin care. *Free Radical Research*. 2017;51(6):555-67.
59. Gonzalez S, Gilaberte Y, Philips N, Juarranz A. Current trends in photoprotection-A new generation of oral photoprotectors. *The Open Dermatology Journal*. 2011;5(1):322-27.
60. Ambati RR, Phang SM, Ravi S, Aswathanarayana RG. Astaxanthin: sources, extraction, stability, biological activities and its commercial applications-a review. *Marine Drugs*. 2014;12(1):128-52.
61. Shanmugapriya K, Kim H, Saravana PS, Chun BS, Kang HW. Astaxanthin-alpha tocopherol nanoemulsion formulation by emulsification methods: investigation on anticancer, wound healing, and antibacterial effects. *Colloids and Surfaces B: Biointerfaces*. 2018;17(2):170-9.

62. Rodriguez-Ruiz V, Salatti-Dorado JA, Barzegari A, Nicolas-Boluda A, Houaoui A, Caballo C, Caballero-Casero N, Sicilia D, Bastias Venegas J, Pauthe E, Omid Y. Astaxanthin-loaded nanostructured lipid carriers for preservation of antioxidant activity. *Molecules*. 2018 ;23(10):2601-11.
63. Lee KW, Porter CJ, Boyd BJ. The effect of administered dose of lipid-based formulations on the in vitro and in vivo performance of cinnarizine as a model poorly water-soluble drug. *Journal of Pharmaceutical Sciences*. 2013;102(2):565-78.
64. Constantinides PP, Scalart JP. Formulation and physical characterization of water-in-oil microemulsions containing long-versus medium-chain glycerides. *International Journal of Pharmaceutics*. 1997;158(1):57-68.
65. Craig DQ, Barker SA, Banning D, Booth SW. An investigation into the mechanisms of self-emulsification using particle size analysis and low frequency dielectric spectroscopy. *International Journal of Pharmaceutics*. 1995;114(1):103-10.
66. Gershanik T, Benita S. Self-dispersing lipid formulations for improving oral absorption of lipophilic drugs. *European Journal of Pharmaceutics and Biopharmaceutics*. 2000;50(1):179-88.
67. Dokania S, Joshi AK. Self-microemulsifying drug delivery system (SMEDDS)-challenges and road ahead. *Drug Delivery*. 2015;22(6):675-90.
68. Gursoy RN, Benita S. Self-emulsifying drug delivery systems (SEDDS) for improved oral delivery of lipophilic drugs. *Biomedicine & Pharmacotherapy*. 2004;58(3):173-82.
69. Porter CJ, Trevaskis NL, Charman WN. Lipids and lipid-based formulations: optimizing the oral delivery of lipophilic drugs. *Nature Reviews Drug Discovery*. 2007;6(3):231-48.
70. Rahman MA, Hussain A, Hussain MS, Mirza MA, Iqbal Z. Role of excipients in successful development of self-emulsifying/microemulsifying drug delivery system (SEDDS/SMEDDS). *Drug Development and Industrial Pharmacy*. 2013;39(1):1-9.
71. Tang B, Cheng G, Gu JC, Xu CH. Development of solid self-emulsifying drug delivery systems: preparation techniques and dosage forms. *Drug Discovery Today*. 2008;13(13-14):606-12.
72. Kimura M, Shizuki M, Miyoshi K, Sakai T, Hidaka H, Takamura H, Matoba T. Relationship between the molecular structures and emulsification properties of edible oils. *Bioscience, Biotechnology, and Biochemistry*. 1994;58(7):1258-61.

73. Perlman ME, Murdande SB, Gumkowski MJ, Shah TS, Rodricks CM, Thornton-Manning J, Freel D, Erhart LC. Development of a self-emulsifying formulation that reduces the food effect for torcetrapib. *International Journal of Pharmaceutics*. 2008;351(1-2):15-22.
74. Prajapati HN, Patel DP, Patel NG, Dalrymple DD, Serajuddin AT. Effect of difference in fatty acid chain lengths of medium-chain lipids on lipid-surfactant-water phase diagrams and drug solubility. *Journal of Excipients and Food Chemicals*. 2011;2(3):73-88.
75. Pouton CW, Porter CJ. Formulation of lipid-based delivery systems for oral administration: materials, methods and strategies. *Advanced Drug Delivery Reviews*. 2008;60(6):625-37.
76. Chen ML. Lipid excipients and delivery systems for pharmaceutical development: a regulatory perspective. *Advanced Drug Delivery Reviews*. 2008;60(6):768-77.
77. Nankervis R, Davis SS, Day NH, Shaw PN. Effect of lipid vehicle on the intestinal lymphatic transport of isotretinoin in the rat. *International Journal of Pharmaceutics*. 1995;119(2):173-81.
78. Constantinides PP, Scalart JP, Lancaster C, Marcello J, Marks G, Ellens H, Smith PL. Formulation and intestinal absorption enhancement evaluation of water-in-oil microemulsions incorporating medium-chain glycerides. *Pharmaceutical Research*. 1994;11(10):1385-90.
79. Porter CJ, Pouton CW, Cuine JF, Charman WN. Enhancing intestinal drug solubilisation using lipid-based delivery systems. *Advanced drug delivery reviews*. 2008;60(6):673-91.
80. Mullertz A, Ogbonna A, Ren S, Rades T. New perspectives on lipid and surfactant based drug delivery systems for oral delivery of poorly soluble drugs. *Journal of pharmacy and pharmacology*. 2010;62(11):1622-36.
81. Date AA, Nagarsenker MS. Parenteral microemulsions: an overview. *International Journal of Pharmaceutics*. 2008;355(1-2):19-30.
82. Hauss DJ, Fogal SE, Ficorilli JV, Price CA, Roy T, Jayaraj AA, Keirns JJ. Lipid-based delivery systems for improving the bioavailability and lymphatic transport of a poorly water-soluble LTB<sub>4</sub> inhibitor. *Journal of Pharmaceutical Sciences*. 1998;87(2):164-9.
83. Stegemann S, Leveiller F, Franchi D, De Jong H, Lindén H. When poor solubility becomes an issue: from early stage to proof of

- concept. *European Journal of Pharmaceutical Sciences*. 2007;31(5):249-61.
84. Nigade PM, Patil SL, Tiwari SS. Self emulsifying drug delivery system (SEDDS): A review. *International Journal of Pharmacy and Biological Sciences*. 2012;2(2):42-52.
  85. N. Politis S, Colombo P, Colombo G, M. Rekkas D. Design of experiments (DoE) in pharmaceutical development. *Drug Development and Industrial Pharmacy*. 2017;43(6):889-901.
  86. Achouri D, Hornebecq V, Piccerelle P, Andrieu V, Sergent M. Self-assembled liquid crystalline nanoparticles as an ophthalmic drug delivery system. Part I: influence of process parameters on their preparation studied by experimental design. *Drug Development and Industrial Pharmacy*. 2015;41(1):109-15.
  87. Achouri D, Sergent M, Tonetto A, Piccerelle P, Andrieu V, Hornebecq V. Self-assembled liquid crystalline nanoparticles as an ophthalmic drug delivery system. Part II: optimization of formulation variables using experimental design. *Drug Development and Industrial Pharmacy*. 2015;41(3):493-501.
  88. Cornell JA. Experiments with mixtures: designs, models, and the analysis of mixture data. John Wiley & Sons;2011;5(1): 6-8.
  89. Aboulfotouh K, Allam AA, El-Badry M, El-Sayed AM. Development and in vitro/in vivo performance of self-nanoemulsifying drug delivery systems loaded with candesartan cilexetil. *European Journal of Pharmaceutical Sciences*. 2017;109:503-13.
  90. Jaiswal P, Aggarwal G, Harikumar SL, Singh K. Development of self-microemulsifying drug delivery system and solid-self-microemulsifying drug delivery system of telmisartan. *International Journal of Pharmaceutical Investigation*. 2014;4(4):195–206.
  91. Qureshi MJ, Mallikarjun C, Kian WG. Enhancement of solubility and therapeutic potential of poorly soluble lovastatin by SMEDDS formulation adsorbed on directly compressed spray dried magnesium aluminometasilicate liquid loadable tablets: a study in diet induced hyperlipidemic rabbits. *Asian Journal of Pharmaceutical Sciences*. 2015;10(1):40-56.
  92. Son HY, Chae BR, Choi JY, Shin DJ, Goo YT, Lee ES, Kang TH, Kim CH, Yoon HY, Choi YW. Optimization of self-microemulsifying drug delivery system for phospholipid complex

- of telmisartan using D-optimal mixture design. *International Journal of Pharmaceutical investigation*. 2018;13(12):121-29.
93. Danaei M, Dehghankhold M, Ataei S, Hasanzadeh Davarani F, Javanmard R, Dokhani A, Khorasani S, Mozafari MR. Impact of particle size and polydispersity index on the clinical applications of lipidic nanocarrier systems. *Pharmaceutics*. 2018;10(2):57.
  94. Joseph E, Singhvi G. Multifunctional nanocrystals for cancer therapy: A potential nanocarrier. *Nanomaterials for Drug Delivery and Therapy*. 2019;11(1):91-116.
  95. Allen LV, Bassani GS, Elder EJ, Parr AF. Strength and stability testing for compounded preparations. *International Journal of Pharmaceutical investigation*. 2016;2(12):96-104.
  96. Shah A, Thakkar V, Gohel M, Baldaniya L, Gandhi T. Optimization of Self Micro Emulsifying Drug Delivery System Containing Curcumin and Artemisinin Using D-Optimal Mixture Design. *Journal of Medical and Pharmaceutical Sciences*. 2017;3(5):388-398.
  97. Singh AK, Chaurasiya A, Awasthi A, Mishra G, Asati D, Khar RK, Mukherjee R. Oral bioavailability enhancement of exemestane from self-microemulsifying drug delivery system (SMEDDS). *Journal of the American Association of Pharmaceutical Scientists*. 2009;10(3):906-16.
  98. Shen H, Zhong M. Preparation and evaluation of self-microemulsifying drug delivery systems (SMEDDS) containing atorvastatin. *Journal of Pharmacy and Pharmacology*. 2006;58(9):1183-91.
  99. Yang R, Huang X, Dou J, Zhai G, Su L. Self-microemulsifying drug delivery system for improved oral bioavailability of oleanolic acid: design and evaluation. *International Journal of Nanomedicine*. 2013;8:2917.
  100. Kassem AA, Mohsen AM, Ahmed RS, Essam TM. Self-nanoemulsifying drug delivery system (SNEDDS) with enhanced solubilization of nystatin for treatment of oral candidiasis: Design, optimization, in vitro and in vivo evaluation. *Journal of Molecular Liquids*. 2016;218:219-32.
  101. Agrawal AG, Kumar A, Gide PS. Self emulsifying drug delivery system for enhanced solubility and dissolution of glipizide. *Colloids and Surfaces B: Biointerfaces*. 2015;126:553-60.
  102. Deshmukh A, Kulkarni S. Solid self-microemulsifying drug delivery system of ritonavir. *Drug Development and Industrial Pharmacy*. 2014;40(4):477-87.

103. Zhang P, Liu Y, Feng N, Xu J. Preparation and evaluation of self-microemulsifying drug delivery system of oridonin. *International Journal of Pharmaceutics*. 2008;355(1-2):269-76.
104. Palamakula A, Khan MA. Evaluation of cytotoxicity of oils used in coenzyme Q10 Self-Emulsifying Drug Delivery Systems (SEDDS). *International Journal of Pharmaceutics*. 2004;273(1-2):63-73.
105. Parmar N, Singla N, Amin S, Kohli K. Study of co-surfactant effect on nanoemulsifying area and development of lercanidipine loaded (SNEDDS) self nanoemulsifying drug delivery system. *Colloids and Surfaces B: Biointerfaces*. 2011;86(2):327-38.
106. Pouton CW, Porter CJ. Formulation of lipid-based delivery systems for oral administration: materials, methods and strategies. *Advanced Drug Delivery Reviews*. 2008;60(6):625-37.
107. Madan JR, Sudarshan B, Kadam VS, Kama D. Formulation and development of self-microemulsifying drug delivery system of pioglitazone. *Asian Journal of Pharmaceutics: Free full text articles from Asian J Pharm*. 2014;8(1):111-19.
108. Tripathi CB, Beg S, Kaur R, Shukla G, Bandopadhyay S, Singh B. Systematic development of optimized SNEDDS of artemether with improved biopharmaceutical and antimalarial potential. *Drug Delivery*. 2016;23(9):3209-23.
109. Prajapati HN, Dalrymple DM, Serajuddin AT. A comparative evaluation of mono-, di- and triglyceride of medium chain fatty acids by lipid/surfactant/water phase diagram, solubility determination and dispersion testing for application in pharmaceutical dosage form development. *Pharmaceutical Research*. 2012;29(1):285-305.
110. Bolko K, Zvonar A, Gasperlin M. Mixed lipid phase SMEDDS as an innovative approach to enhance resveratrol solubility. *Drug Development and Industrial Pharmacy*. 2014;40(1):102-9.
111. Lee SY, Pung YY, Khor BK, Kong WE, Tan CT, Teo SY. Lipid-based delivery system for topical phenytoin. *Journal of Applied Pharmaceutical Science*. 2016;6:014-20.
112. Azeem A, Rizwan M, Ahmad FJ, Iqbal Z, Khar RK, Aqil M, Talegaonkar S. Nanoemulsion components screening and selection: a technical note. *Journal of American Association of Pharmaceutical Scientists*. 2009;10(1):69-76.
113. Elnaggar YS, El-Massik MA, Abdallah OY. Self-nanoemulsifying drug delivery systems of tamoxifen citrate: design and

- optimization. *International Journal of Pharmaceutics*. 2009 ;380(1-2):133-41.
114. Yeom DW, Song YS, Kim SR, Lee SG, Kang MH, Lee S, Choi YW. Development and optimization of a self-microemulsifying drug delivery system for atorvastatin calcium by using D-optimal mixture design. *International Journal of Nanomedicine*. 2015;10(2):3865-72.
  115. Phillips GO, Williams PA, editors. *Handbook of Hydrocolloids (Second Edition)*. Woodhead Publishing. 2009;10(2):359-82.
  116. Pol AS, Patel PA, Hegde D. Peppermint oil based drug delivery system of aceclofenac with improved anti-inflammatory activity and reduced Ulcerogenecity. *Internation Journal of Pharma and Biosciences Technology*. 2013;1(2):89-101.
  117. Lawrence MJ. Microemulsions as drug delivery vehicles. *Current Opinion in Colloid & Interface Science*. 1996;1(6):826-32.
  118. Bandivadekar M, Pancholi S, Kaul-Ghanekar R, Choudhari A, Koppikar S. Single non-ionic surfactant based self-nanoemulsifying drug delivery systems: formulation, characterization, cytotoxicity and permeability enhancement study. *Drug Development and Industrial Pharmacy*. 2013;39(5):696-703.
  119. Wakerly MG, Pouton CW, Meakin BJ. Evaluation of the self-emulsifying performance of a non-ionic surfactant-vegetable oil mixture. *Journal of Pharmacy and Pharmacology*. 1987;39(6):70-86.
  120. Chen ML. Lipid excipients and delivery systems for pharmaceutical development: a regulatory perspective. *Advanced Drug Delivery Reviews*. 2008;60(6):768-77.
  121. Cerpnjak K, Zvonar A, Gasperlin M, Vrecer F. Lipid-based systems as a promising approach for enhancing the bioavailability of poorly water-soluble drugs. *Drug Development and Industrial Pharmacy*. 2013;63(4):427-45.
  122. Rao BC, Vidyadhara S, Sasidhar RL, Chowdary YA. Formulation and evaluation of liquid loaded tablets containing docetaxel-self nano emulsifying drug delivery systems. *Tropical Journal of Pharmaceutical Research*. 2015;14(4):567-73.
  123. Prajapat MD, Patel NJ, Bariya A, Patel SS, Butani SB. Formulation and evaluation of self-emulsifying drug delivery system for nimodipine, a BCS class II drug. *Journal Drug Delivery Sciences and Technology*. 2017;39:59-68.

124. Constantinides PP. Lipid microemulsions for improving drug dissolution and oral absorption: physical and biopharmaceutical aspects. *Pharmaceutical Research*. 1995;12(11):1561-72.
125. Lawrence MJ, Rees GD. Microemulsion-based media as novel drug delivery systems. *Advanced Drug Delivery Reviews*. 2000;45(1):89-121.
126. Patel AR, Vavia PR. Preparation and in vivo evaluation of SMEDDS (self-microemulsifying drug delivery system) containing fenofibrate. *Journal of American Association of Pharmaceutical Scientists*. 2007;9(3):344-52.
127. Dixit AR, Rajput SJ, Patel SG. Preparation and bioavailability assessment of SMEDDS containing valsartan. *Journal of American Association of Pharmaceutical Scientists*. 2010;11(1):314-21.
128. Yeom DW, Song YS, Kim SR, Lee SG, Kang MH, Lee S, Choi YW. Development and optimization of a self-microemulsifying drug delivery system for atorvastatin calcium by using D-optimal mixture design. *International Journal of Nanomedicine*. 2015;10(1):3865-73.
129. Kamboj S, Rana V. Quality-by-design based development of a self-microemulsifying drug delivery system to reduce the effect of food on Nelfinavir mesylate. *International Journal of Pharmaceutics*. 2016;501(1-2):311-25.
130. Constantinides PP, Scalart JP. Formulation and physical characterization of water-in-oil microemulsions containing long-versus medium-chain glycerides. *International Journal of Pharmaceutics*. 1997;158(1):57-68.
131. Baboota S, Shakeel F, Ahuja A, Ali J, Shafiq S. Design, development and evaluation of novel nanoemulsion formulations for transdermal potential of celecoxib. *A Quarterly Journal of Croatian Pharmaceutical Society and Slovenian Pharmaceutical Society*. 2007;57(3):315-32.
132. Prajapat MD, Patel NJ, Bariya A, Patel SS, Butani SB. Formulation and evaluation of self-emulsifying drug delivery system for nimodipine, a BCS class II drug. *Journal of Drug Delivery Sciences and Technology*. 2017;39(1):59-68.
133. Mundada V, Sawant K. Enhanced oral bioavailability and anticoagulant activity of dabigatran etexilate by self-micro emulsifying drug delivery system: systematic development. *Journal of Nanomedicine and Nanotechnology*. 2018;9(1):480-92.
134. Qi X, Wang L, Zhu J, Hu Z, Zhang J. Self-double-emulsifying drug delivery system (SDEDDS): a new way for oral delivery of



- drugs with high solubility and low permeability. *International Journal of Pharmaceutics*. 2011;409(1-2):245-51.
135. Pandey V, Kohli S. SMEDDS of pioglitazone: Formulation, *in-vitro* evaluation and stability studies. *Future Journal of Pharmaceutical Sciences*. 2017;3(1):53-59.
136. Saritha D, Bose P, Nagaraju R. Formulation and evaluation of self emulsifying drug delivery system (SEDDS) of Ibuprofen. *International Journal of Pharmaceutical Sciences and Research*. 2014;5(9):3511-9.
137. Hassan S, Prakash G, Ozturk AB, Saghazadeh S, Sohail MF, Seo J, Dokmeci MR, Zhang YS, Khademhosseini A. Evolution and clinical translation of drug delivery nanomaterials. *Nano Today*. 2017;15(1):91-106.
138. Cui J, Yu B, Zhao Y, Zhu W, Li H, Lou H, Zhai G. Enhancement of oral absorption of curcumin by self-microemulsifying drug delivery systems. *International Journal of Pharmaceutics*. 2009;371(1-2):148-55.
139. Patel MJ, Patel NM, Patel RB, Patel RP. Formulation and evaluation of self-microemulsifying drug delivery system of lovastatin. *Asian Journal of Pharmaceutical Sciences*. 2010;5(6):266-75.
140. Bachhav YG, Patravale VB. SMEDDS of glyburide: formulation, *in vitro* evaluation, and stability studies. *Journal of American Association of Pharmaceutical Scientists*. 2009;10(2):482-7.
141. Chuong MC, Christensen JM, Ayres JW. New dissolution method for mesalamine tablets and capsules. *Dissolution Technology*. 2008;15(3):7-14



**APPENDIX**

จุฬาลงกรณ์มหาวิทยาลัย  
**CHULALONGKORN UNIVERSITY**



**APPENDIX A**

**Titration charts used in the construction of pseudoternary  
phase diagram**

จุฬาลงกรณ์มหาวิทยาลัย  
**CHULALONGKORN UNIVERSITY**

Titration chart of LCT-SMEDS

Oil ( $\mu\text{L}$ )	$S_{\text{mix}}$ ( $\mu\text{L}$ )	Water ( $\mu\text{L}$ )	Water added ( $\mu\text{L}$ )	Total ( $\mu\text{L}$ )	Oil (%)	$S_{\text{mix}}$ (%)	Water (%)	Visual observation				
								(1:1)	(2:1)	(3:1)	(4:1)	(5:1)
10	90	10	10	110	9.09	81.82	9.09	TG	TG	TG	TG	TG
10	90	20	10	120	8.33	75	16.67	TG	TG	TG	TG	TG
10	90	25	5	125	8	72	20	TG	TG	TG	TG	TG
10	90	35	10	135	7.41	66.67	25.93	TG	TG	TG	TG	TG
10	90	45	10	145	6.9	62.07	31.03	TG	TG	TG	TG	TG
10	90	55	10	155	6.45	58.06	35.48	TG	TG	TG	TG	TG
10	90	70	15	170	5.88	52.94	41.18	TG	TG	TG	TG	TG
10	90	80	10	180	5.56	50	44.44	TG	TG	TG	TG	TG
10	90	100	20	200	5	45	50	TG	TG	TG	TG	TG
10	90	120	20	220	4.55	40.91	54.55	TG	TG	TG	TG	TG
10	90	155	35	255	3.92	35.29	60.78	TG	TG	TG	TG	TG
10	90	190	35	290	3.45	31.03	65.52	TG	TG	TG	TG	TG
10	90	240	50	340	2.94	26.47	70.59	M	M	M	M	M
10	90	300	60	400	2.5	22.5	75	M	M	M	M	M
10	90	410	110	510	1.96	17.65	80.39	M	M	M	M	M
10	90	570	160	670	1.49	13.43	85.07	M	M	M	M	M
10	90	900	330	1000	1	9	90	M	M	M	M	M
10	90	2000	1100	2100	0.48	4.29	95.24	M	M	M	M	M

Continue

Oil ( $\mu\text{L}$ )	$S_{\text{mix}}$ ( $\mu\text{L}$ )	Water ( $\mu\text{L}$ )	Water added ( $\mu\text{L}$ )	Total ( $\mu\text{L}$ )	Oil (%)	$S_{\text{mix}}$ (%)	Water (%)	Visual observation					
								(1:1)	(2:1)	(3:1)	(4:1)	(5:1)	
20	80	10	10	110	18.18	72.73	9.09	EG	TG	TG	TG	TG	TG
20	80	20	10	120	16.67	66.67	16.67	EG	TG	TG	TG	TG	TG
20	80	25	5	125	16	64	20	EG	TG	TG	TG	TG	TG
20	80	35	10	135	14.81	59.26	25.93	EG	TG	TG	TG	TG	TG
20	80	45	10	145	13.79	55.17	31.03	EG	TG	TG	TG	TG	TG
20	80	55	10	155	12.9	51.61	35.48	EG	TG	TG	TG	TG	TG
20	80	70	15	170	11.76	47.06	41.18	EG	TG	TG	TG	TG	TG
20	80	85	15	185	10.81	43.24	45.95	EG	TG	TG	TG	TG	TG
20	80	100	15	200	10	40	50	EG	TG	M	TG	TG	TG
20	80	125	25	225	8.89	35.56	55.56	EG	TG	M	TG	TG	TG
20	80	155	30	255	7.84	31.37	60.78	E	M	M	TG	TG	TG
20	80	190	35	290	6.9	27.59	65.52	E	M	M	M	M	M
20	80	240	50	340	5.88	23.53	70.59	E	M	M	M	M	M
20	80	310	70	410	4.88	19.51	75.61	E	M	M	M	M	M
20	80	400	90	500	4	16	80	E	M	M	M	M	M
20	80	570	170	670	2.99	11.94	85.07	E	M	M	M	M	M
20	80	1000	430	1100	1.82	7.27	90.91	E	M	M	M	M	M
20	80	2000	1000	2100	0.95	3.81	95.24	E	M	M	M	M	M

Continue

Oil ( $\mu\text{L}$ )	$S_{\text{mix}}$ ( $\mu\text{L}$ )	Water ( $\mu\text{L}$ )	Water added ( $\mu\text{L}$ )	Total ( $\mu\text{L}$ )	Oil (%)	$S_{\text{mix}}$ (%)	Water (%)	Visual observation				
								(1:1)	(2:1)	(3:1)	(4:1)	(5:1)
30	70	10	10	110	27.27	63.64	9.09	EG	EG	EG	TG	TG
30	70	20	10	120	25	58.33	16.67	EG	EG	EG	TG	TG
30	70	25	5	125	24	56	20	EG	EG	EG	TG	TG
30	70	35	10	135	22.22	51.85	25.93	EG	EG	EG	TG	TG
30	70	45	10	145	20.69	48.28	31.03	EG	EG	EG	TG	TG
30	70	55	10	155	19.35	45.16	35.48	EG	EG	EG	TG	TG
30	70	65	10	165	18.18	42.42	39.39	EG	EG	EG	TG	TG
30	70	80	15	180	16.67	38.89	44.44	EG	EG	EG	TG	TG
30	70	100	20	200	15	35	50	EG	EG	EG	TG	TG
30	70	120	20	220	13.33	31.11	55.56	EG	EG	E	M	M
30	70	150	30	250	11.76	27.45	60.78	EG	E	E	M	M
30	70	185	35	285	10.53	24.56	64.91	E	E	E	M	M
30	70	235	50	335	9.09	21.21	69.7	E	E	E	M	M
30	70	300	65	400	7.5	17.5	75	E	E	E	M	M
30	70	400	100	500	6	14	80	E	E	E	M	M
30	70	550	150	650	4.48	10.45	85.07	E	E	E	M	M
30	70	900	350	1000	2.94	6.86	90.2	E	E	E	M	M
30	70	2000	1100	2100	1.43	3.33	95.24	E	E	E	M	M

Continue

Oil ( $\mu\text{L}$ )	$S_{\text{mix}}$ ( $\mu\text{L}$ )	Water ( $\mu\text{L}$ )	Water added ( $\mu\text{L}$ )	Total ( $\mu\text{L}$ )	Oil (%)	$S_{\text{mix}}$ (%)	Water (%)	Visual observation				
								(1:1)	(2:1)	(3:1)	(4:1)	(5:1)
40	60	10	10	110	36.36	54.55	9.09	EG	EG	EG	EG	EG
40	60	20	10	120	33.33	50	16.67	EG	EG	EG	EG	EG
40	60	25	5	125	32	48	20	EG	EG	EG	EG	EG
40	60	35	10	135	29.63	44.44	25.93	EG	EG	EG	EG	EG
40	60	45	10	145	27.59	41.38	31.03	EG	EG	EG	EG	EG
40	60	55	10	155	25.81	38.71	35.48	EG	EG	EG	EG	EG
40	60	65	10	165	23.53	35.29	41.18	EG	EG	EG	EG	EG
40	60	80	15	180	21.62	32.43	45.95	EG	EG	EG	EG	EG
40	60	100	20	200	20	30	50	EG	EG	EG	EG	EG
40	60	120	20	220	17.78	26.67	55.55	E	E	E	M	E
40	60	150	30	250	15.69	23.53	60.78	E	E	E	M	E
40	60	185	35	285	14.04	21.05	64.91	E	E	E	M	E
40	60	235	50	335	11.94	17.91	70.15	E	E	E	M	E
40	60	300	65	400	10	15	75	E	E	E	M	E
40	60	400	100	500	8	12	80	E	E	E	M	E
40	60	550	150	650	5.97	8.96	85.07	E	E	E	M	E
40	60	900	350	1000	3.92	5.88	90.2	E	E	E	M	E
40	60	2000	1100	2100	1.9	2.86	95.24	E	E	E	M	E

Continue

Oil ( $\mu\text{L}$ )	$S_{\text{mix}}$ ( $\mu\text{L}$ )	Water ( $\mu\text{L}$ )	Water added ( $\mu\text{L}$ )	Total ( $\mu\text{L}$ )	Oil (%)	$S_{\text{mix}}$ (%)	Water (%)	Visual observation				
								(1:1)	(2:1)	(3:1)	(4:1)	(5:1)
50	50	10	10	110	45.45	45.45	9.1	EG	EG	EG	EG	EG
50	50	20	10	120	41.67	41.67	16.66	EG	EG	EG	EG	EG
50	50	25	5	125	40	40	20	EG	EG	EG	EG	EG
50	50	35	10	135	37.04	37.04	25.92	EG	EG	EG	EG	EG
50	50	45	10	145	34.48	34.48	31.04	EG	EG	EG	EG	EG
50	50	55	10	155	32.26	32.26	35.48	EG	EG	EG	EG	EG
50	50	65	10	165	29.41	29.41	41.18	EG	EG	EG	EG	EG
50	50	80	15	180	27.03	27.03	45.94	E	E	E	E	E
50	50	100	20	200	25	25	50	E	E	E	E	E
50	50	120	20	220	22.22	22.22	55.56	E	E	E	E	E
50	50	150	30	250	19.61	19.61	60.78	E	E	E	E	E
50	50	185	35	285	17.54	17.54	64.92	E	E	E	E	E
50	50	235	50	335	14.93	14.93	70.14	E	E	E	E	E
50	50	300	65	400	12.5	12.5	75	E	E	E	E	E
50	50	400	100	500	10	10	80	E	E	E	E	E
50	50	550	150	650	7.46	7.46	85.08	E	E	E	E	E
50	50	900	350	1000	4.9	4.9	90.2	E	E	E	E	E
50	50	2000	1100	2100	2.38	2.38	95.24	E	E	E	E	E



Continue

Oil ( $\mu\text{L}$ )	$S_{\text{mix}}$ ( $\mu\text{L}$ )	Water ( $\mu\text{L}$ )	Water added ( $\mu\text{L}$ )	Total ( $\mu\text{L}$ )	Oil (%)	$S_{\text{mix}}$ (%)	Water (%)	Visual observation				
								(1:1)	(2:1)	(3:1)	(4:1)	(5:1)
60	40	10	10	110	54.55	36.36	9.09	EG	EG	EG	EG	EG
60	40	20	10	120	50	33.33	16.67	EG	EG	EG	EG	EG
60	40	25	5	125	48	32	20	EG	EG	EG	EG	EG
60	40	35	10	135	44.44	29.63	25.93	EG	EG	EG	EG	EG
60	40	45	10	145	41.38	27.59	31.03	EG	EG	EG	EG	EG
60	40	55	10	155	38.71	25.81	35.48	EG	EG	EG	EG	EG
60	40	65	10	165	35.29	23.53	41.18	EG	EG	EG	EG	EG
60	40	80	15	180	32.43	21.62	45.95	E	E	E	E	E
60	40	100	20	200	30	20	50	E	E	E	E	E
60	40	120	20	220	26.67	17.78	55.55	E	E	E	E	E
60	40	150	30	250	23.53	15.69	60.78	E	E	E	E	E
60	40	185	35	285	21.05	14.04	64.91	E	E	E	E	E
60	40	235	50	335	17.91	11.94	70.15	E	E	E	E	E
60	40	300	65	400	15	10	75	E	E	E	E	E
60	40	400	100	500	12	8	80	E	E	E	E	E
60	40	550	150	650	8.96	5.97	85.07	E	E	E	E	E
60	40	900	350	1000	5.88	3.92	90.2	E	E	E	E	E
60	40	2000	1100	2100	2.86	1.9	95.24	E	E	E	E	E

Continue

Oil ( $\mu\text{L}$ )	$S_{\text{mix}}$ ( $\mu\text{L}$ )	Water ( $\mu\text{L}$ )	Water added ( $\mu\text{L}$ )	Total ( $\mu\text{L}$ )	Oil (%)	$S_{\text{mix}}$ (%)	Water (%)	Visual observation				
								(1:1)	(2:1)	(3:1)	(4:1)	(5:1)
70	30	10	10	110	63.64	27.27	9.09	EG	EG	EG	EG	EG
70	30	20	10	120	58.33	25	16.67	EG	EG	EG	EG	EG
70	30	25	5	125	56	24	20	EG	EG	EG	EG	EG
70	30	35	10	135	51.85	22.22	25.93	EG	EG	EG	EG	EG
70	30	45	10	145	48.28	20.69	31.03	EG	EG	EG	EG	EG
70	30	55	10	155	45.16	19.35	35.48	EG	EG	EG	EG	EG
70	30	65	10	165	42.42	18.18	39.39	EG	EG	EG	EG	EG
70	30	80	15	180	38.89	16.67	44.44	E	E	E	E	E
70	30	100	20	200	35	15	50	E	E	E	E	E
70	30	120	20	220	31.11	13.33	55.56	E	E	E	E	E
70	30	150	30	250	27.45	11.76	60.78	E	E	E	E	E
70	30	185	35	285	24.56	10.53	64.91	E	E	E	E	E
70	30	235	50	335	21.21	9.09	69.7	E	E	E	E	E
70	30	300	65	400	17.5	7.5	75	E	E	E	E	E
70	30	400	100	500	14	6	80	E	E	E	E	E
70	30	550	150	650	10.45	4.48	85.07	E	E	E	E	E
70	30	900	350	1000	6.86	2.94	90.2	E	E	E	E	E
70	30	2000	1100	2100	3.33	1.43	95.24	E	E	E	E	E

Continue

Oil ( $\mu\text{L}$ )	$S_{\text{mix}}$ ( $\mu\text{L}$ )	Water ( $\mu\text{L}$ )	Water added ( $\mu\text{L}$ )	Total ( $\mu\text{L}$ )	Oil (%)	$S_{\text{mix}}$ (%)	Water (%)	Visual observation				
								(1:1)	(2:1)	(3:1)	(4:1)	(5:1)
80	20	10	10	110	72.73	18.18	9.09	EG	EG	EG	EG	EG
80	20	20	10	120	66.67	16.67	16.67	EG	EG	EG	EG	EG
80	20	25	5	125	64	16	20	EG	EG	EG	EG	EG
80	20	35	10	135	59.26	14.81	25.93	EG	EG	EG	EG	EG
80	20	45	10	145	55.17	13.79	31.03	EG	EG	EG	EG	EG
80	20	55	10	155	51.61	12.9	35.48	EG	EG	EG	EG	EG
80	20	65	10	165	47.06	11.76	41.18	EG	EG	EG	EG	EG
80	20	80	15	180	43.24	10.81	45.95	E	E	E	E	E
80	20	100	20	200	40	10	50	E	E	E	E	E
80	20	120	20	220	35.56	8.89	55.56	E	E	E	E	E
80	20	150	30	250	31.37	7.84	60.78	E	E	E	E	E
80	20	185	35	285	27.59	6.9	65.52	E	E	E	E	E
80	20	235	50	335	23.53	5.88	70.59	E	E	E	E	E
80	20	300	65	400	19.51	4.88	75.61	E	E	E	E	E
80	20	400	100	500	16	4	80	E	E	E	E	E
80	20	550	150	650	11.94	2.99	85.07	E	E	E	E	E
80	20	900	350	1000	7.27	1.82	90.91	E	E	E	E	E
80	20	2000	1100	2100	3.81	0.95	95.24	E	E	E	E	E

Continue

Oil ( $\mu\text{L}$ )	$S_{\text{mix}}$ ( $\mu\text{L}$ )	Water ( $\mu\text{L}$ )	Water added ( $\mu\text{L}$ )	Total ( $\mu\text{L}$ )	Oil (%)	$S_{\text{mix}}$ (%)	Water (%)	Visual observation				
								(1:1)	(2:1)	(3:1)	(4:1)	(5:1)
90	10	10	10	110	81.82	9.09	9.09	EG	EG	EG	EG	EG
90	10	20	10	120	75	8.33	16.67	EG	EG	EG	EG	EG
90	10	25	5	125	72	8	20	EG	EG	EG	EG	EG
90	10	35	10	135	66.67	7.41	25.93	EG	EG	EG	EG	EG
90	10	45	10	145	62.07	6.9	31.03	EG	EG	EG	EG	EG
90	10	55	10	155	58.06	6.45	35.48	EG	EG	EG	EG	EG
90	10	65	10	165	52.94	5.88	41.18	EG	EG	EG	EG	EG
90	10	80	15	180	50	5.56	44.44	E	E	E	E	E
90	10	100	20	200	45	5	50	E	E	E	E	E
90	10	120	20	220	40.91	4.55	54.55	E	E	E	E	E
90	10	150	30	250	35.29	3.92	60.78	E	E	E	E	E
90	10	185	35	285	31.03	3.45	65.52	E	E	E	E	E
90	10	235	50	335	26.47	2.94	70.59	E	E	E	E	E
90	10	300	65	400	22.5	2.5	75	E	E	E	E	E
90	10	400	100	500	17.65	1.96	80.39	E	E	E	E	E
90	10	550	150	650	13.43	1.49	85.07	E	E	E	E	E
90	10	900	350	1000	9	1	90	E	E	E	E	E
90	10	2000	1100	2100	4.29	0.48	95.24	E	E	E	E	E

TG; Translucent gel (clear), EG; Emulgel (milky), M; Microemulsion(clear), E; Emulsion (milky)

Titration chart of MCT-SMEDS

Oil ( $\mu\text{L}$ )	$S_{\text{mix}}$ ( $\mu\text{L}$ )	Water ( $\mu\text{L}$ )	Water added ( $\mu\text{L}$ )	Total ( $\mu\text{L}$ )	Oil (%)	$S_{\text{mix}}$ (%)	Water (%)	Visual observation					
								(1:1)	(2:1)	(3:1)	(4:1)	(5:1)	
10	90	10	10	110	9.09	81.82	9.09	TG	TG	TG	TG	TG	TG
10	90	20	10	120	8.33	75	16.67	TG	TG	TG	TG	TG	TG
10	90	25	5	125	8	72	20	TG	TG	TG	TG	TG	TG
10	90	35	10	135	7.41	66.67	25.93	TG	TG	TG	TG	TG	TG
10	90	45	10	145	6.9	62.07	31.03	TG	TG	TG	TG	TG	TG
10	90	55	10	155	6.45	58.06	35.48	TG	TG	TG	TG	TG	TG
10	90	70	15	170	5.88	52.94	41.18	TG	TG	TG	TG	TG	TG
10	90	80	10	180	5.56	50	44.44	TG	TG	TG	TG	TG	TG
10	90	100	20	200	5	45	50	TG	TG	TG	TG	TG	TG
10	90	120	20	220	4.55	40.91	54.55	TG	TG	TG	TG	TG	TG
10	90	155	35	255	3.92	35.29	60.78	M	M	M	M	M	M
10	90	190	35	290	3.45	31.03	65.52	M	M	M	M	M	M
10	90	240	50	340	2.94	26.47	70.59	M	M	M	M	M	M
10	90	300	60	400	2.5	22.5	75	M	M	M	M	M	M
10	90	410	110	510	1.96	17.65	80.39	M	M	M	M	M	M
10	90	570	160	670	1.49	13.43	85.07	M	M	M	M	M	M
10	90	900	330	1000	1	9	90	M	M	M	M	M	M
10	90	2000	1100	2100	0.48	4.29	95.24	M	M	M	M	M	M

Continue

Oil ( $\mu\text{L}$ )	$S_{\text{mix}}$ ( $\mu\text{L}$ )	Water ( $\mu\text{L}$ )	Water added ( $\mu\text{L}$ )	Total ( $\mu\text{L}$ )	Oil (%)	$S_{\text{mix}}$ (%)	Water (%)	Visual observation					
								(1:1)	(2:1)	(3:1)	(4:1)	(5:1)	
20	80	10	10	110	18.18	72.73	9.09	TG	TG	TG	TG	TG	TG
20	80	20	10	120	16.67	66.67	16.67	TG	TG	TG	TG	TG	TG
20	80	25	5	125	16	64	20	TG	TG	TG	TG	TG	TG
20	80	35	10	135	14.81	59.26	25.93	TG	TG	TG	TG	TG	TG
20	80	45	10	145	13.79	55.17	31.03	TG	TG	TG	TG	TG	TG
20	80	55	10	155	12.9	51.61	35.48	TG	TG	TG	TG	TG	TG
20	80	70	15	170	11.76	47.06	41.18	TG	TG	TG	TG	TG	TG
20	80	85	15	185	10.81	43.24	45.95	TG	TG	TG	TG	TG	TG
20	80	100	15	200	10	40	50	M	TG	TG	TG	TG	TG
20	80	125	25	225	8.89	35.56	55.56	M	TG	TG	TG	TG	TG
20	80	155	30	255	7.84	31.37	60.78	M	M	M	M	M	M
20	80	190	35	290	6.9	27.59	65.52	M	M	M	M	M	M
20	80	240	50	340	5.88	23.53	70.59	M	M	M	M	M	M
20	80	310	70	410	4.88	19.51	75.61	M	M	M	M	M	M
20	80	400	90	500	4	16	80	M	M	M	M	M	M
20	80	570	170	670	2.99	11.94	85.07	M	M	M	M	M	M
20	80	1000	430	1100	1.82	7.27	90.91	M	M	M	M	M	M
20	80	2000	1000	2100	0.95	3.81	95.24	M	M	M	M	M	M

Continue

Oil ( $\mu\text{L}$ )	$S_{\text{mix}}$ ( $\mu\text{L}$ )	Water ( $\mu\text{L}$ )	Water added ( $\mu\text{L}$ )	Total ( $\mu\text{L}$ )	Oil (%)	$S_{\text{mix}}$ (%)	Water (%)	Visual observation					
								(1:1)	(2:1)	(3:1)	(4:1)	(5:1)	
30	70	10	10	110	27.27	63.64	9.09	TG	TG	TG	TG	TG	TG
30	70	20	10	120	25	58.33	16.67	TG	TG	TG	TG	TG	TG
30	70	25	5	125	24	56	20	TG	TG	TG	TG	TG	TG
30	70	35	10	135	22.22	51.85	25.93	TG	TG	TG	TG	TG	TG
30	70	45	10	145	20.69	48.28	31.03	TG	TG	TG	TG	TG	TG
30	70	55	10	155	19.35	45.16	35.48	TG	TG	TG	TG	TG	TG
30	70	65	10	165	18.18	42.42	39.39	TG	TG	TG	TG	TG	TG
30	70	80	15	180	16.67	38.89	44.44	TG	TG	TG	TG	TG	TG
30	70	100	20	200	15	35	50	TG	TG	TG	TG	TG	TG
30	70	120	20	220	13.33	31.11	55.56	TG	TG	TG	TG	TG	TG
30	70	150	30	250	11.76	27.45	60.78	TG	TG	TG	TG	TG	TG
30	70	185	35	285	10.53	24.56	64.91	M	TG	TG	TG	TG	TG
30	70	235	50	335	9.09	21.21	69.7	M	TG	TG	TG	TG	TG
30	70	300	65	400	7.5	17.5	75	M	M	M	M	M	M
30	70	400	100	500	6	14	80	M	M	M	M	M	M
30	70	550	150	650	4.48	10.45	85.07	M	M	M	M	M	M
30	70	900	350	1000	2.94	6.86	90.2	M	M	M	M	M	M
30	70	2000	1100	2100	1.43	3.33	95.24	M	M	M	M	M	M

Continue

Oil ( $\mu\text{L}$ )	$S_{\text{mix}}$ ( $\mu\text{L}$ )	Water ( $\mu\text{L}$ )	Water added ( $\mu\text{L}$ )	Total ( $\mu\text{L}$ )	Oil (%)	$S_{\text{mix}}$ (%)	Water (%)	Visual observation					
								(1:1)	(2:1)	(3:1)	(4:1)	(5:1)	
40	60	10	10	110	36.36	54.55	9.09	TG	TG	TG	TG	TG	TG
40	60	20	10	120	33.33	50	16.67	TG	TG	TG	TG	TG	TG
40	60	25	5	125	32	48	20	TG	TG	TG	TG	TG	TG
40	60	35	10	135	29.63	44.44	25.93	TG	TG	TG	TG	TG	TG
40	60	45	10	145	27.59	41.38	31.03	TG	TG	TG	TG	TG	TG
40	60	55	10	155	25.81	38.71	35.48	EG	EG	EG	EG	EG	EG
40	60	65	10	165	23.53	35.29	41.18	EG	EG	EG	EG	EG	EG
40	60	80	15	180	21.62	32.43	45.95	EG	EG	EG	EG	EG	EG
40	60	100	20	200	20	30	50	EG	EG	EG	EG	EG	EG
40	60	120	20	220	17.78	26.67	55.55	EG	EG	EG	EG	EG	EG
40	60	150	30	250	15.69	23.53	60.78	EG	EG	EG	EG	EG	EG
40	60	185	35	285	14.04	21.05	64.91	E	E	E	E	E	E
40	60	235	50	335	11.94	17.91	70.15	E	E	E	E	E	E
40	60	300	65	400	10	15	75	E	E	E	E	E	E
40	60	400	100	500	8	12	80	E	E	E	E	E	E
40	60	550	150	650	5.97	8.96	85.07	E	E	E	E	E	E
40	60	900	350	1000	3.92	5.88	90.2	E	E	E	E	E	E
40	60	2000	1100	2100	1.9	2.86	95.24	E	E	E	E	E	E



Continue

Oil ( $\mu\text{L}$ )	$S_{\text{mix}}$ ( $\mu\text{L}$ )	Water ( $\mu\text{L}$ )	Water added ( $\mu\text{L}$ )	Total ( $\mu\text{L}$ )	Oil (%)	$S_{\text{mix}}$ (%)	Water (%)	Visual observation					
								(1:1)	(2:1)	(3:1)	(4:1)	(5:1)	
50	50	10	10	110	45.45	45.45	9.1	TG	TG	TG	TG	TG	TG
50	50	20	10	120	41.67	41.67	16.66	EG	EG	EG	EG	EG	EG
50	50	25	5	125	40	40	20	EG	EG	EG	EG	EG	EG
50	50	35	10	135	37.04	37.04	25.92	EG	EG	EG	EG	EG	EG
50	50	45	10	145	34.48	34.48	31.04	EG	EG	EG	EG	EG	EG
50	50	55	10	155	32.26	32.26	35.48	EG	EG	EG	EG	EG	EG
50	50	65	10	165	29.41	29.41	41.18	EG	EG	EG	EG	EG	EG
50	50	80	15	180	27.03	27.03	45.94	EG	EG	EG	EG	EG	EG
50	50	100	20	200	25	25	50	EG	EG	EG	EG	EG	EG
50	50	120	20	220	22.22	22.22	55.56	E	E	E	E	E	E
50	50	150	30	250	19.61	19.61	60.78	E	E	E	E	E	E
50	50	185	35	285	17.54	17.54	64.92	E	E	E	E	E	E
50	50	235	50	335	14.93	14.93	70.14	E	E	E	E	E	E
50	50	300	65	400	12.5	12.5	75	E	E	E	E	E	E
50	50	400	100	500	10	10	80	E	E	E	E	E	E
50	50	550	150	650	7.46	7.46	85.08	E	E	E	E	E	E
50	50	900	350	1000	4.9	4.9	90.2	E	E	E	E	E	E
50	50	2000	1100	2100	2.38	2.38	95.24	E	E	E	E	E	E

Continue

Oil ( $\mu\text{L}$ )	$S_{\text{mix}}$ ( $\mu\text{L}$ )	Water ( $\mu\text{L}$ )	Water added ( $\mu\text{L}$ )	Total ( $\mu\text{L}$ )	Oil (%)	$S_{\text{mix}}$ (%)	Water (%)	Visual observation				
								(1:1)	(2:1)	(3:1)	(4:1)	(5:1)
60	40	10	10	110	54.55	36.36	9.09	TG	TG	TG	TG	TG
60	40	20	10	120	50	33.33	16.67	EG	EG	EG	EG	EG
60	40	25	5	125	48	32	20	EG	EG	EG	EG	EG
60	40	35	10	135	44.44	29.63	25.93	EG	EG	EG	EG	EG
60	40	45	10	145	41.38	27.59	31.03	EG	EG	EG	EG	EG
60	40	55	10	155	38.71	25.81	35.48	EG	EG	EG	EG	EG
60	40	65	10	165	35.29	23.53	41.18	EG	EG	EG	EG	EG
60	40	80	15	180	32.43	21.62	45.95	EG	EG	EG	EG	EG
60	40	100	20	200	30	20	50	EG	EG	EG	EG	EG
60	40	120	20	220	26.67	17.78	55.55	E	E	E	E	E
60	40	150	30	250	23.53	15.69	60.78	E	E	E	E	E
60	40	185	35	285	21.05	14.04	64.91	E	E	E	E	E
60	40	235	50	335	17.91	11.94	70.15	E	E	E	E	E
60	40	300	65	400	15	10	75	E	E	E	E	E
60	40	400	100	500	12	8	80	E	E	E	E	E
60	40	550	150	650	8.96	5.97	85.07	E	E	E	E	E
60	40	900	350	1000	5.88	3.92	90.2	E	E	E	E	E
60	40	2000	1100	2100	2.86	1.9	95.24	E	E	E	E	E

Continue

Oil ( $\mu\text{L}$ )	$S_{\text{mix}}$ ( $\mu\text{L}$ )	Water ( $\mu\text{L}$ )	Water added ( $\mu\text{L}$ )	Total ( $\mu\text{L}$ )	Oil (%)	$S_{\text{mix}}$ (%)	Water (%)	Visual observation					
								(1:1)	(2:1)	(3:1)	(4:1)	(5:1)	
70	30	10	10	110	63.64	27.27	9.09	TG	TG	TG	TG	TG	TG
70	30	20	10	120	58.33	25	16.67	EG	EG	EG	EG	EG	EG
70	30	25	5	125	56	24	20	EG	EG	EG	EG	EG	EG
70	30	35	10	135	51.85	22.22	25.93	EG	EG	EG	EG	EG	EG
70	30	45	10	145	48.28	20.69	31.03	EG	EG	EG	EG	EG	EG
70	30	55	10	155	45.16	19.35	35.48	EG	EG	EG	EG	EG	EG
70	30	65	10	165	42.42	18.18	39.39	EG	EG	EG	EG	EG	EG
70	30	80	15	180	38.89	16.67	44.44	EG	EG	EG	EG	EG	EG
70	30	100	20	200	35	15	50	EG	EG	EG	EG	EG	EG
70	30	120	20	220	31.11	13.33	55.56	E	E	E	E	E	E
70	30	150	30	250	27.45	11.76	60.78	E	E	E	E	E	E
70	30	185	35	285	24.56	10.53	64.91	E	E	E	E	E	E
70	30	235	50	335	21.21	9.09	69.7	E	E	E	E	E	E
70	30	300	65	400	17.5	7.5	75	E	E	E	E	E	E
70	30	400	100	500	14	6	80	E	E	E	E	E	E
70	30	550	150	650	10.45	4.48	85.07	E	E	E	E	E	E
70	30	900	350	1000	6.86	2.94	90.2	E	E	E	E	E	E
70	30	2000	1100	2100	3.33	1.43	95.24	E	E	E	E	E	E

Continue

Oil ( $\mu\text{L}$ )	$S_{\text{mix}}$ ( $\mu\text{L}$ )	Water ( $\mu\text{L}$ )	Water added ( $\mu\text{L}$ )	Total ( $\mu\text{L}$ )	Oil (%)	$S_{\text{mix}}$ (%)	Water (%)	Visual observation				
								(1:1)	(2:1)	(3:1)	(4:1)	(5:1)
80	20	10	10	110	72.73	18.18	9.09	TG	TG	TG	TG	TG
80	20	20	10	120	66.67	16.67	16.67	EG	EG	EG	EG	EG
80	20	25	5	125	64	16	20	EG	EG	EG	EG	EG
80	20	35	10	135	59.26	14.81	25.93	EG	EG	EG	EG	EG
80	20	45	10	145	55.17	13.79	31.03	EG	EG	EG	EG	EG
80	20	55	10	155	51.61	12.9	35.48	EG	EG	EG	EG	EG
80	20	65	10	165	47.06	11.76	41.18	EG	EG	EG	EG	EG
80	20	80	15	180	43.24	10.81	45.95	EG	EG	EG	EG	EG
80	20	100	20	200	40	10	50	EG	EG	EG	EG	EG
80	20	120	20	220	35.56	8.89	55.56	E	E	E	E	E
80	20	150	30	250	31.37	7.84	60.78	E	E	E	E	E
80	20	185	35	285	27.59	6.9	65.52	E	E	E	E	E
80	20	235	50	335	23.53	5.88	70.59	E	E	E	E	E
80	20	300	65	400	19.51	4.88	75.61	E	E	E	E	E
80	20	400	100	500	16	4	80	E	E	E	E	E
80	20	550	150	650	11.94	2.99	85.07	E	E	E	E	E
80	20	900	350	1000	7.27	1.82	90.91	E	E	E	E	E
80	20	2000	1100	2100	3.81	0.95	95.24	E	E	E	E	E

Continue

Oil ( $\mu\text{L}$ )	$S_{\text{mix}}$ ( $\mu\text{L}$ )	Water ( $\mu\text{L}$ )	Water added ( $\mu\text{L}$ )	Total ( $\mu\text{L}$ )	Oil (%)	$S_{\text{mix}}$ (%)	Water (%)	Visual observation				
								(1:1)	(2:1)	(3:1)	(4:1)	(5:1)
90	10	10	10	110	81.82	9.09	9.09	TG	TG	TG	TG	TG
90	10	20	10	120	75	8.33	16.67	EG	EG	EG	EG	EG
90	10	25	5	125	72	8	20	EG	EG	EG	EG	EG
90	10	35	10	135	66.67	7.41	25.93	EG	EG	EG	EG	EG
90	10	45	10	145	62.07	6.9	31.03	EG	EG	EG	EG	EG
90	10	55	10	155	58.06	6.45	35.48	EG	EG	EG	EG	EG
90	10	65	10	165	52.94	5.88	41.18	EG	EG	EG	EG	EG
90	10	80	15	180	50	5.56	44.44	EG	EG	EG	EG	EG
90	10	100	20	200	45	5	50	EG	EG	EG	EG	EG
90	10	120	20	220	40.91	4.55	54.55	E	E	E	E	E
90	10	150	30	250	35.29	3.92	60.78	E	E	E	E	E
90	10	185	35	285	31.03	3.45	65.52	E	E	E	E	E
90	10	235	50	335	26.47	2.94	70.59	E	E	E	E	E
90	10	300	65	400	22.5	2.5	75	E	E	E	E	E
90	10	400	100	500	17.65	1.96	80.39	E	E	E	E	E
90	10	550	150	650	13.43	1.49	85.07	E	E	E	E	E
90	10	900	350	1000	9	1	90	E	E	E	E	E
90	10	2000	1100	2100	4.29	0.48	95.24	E	E	E	E	E

TG; Translucent gel (clear), EG; Emulgel (milky), M; Microemulsion(clear), E; Emulsion (milky)



**APPENDIX B**  
**Residual plots for optimization**

จุฬาลงกรณ์มหาวิทยาลัย  
**CHULALONGKORN UNIVERSITY**

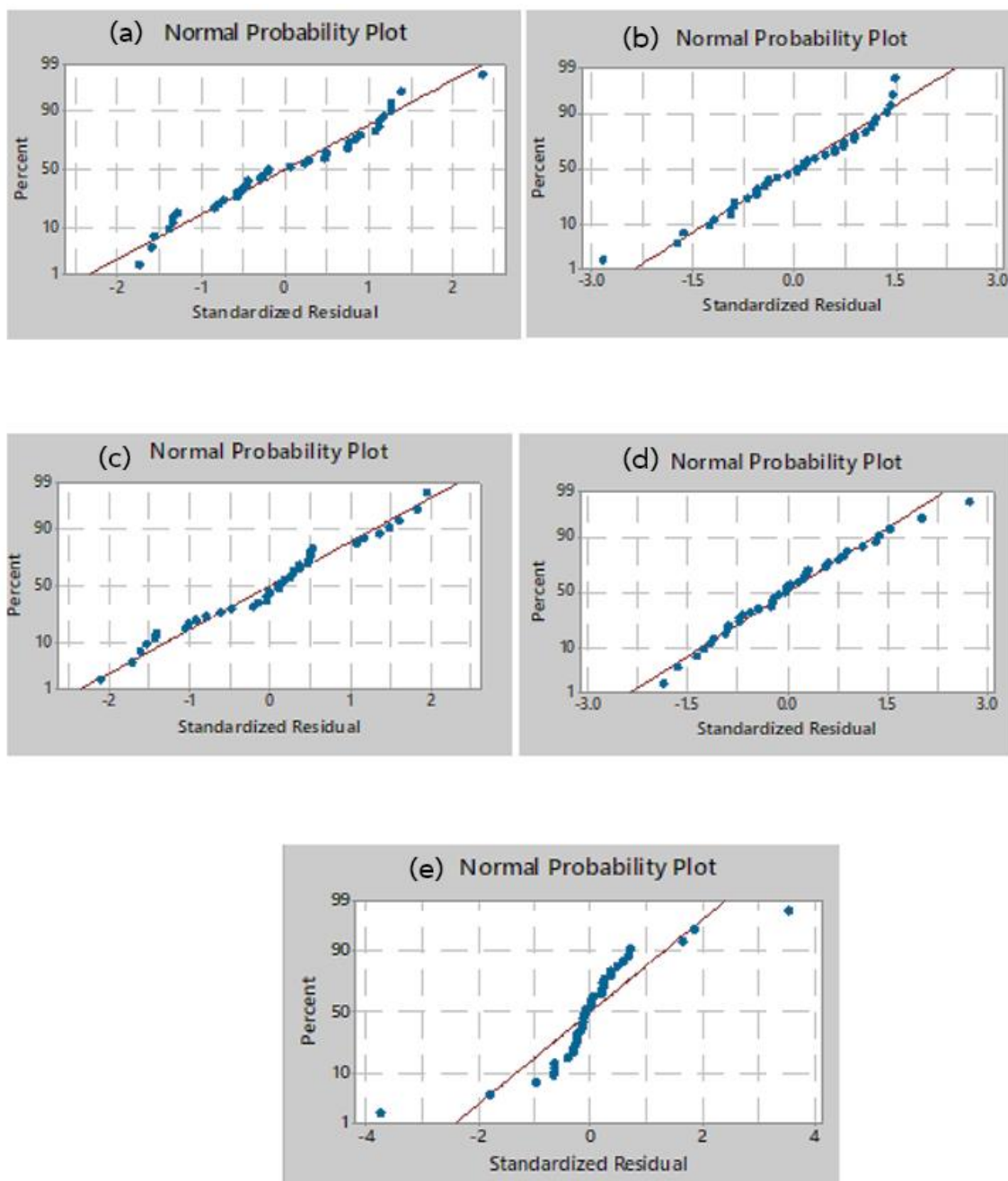


Figure: Residual plots for (a) droplet size, (b) polydispersity index, (c) zeta potential, (d) active ingredient content, and (e) %transmittance of LCT-SMEDS

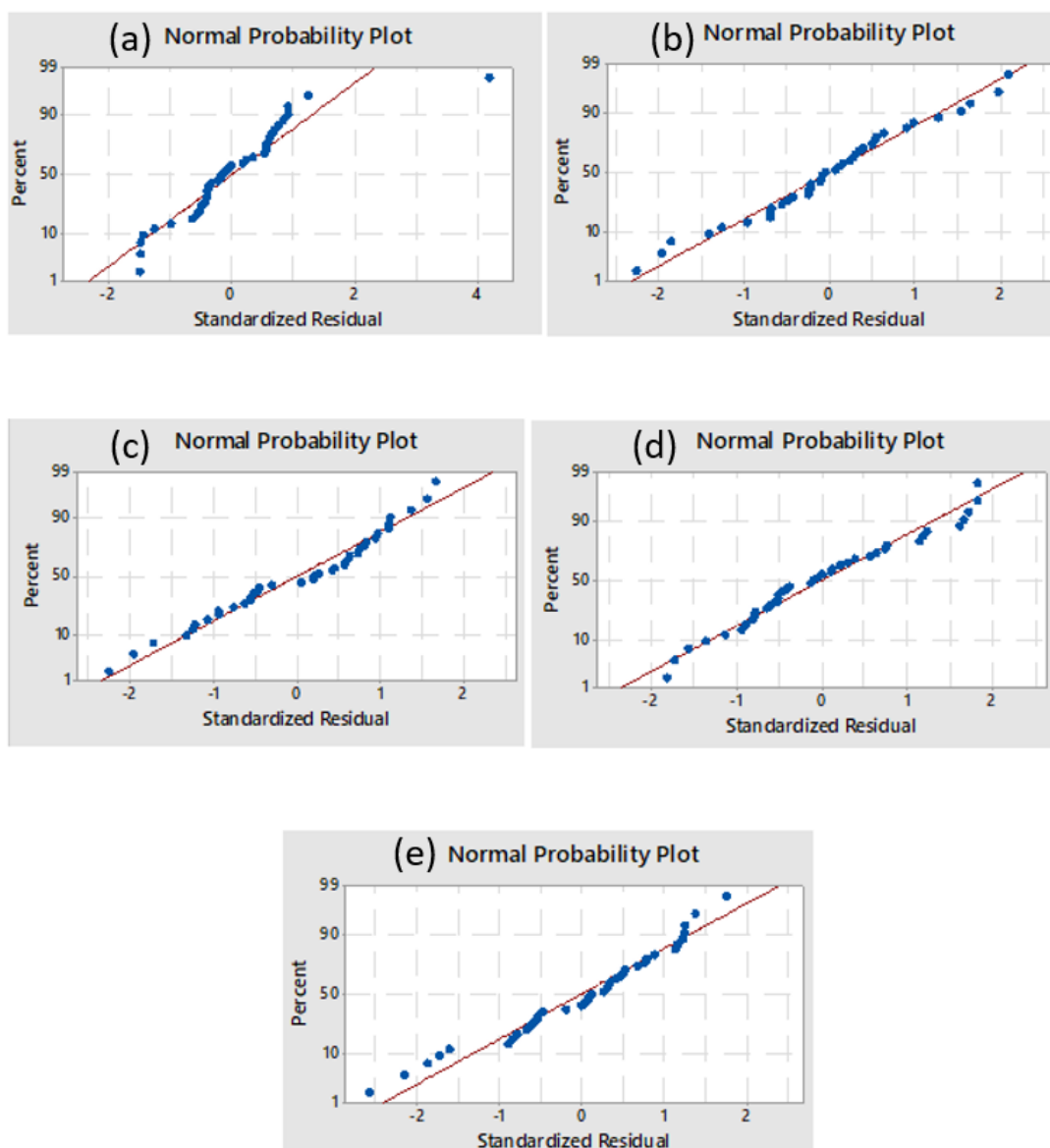


Figure: Residual plots for (a) droplet size, (b) polydispersity index, (c) zeta potential, (d) active ingredient content, and (e) %transmittance of MCT-SMEDS



**VITA**

**NAME** Miss Mo Mo Ko Zin

**DATE OF BIRTH** 20 February 1992

**PLACE OF BIRTH** Yangon, Myanmar

**INSTITUTIONS  
ATTENDED** University of Pharmacy (Yangon)

**HOME ADDRESS** No 303, Yazadirit road, 72 quarter, Dagon Myothit (South),  
Yangon, Myanmar.



จุฬาลงกรณ์มหาวิทยาลัย  
**CHULALONGKORN UNIVERSITY**